Surface-No. 14-MOC-CMA

Report on the Quality of Land Surface Observations in Region II (Asia)

July – December 2024

No. 14

Regional WIGOS Centre, Beijing

China Meteorological Administration

No. 46 Zhongguancun Nandajie

Beijing, CHINA

Contents

Report on the Quality of Land Surface Observations in Region II
(No. 14)
July – December 2024

Introduction

In its role as Regional WMO Integrated Global Observing System (WIGOS) Centre, Beijing (RWC-Beijing) in Regional Association (RA) II, China Meteorological Administration (CMA) has issued the 14th report on the land surface observation quality monitoring for the period from July to December 2024. The report includes a consolidated list of stations suspected of producing low-quality observational data.

RWC-Beijing was designated as RWC in 2021, in support to the Members of the Region as an operational RWC with a certification. It is responsible for monitoring the availability and quality of meteorological observations and maintaining consolidated lists of stations suspected of reporting low-quality observational data together with adequate evidence. The lists are to be passed on to the WMO Secretariat as well as to Members of RA II for their reference.

1. Monitored Data

Monitored surface observational data are obtained at 00, 06, 12 and 18 UTC and collected at CMA before the data cut-off time, defined as the end of the period in which observational data are gathered for operational analysis. The cut-off times for CMA global analysis are shown in Table 1.

Table 1 Data cut-off times for CMA global analysis

Analysis time	Data cut-off time
00 UTC	11:50 UTC
06 UTC	17:50 UTC
12 UTC	23:50 UTC
18 UTC	05:50 UTC

The observation elements monitored are (1) station level pressure, (2) mean sea level pressure, and (3) geopotential height, hereafter referred to as SLP, MSLP, and GZ respectively. In accordance with the Manual on Codes (WMO No. 306) Volume II, GZ data on an agreed standard pressure level are reported at the stations whose elevation is higher than 800 m. Standard pressure levels defined in line with station elevation are shown in Table 2.

Table 2 Elevation of stations reporting GZ data and corresponding standard pressure Levels

Station elevation (m)	Pressure level (hPa)
800 – 2,300	850
2,300 – 3,700	700
Higher than 3,700	500

The numbers of stations reporting SLP, MSLP and/or GZ data in Region II are shown in Table 3, and the data availability of these land surface stations are shown in Figure 1.

Table 3 Numbers of stations reporting SLP, MSLP and/or GZ data in Region II

Element	Number of stations	Number of GBON staions
SLP	2214	1570
MSLP	2266	1535
GZ	180	103

2. Monitoring Methods

The three items described below are examined for each element.

(i) Monthly statistics on observation deviations from the most recent forecast of CMA's global model (referred to as first-guess values) (observation minus guess, hereafter referred to as O-G) and on related trends over the monitoring period

(ii) Reference information from other monitoring centres

Information on the latitude, longitude and altitude of each station is necessary for calculation of first-guess values. Such data for land surface station locations are retrieved from the surface-based observing system component of the Observing Systems Capability Analysis and Review Tool (OSCAR/Surface) *.

* https://oscar.wmo.int/surface/index.html#/

The monitoring procedure has two steps as outlined below.

(1) Exclusion of data with gross errors from the statistical calculation sample

The following thresholds are applied for the gross error check in the first step:

|O-G| >= 15 hPa for SLP and MSLP

|O-G| >= 100 gpm for GZ

Gross error data are excluded from the calculation of BIAS (the mean of O-G) and SD (the standard deviation of O-G).

(2) Identification of suspect stations

When the total number of observations (NOBS) is 184 or more, the next criteria are applied:

- BIAS |BIAS| >= 3 hPa for SLP and MSLP
  |BIAS| >= 30 gpm for GZ

- SD SD >= 5 hPa for SLP and MSLP
  SD >= 40 gpm for GZ

- Percentage of gross errors (PGE) PGE >= 25%

Stations with even one statistic exceeding the threshold are considered suspect.

Note:
(i) The quality of observational data from stations are not checked when the NOBS value is less than 184 or the difference between H and HM is greater than 1,000 m. MSLP reports are also not checked for stations located at altitudes higher than 1,000 m above sea level.
(ii) In case of low quality of the first-guess field, those statistics can exceed the threshold and the stations are listed in the consolidated list. To avoid such situations, statistics of surrounding stations and information from other monitoring centres are also used to judge whether the quality of the station's first-guess field value is appropriate.

3. Monitoring Results

3.1 Consolidated list of suspect stations throughout the period

Table 4 List of suspect land surface stations throughout the period

WMO IDENT	LAT (N)	LON (E)	H (m)	HM (m)	ELEM	NUM OBS	PGE %	SD	BIAS	RMS
36914*	42.73	75.02	1775	1692.6	P	655	96	-	-	-
					GZ850	657	0	13.13	1.18	13.19
38262*	42.95	59.80	94.5	58.5	P	688	0	0.93	3.95	4.06
					MSLP	688	0	0.82	0.45	0.94
38349*	42.16	72.89	2000	2874.9	P	645	0	1.31	4.81	4.99
					GZ850	643	0	17.45	50.82	53.73
38359*	42.32	73.80	3500	3104.3	P	653	95	-	-	-
					GZ700	649	0	10.22	-37.85	39.21
38471*	41.95	71.38	2027	2939	P	655	86	1.14	-13.7	13.75
					GZ850	653	96	-	-	-

38476*	41.29	72.83	1748	2017.9	P	648	1	0.88	9.25	9.29
					GZ850	649	16	7.8	88.56	88.91
38829	38.27	67.90	520.7	653.8	P	679	0	1.2	-3.15	3.37
					MSLP	677	0	1.56	-4.36	4.63
38875	39.02	73.55	3930	4307.8	P	320	96	-	-	-
					GZ700	3	100	-	-	-
38880*	37.99	58.36	312	484.6	P	693	1	1.61	12.12	12.22
					MSLP	692	0	1.47	-0.22	1.49
38944*	37.48	69.38	447	563.3	P	687	0	1.1	-5.5	5.61
					MSLP	687	0	1.59	-6.71	6.89
41315*	17.25	54.09	881	512.9	P	598	95	0.63	14.17	14.18
					GZ850	543	94	42.69	-30.5	52.46
42083	31.10	77.17	2270	1502.2	P	343	96	-	-	-
					GZ850	11	100	-	-	-
42114	30.38	78.43	1931	1547.3	P	354	0	0.72	3.71	3.78
					MSLP	-	-	-	-	-
42147	29.47	79.65	2311	1609.7	P	354	0	0.75	5.53	5.58
					MSLP	-	-	-	-	-
42515	25.25	91.73	1300	494	P	359	0	0.82	3.34	3.44
					MSLP	-	-	-	-	-
47037*	39.98	125.25	101	198.6	P	695	0	1.66	-3.98	4.31
					MSLP	695	0	1.66	-4.4	4.71
48018*	24.17	96.33	109.4	172.2	P	204	0	1.28	4.92	5.09
					MSLP	204	0	1.09	-0.05	1.09
48921	21.63	101.88	1360	1068.8	P	459	1	1.25	-3.68	3.89
					GZ850	457	96	0	48	48
48925	20.68	102.00	636	960.9	P	413	1	1.01	-3.49	3.63
					MSLP	413	0	1.31	-4.58	4.76
48926	20.25	100.43	531.8	506.6	P	426	11	1.39	13.64	13.71
					MSLP	426	0	1.16	-0.75	1.38

48944	18.28	102.63	185	309.5	P	339	95	0	5.4	5.4
					MSLP	339	0	3.49	-6.08	7.01
48952	15.68	106.43	180	302.8	P	464	1	1.38	3.49	3.75
					MSLP	464	0	1.27	1.47	1.94

WMO IDENT:	WMO station identification number ("*" represents GBON station)
LAT:	station latitude
LON:	station longitude
H:	station elevation
HM:	model elevation
ELEM:	observed element
NOBS:	total number of observations during the period
PGE:	percentage gross error
SD:	standard deviation of (observation - guess)
BIAS:	bias of (observation - guess)
RMS:	root mean square of (observation - guess)

Kyrgyzstan

36914* – Positive bias of O-G at the station level (Figures 2)
38349* – Positive bias of O-G at the station level (Figures 5 and 6)
38359* – Positive bias of O-G at the station level (Figures 7)
38471* – Negative bias of O-G at the station level (Figures 8)
38476* – Positive bias of O-G at the station level (Figures 9 and 10)

Uzbekistan

38262* – Positive bias of O-G at the station level (Figures 3 and 4)
38829 – Negative bias of O-G at the station level (Figures 11 and 12)

Tajikistan

38875 – Positive bias of O-G at the station level (Figures 13)
38944* – Negative bias of O-G at the station level (Figures 16 and 17)

Turkmenistan

38880* – Positive bias of O-G at the station level (Figures 14 and 15)

Oman

41315* – Positive bias of O-G at the station level (Figures 18)

India

42083 – Positive bias of O-G at the station level (Figures 19)

42114 – Positive bias of O-G at the station level (Figures 20 and 21)
42147 – Positive bias of O-G at the station level (Figures 22 and 23)
42515 – Positive bias of O-G at the station level (Figures 24 and 25)

Democratic People's Republic of Korea
47037* – Negative bias of O-G at the station level (Figures 26 and 27)

Myanmar
48018* – Positive bias of O-G at the station level (Figures 28 and 29)

Lao People's Democratic Republic
48921 – Negative bias of O-G at the station level (Figures 30 and 31)
48925 – Negative bias of O-G at the station level (Figures 32 and 33)
48926 – Positive bias of O-G at the station level (Figures 34 and 35)
48944 – Positive bias of O-G at the station level (Figures 36)
48952 – Positive bias of O-G at the station level (Figures 37 and 38)

3.2 Stations where quality deteriorated during the period

Table 5 List of suspect stations where quality deteriorated during the period

WMO IDENT	LAT (N)	LON (E)	H (m)	HM (m)	ELEM	NUM OBS	PGE %	SD	BIAS	RMS
36729	46.19	80.96	387	457.5	P	687	7	5.27	4.06	6.66
					MSLP	687	9	5.67	3.41	6.62
36934*	42.64	77.07	1613	2536.7	P	611	0	5.49	-7.36	9.18
					GZ850	613	55	44.28	-33.47	55.51
38567	40.13	65.35	341.4	444.5	P	684	0	1.38	-6.66	6.8
					MSLP	684	0	1.81	-7.51	7.72
41565	33.82	71.88	1371	533.7	P	230	0	1.83	4.23	4.61
					GZ850	229	90	19.27	18.48	26.7
41757	25.13	62.33	96	23.8	P	229	0	0.83	10.9	10.93
					MSLP	229	0	0.77	0.95	1.22
42045	33.50	75.17	1624	2401.2	P	526	0	2.03	-4.2	4.67
					GZ850	526	0	18.59	-54.68	57.75
48973	13.73	106.98	330	211	P	259	94	0	3.4	3.4
					MSLP	259	94	0	0.4	0.4

48986	11.63	102.98	13	147	P	220	40	4.64	3.69	5.93
					MSLP	220	37	4.88	2.05	5.29

Kazakhstan

36729 – Positive bias of O-G at the station level has gradually become wild since October 2024. (Figures 39 and 40) In addition, we noticed the bias of O-G at the station level has improved since February this year.

Kyrgyzstan

36934* – Negative bias of O-G at the station level suddenly got bigger since the end of August. (Figures 41 and 42)

Uzbekistan

38567 – Negative bias of O-G at the station level (Figures 43 and 44)

Pakistan

41565 – Positive bias of O-G at the station level (Figures 45 and 46)

41757 – Positive bias of O-G at the station level (Figures 47 and 48)

India

42045 – Negative bias of O-G at the station level (Figures 49 and 50)

Cambodia

48973 – Positive bias of O-G at the station level (Figures 51)

48986 – Positive bias of O-G at the station level, no observations have been received since October, 2024. (Figures 52)

3.3 Stations improved and excluded from the previous consolidated list

Kazakhstan

38318 – The negative pressure bias of O-G at the station level has improved since the end of September. (Figures 53) In addition, since RWC-Beijing worked with NFP (Kazakhstan) using the Incident Management System and station's elevation above sea level was changed in CMA's records based on OSCAR/Surface, the bias of O-G at the station level has improved.

Tajikistan

38719* – The positive pressure bias of O-G at the station level has improved. But the bias of O-G at the station level became bigger again starting from November, 2024. (Figures 54)

Pakistan

41508* – Although station 41508 still displays positive pressure biases of O-G at the station level, it was removed from the consolidated list because the biases did not exceed the threshold. (Figures 55)

Myanmar

48107* – Although station 48107 still displays negative biases of O-G at the station level, it was removed from the consolidated list because the biases did not exceed the threshold. (Figures 56)

3.4 Stations removed from the previous consolidated list

Cambodia

48963 – Although station 48963 still displays positive biases of O-G at the station level, it was removed from the consolidated list because the number of reports (2) was insufficient for quality checking. (Figure 57)

48966 – Although station 48966 still displays positive biases of O-G at the station level, it was removed from the consolidated list because the number of reports (2) was insufficient for quality checking. (Figure 58)

4. Possible Causes of Remarkable and Sustained Biases

The following are possible causes of remarkable and sustained biases

a. The barometer used for observation is not correctly calibrated.

b. The latitude, longitude or altitude of the station in OSCAR/Surface has not been updated in a timely and appropriate manner. This could result in remarkable biases because it may cause incorrect calculated first-guess field values.

c. Biases are specific to the NWP model used in quality monitoring.

Note: Model biases are likely to appear in relatively large areas.

5. Technical Support

Any comments on the contents and the format of the report are welcome and could be sent to us.

Project Leader:

Shi Lijuan (Ms.), Qin Shiguang (Mr.)

Technical director:

Cui Xiai (Ms.)

Technical employee:

Dai Zhiying (Ms.), Guan Yunong (Ms.), Sun Hao (Mr.)

Tel: 86-010-58991513

E-mail: rwc-bj@cma.gov.cn

Regional WIGOS Centre, Beijing

Meteorological Observation Centre of China Meteorological Administration

6. Figures

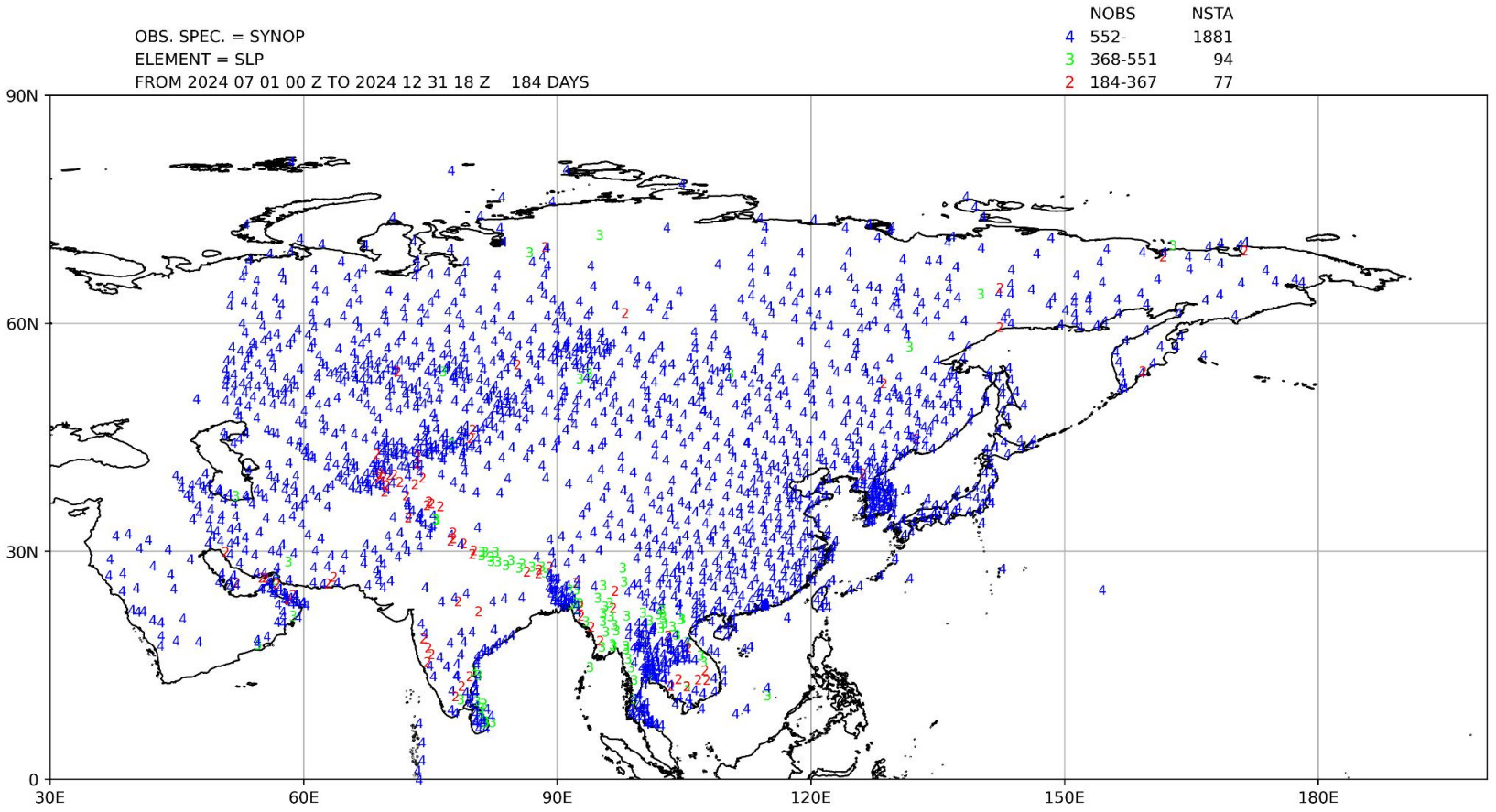

Figure 1(a) Location of all land surface stations reporting station level pressure (SLP) observations in Region II over the six-month period from July to December 2024. Numbers (2, 3, 4) show the total number of observations (NOBS) received at RWC-Beijing. The total numbers of stations (NSTA) reporting SLP are shown at the top of the figure. (Data availability)

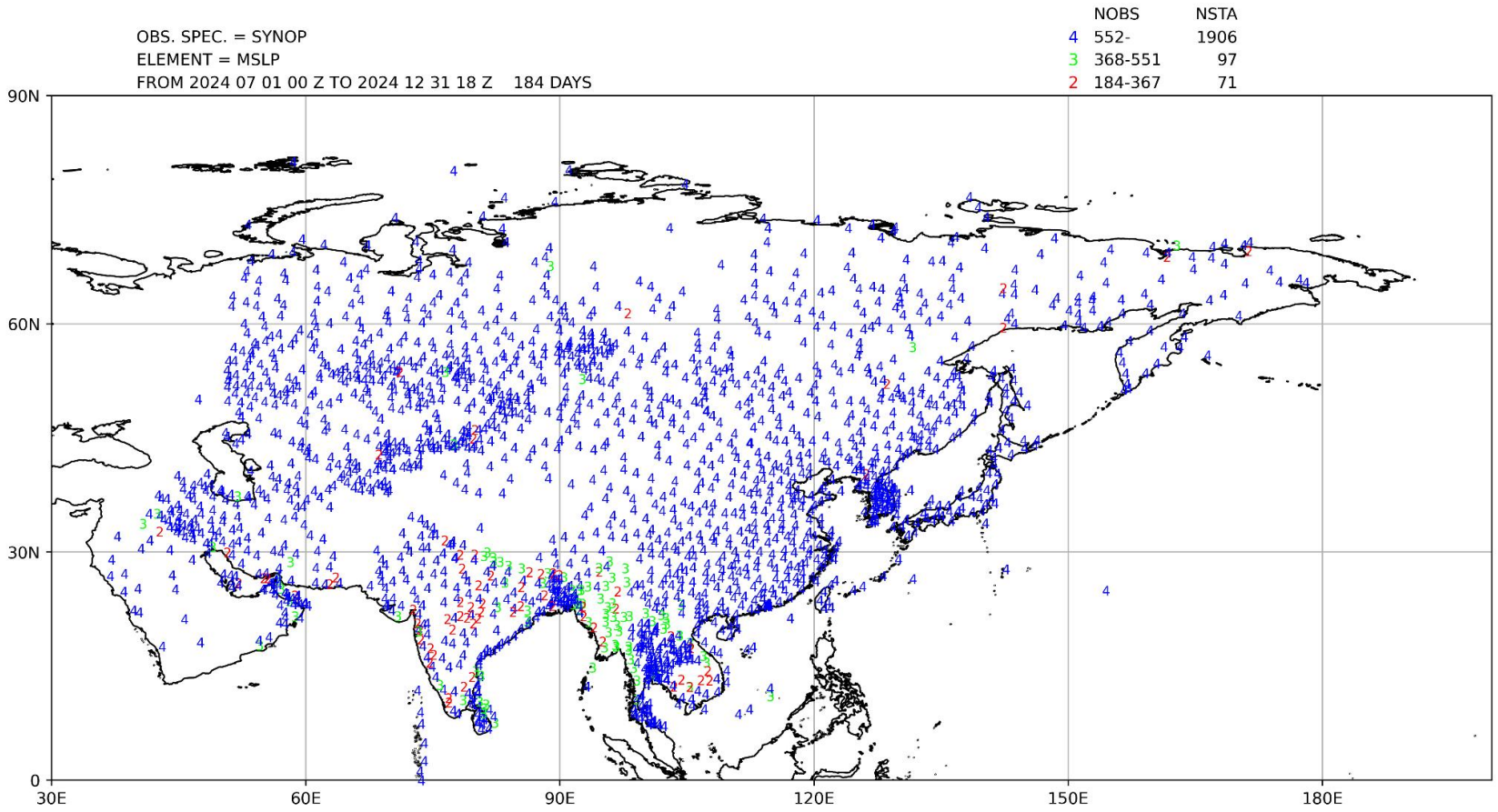

Figure 1(b) Location of all land surface stations reporting mean sea level pressure (MSLP) observations in Region II over the six-month period from July to December 2024. Numbers (2, 3, 4) show the total number of observations (NOBS) received at RWC-Beijing. The total numbers of stations (NSTA) reporting MSLP are shown at the top of the figure. (Data availability)

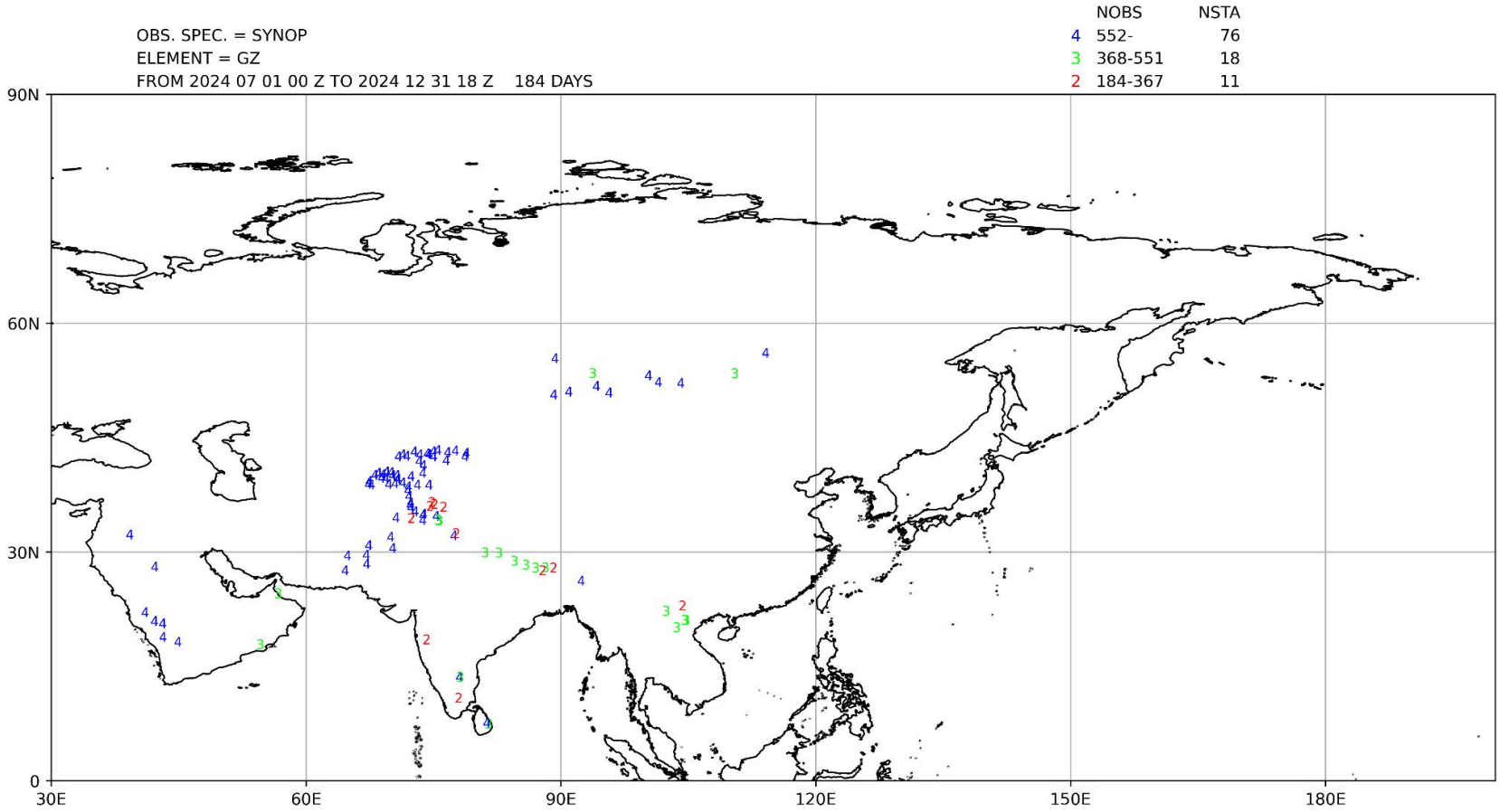

Figure 1(c) Location of all land surface stations reporting geopotential height (GZ) observations in Region II over the six-month period from July to December 2024. Numbers (2, 3, 4) show the total number of observations (NOBS) received at RWC-Beijing. The total numbers of stations (NSTA) reporting GZ are shown at the top of the figure. (Data availability)

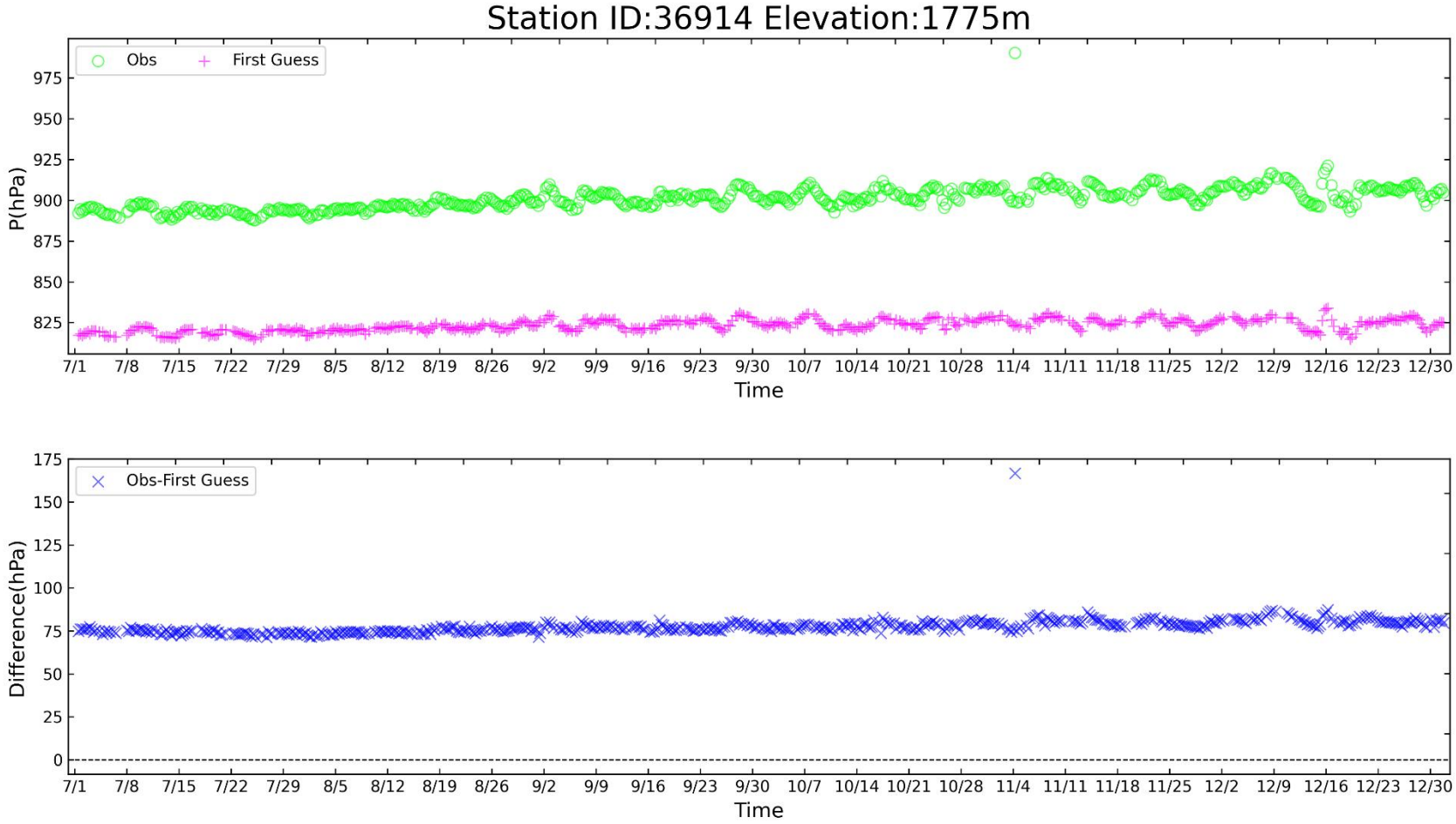

Figure 2 Time-series representation of SLP Obs minus FirstGuess for station 36914*

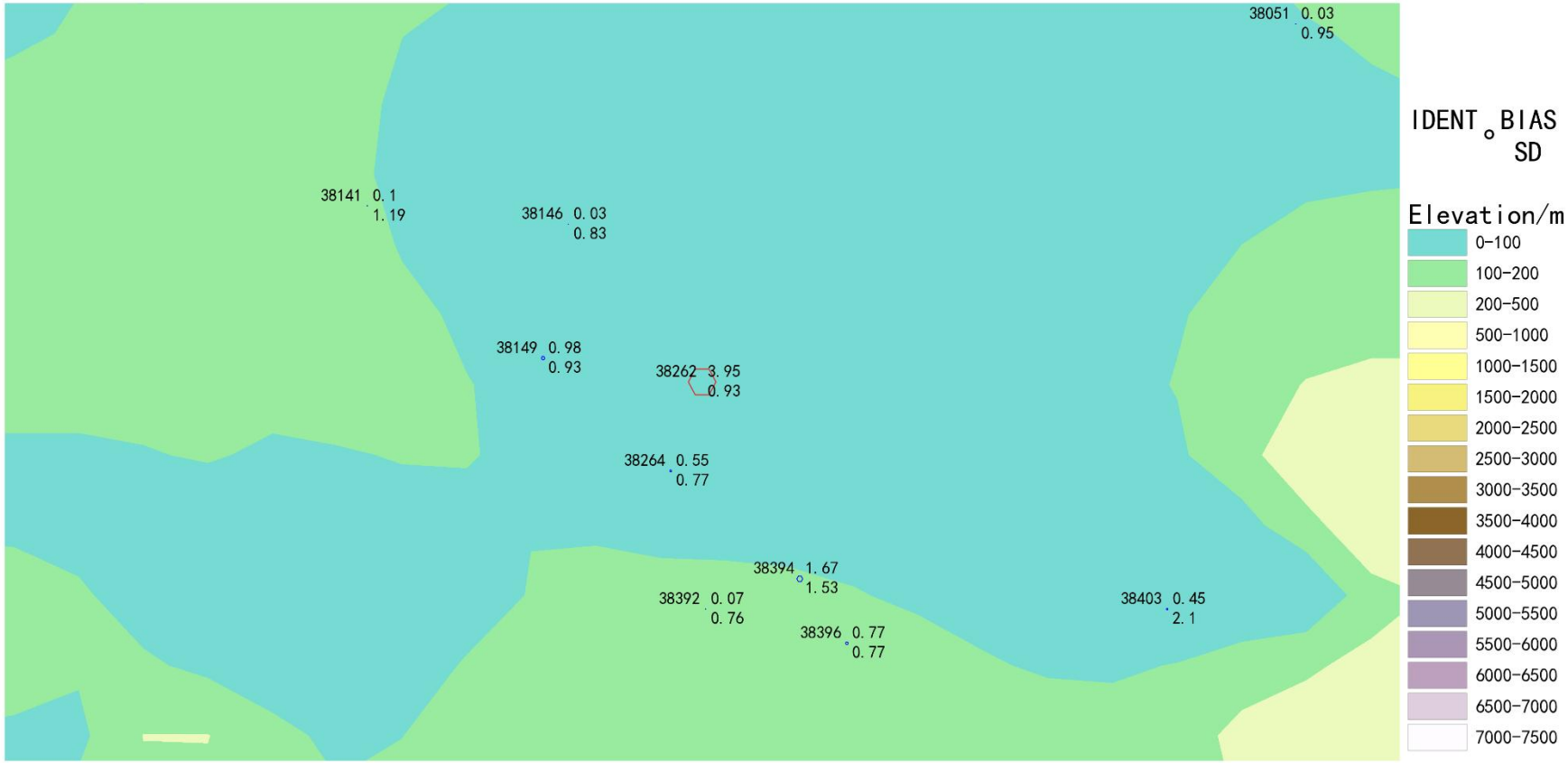

Figure 3 BIAS and SD of SLP for station 38262* (red) and surrounding stations (blue).

The number to the upper left of each symbol is the WMO IDENT, and those to the upper right are the values of BIAS and SD.

The size of each symbol is proportional to the value of BIAS, with hexagonal forms representing positive bias and triangular forms representing negative bias.

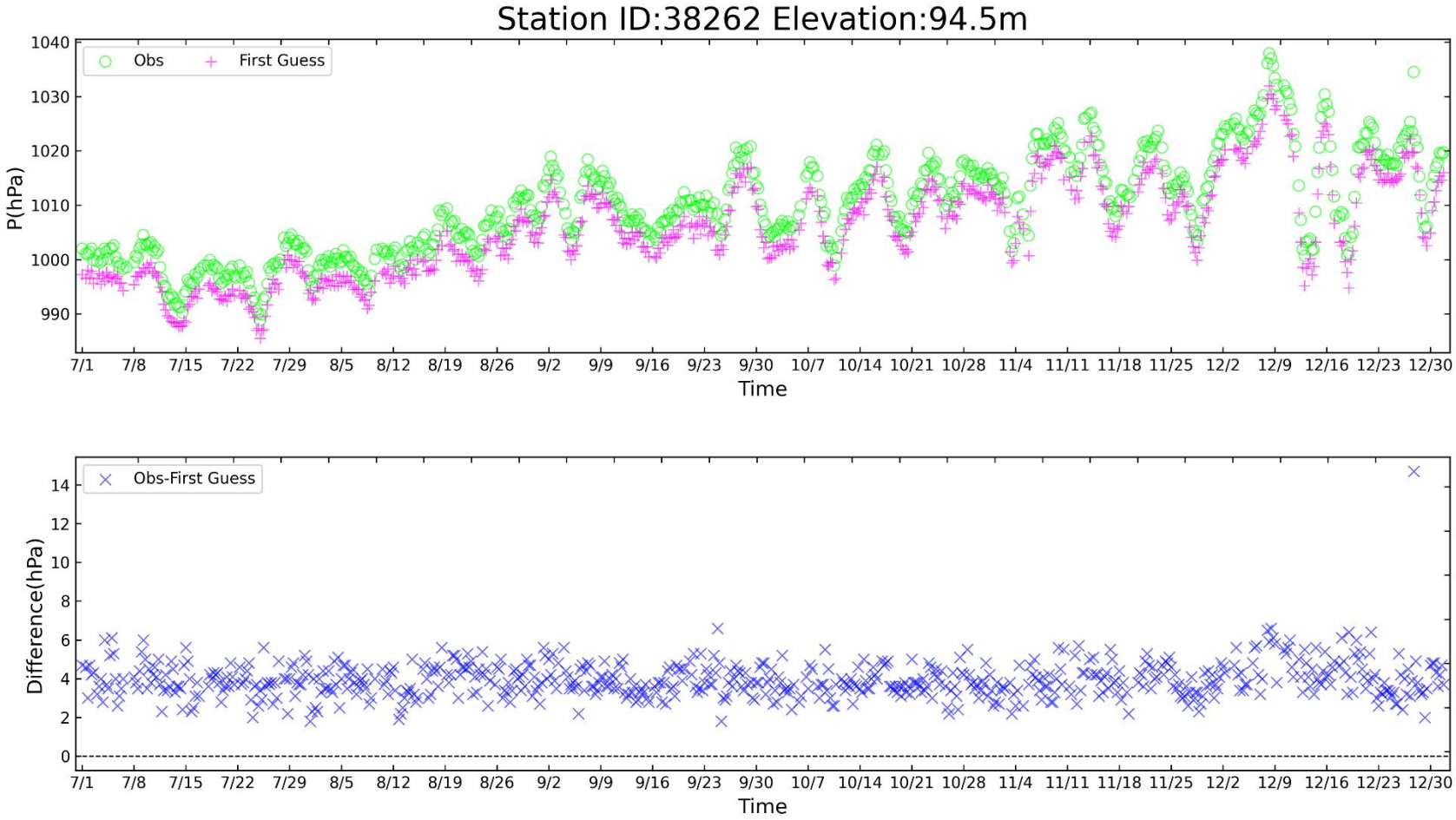

Figure 4 Time-series representation of SLP Obs minus FirstGuess for station 38262*

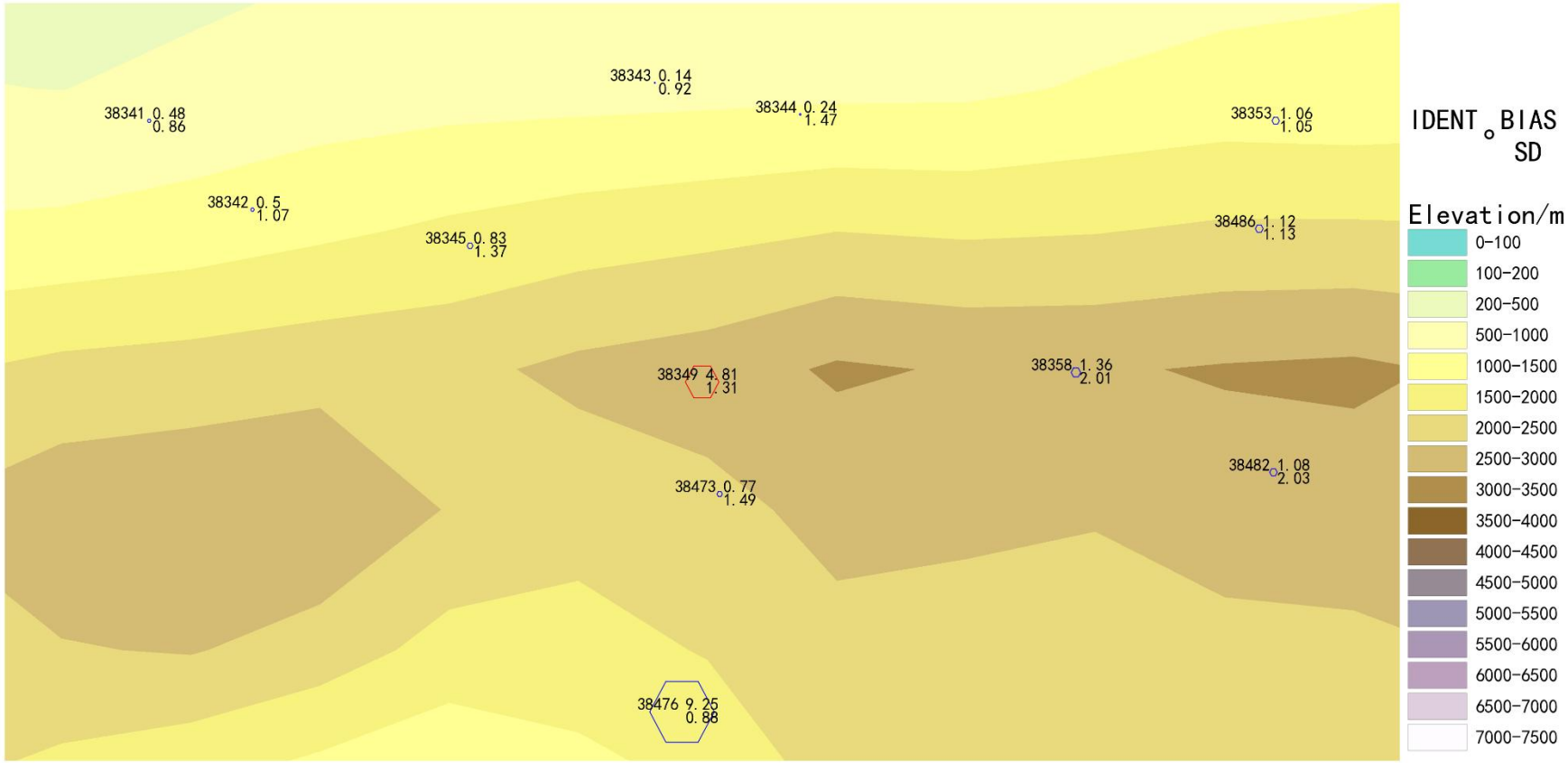

Figure 5 BIAS and SD of SLP for station 38349* (red) and surrounding stations (blue).

The number to the upper left of each symbol is the WMO IDENT, and those to the upper right are the values of BIAS and SD.

The size of each symbol is proportional to the value of BIAS, with hexagonal forms representing positive bias and triangular forms representing negative bias.

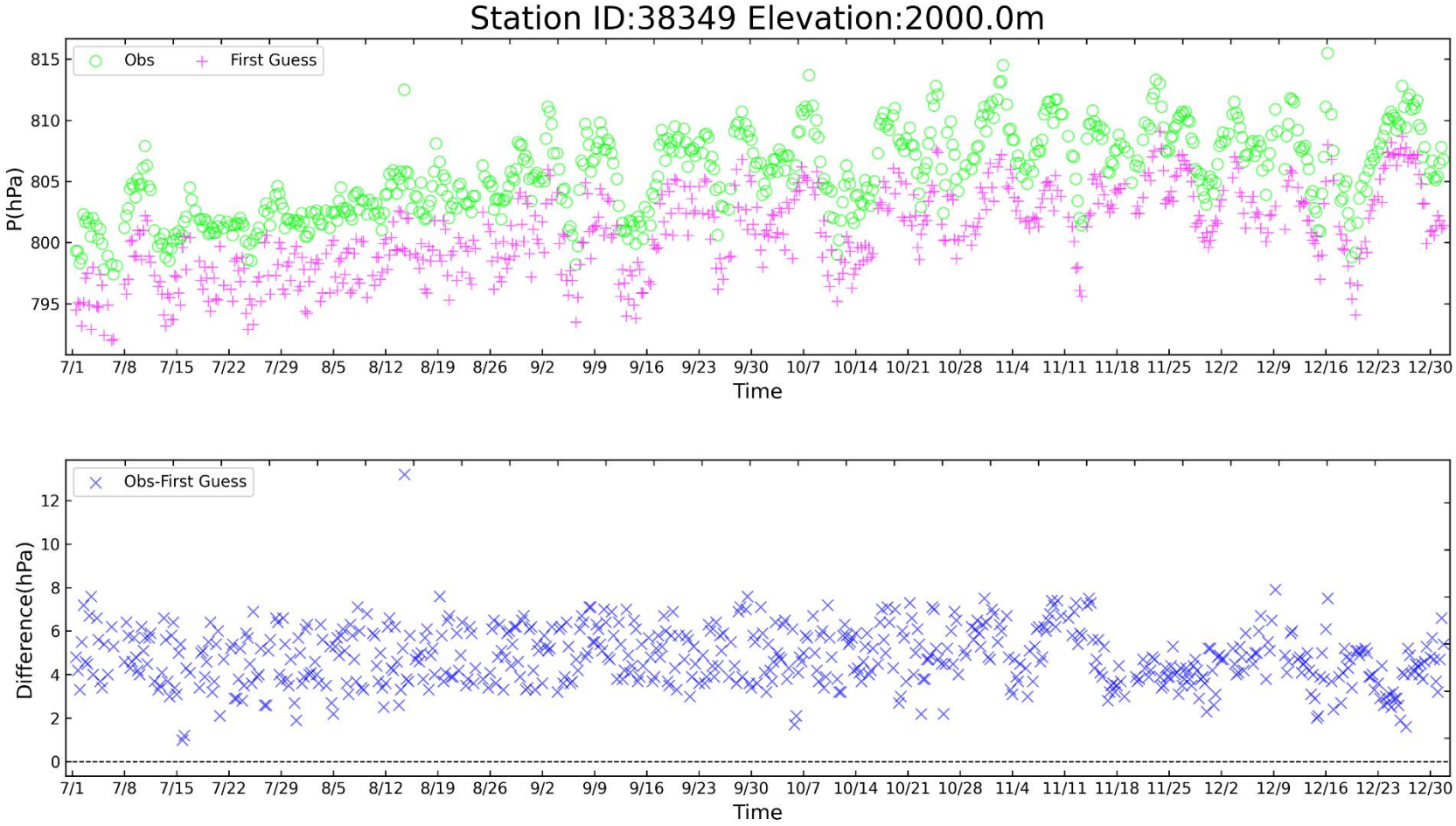

Figure 6 Time-series representation of SLP Obs minus FirstGuess for station 38349*

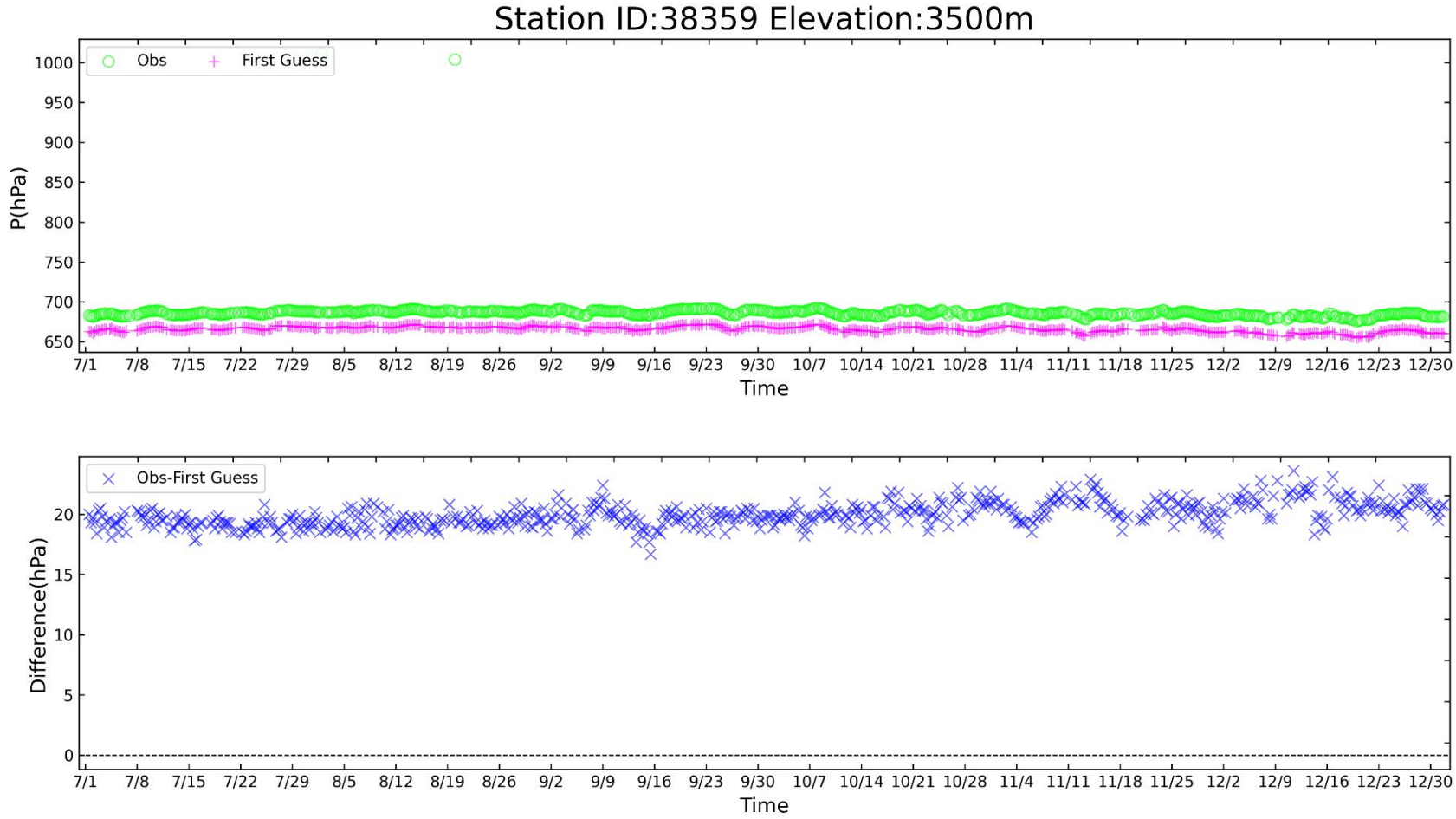

Figure 7 Time-series representation of SLP Obs minus FirstGuess for station 38359*

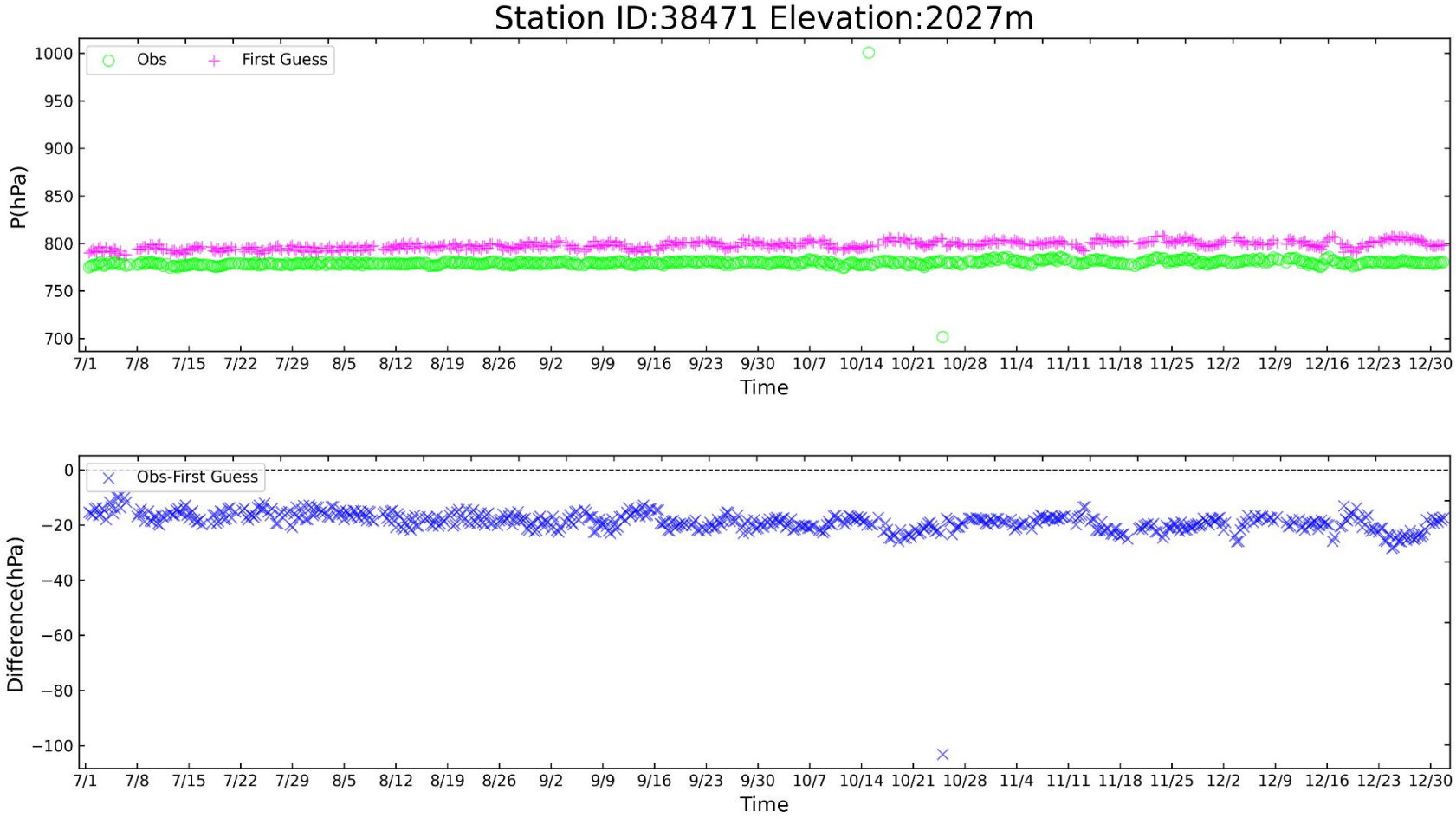

Figure 8 Time-series representation of SLP Obs minus FirstGuess for station 38471*

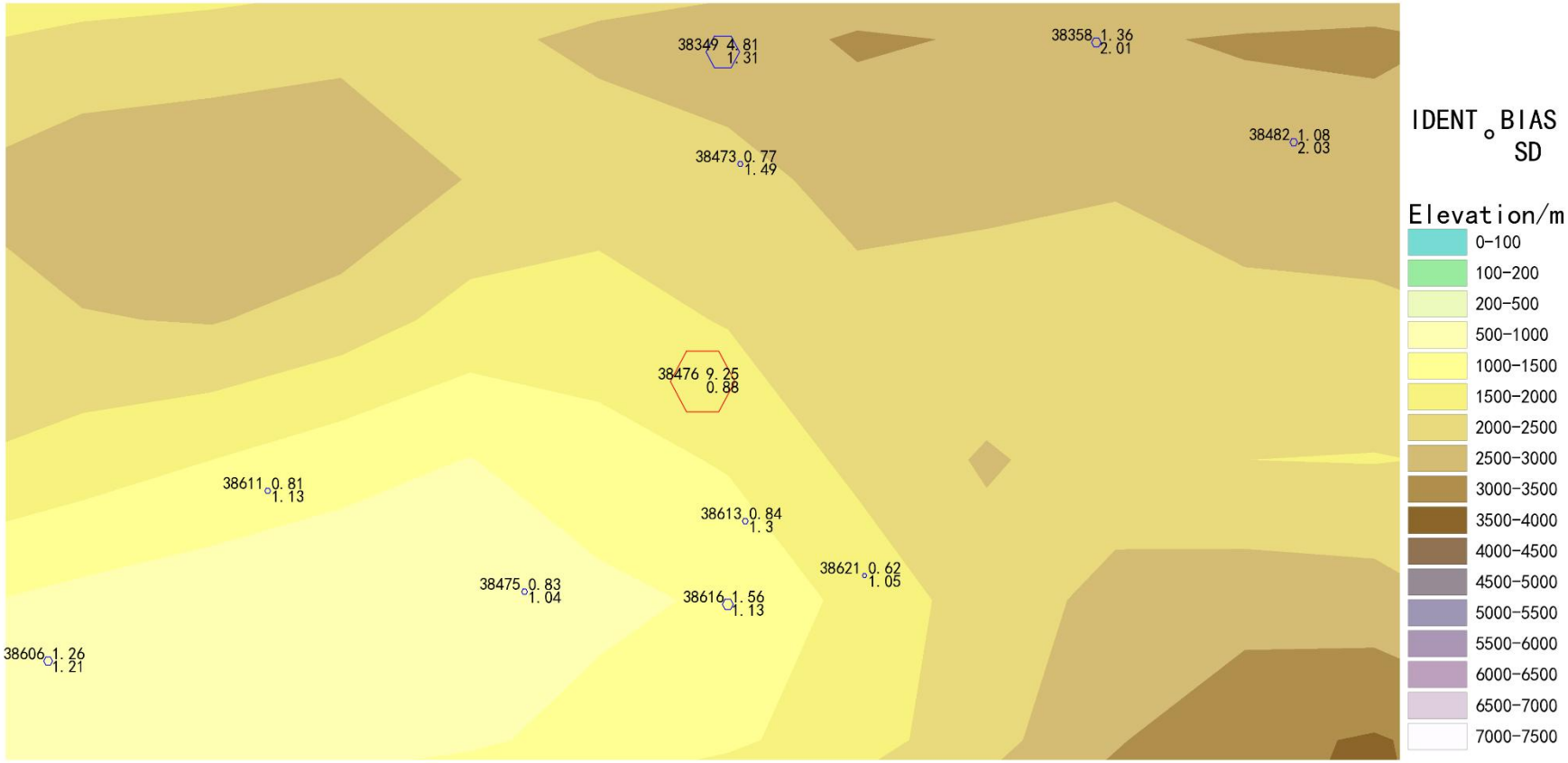

Figure 9 BIAS and SD of SLP for station 38476* (red) and surrounding stations (blue).

The number to the upper left of each symbol is the WMO IDENT, and those to the upper right are the values of BIAS and SD.

The size of each symbol is proportional to the value of BIAS, with hexagonal forms representing positive bias and triangular forms representing negative bias.

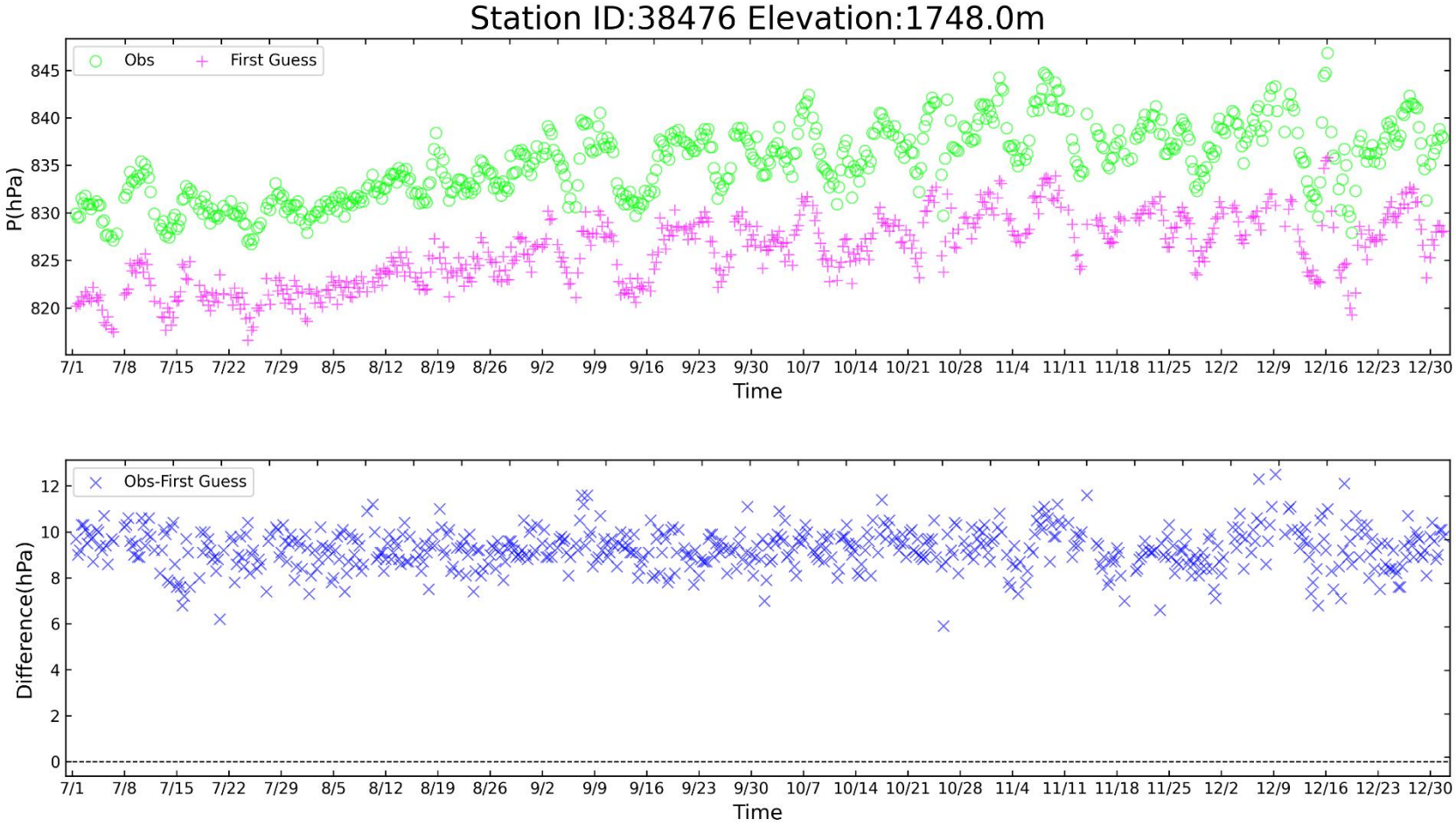

Figure 10 Time-series representation of SLP Obs minus FirstGuess for station 38476*

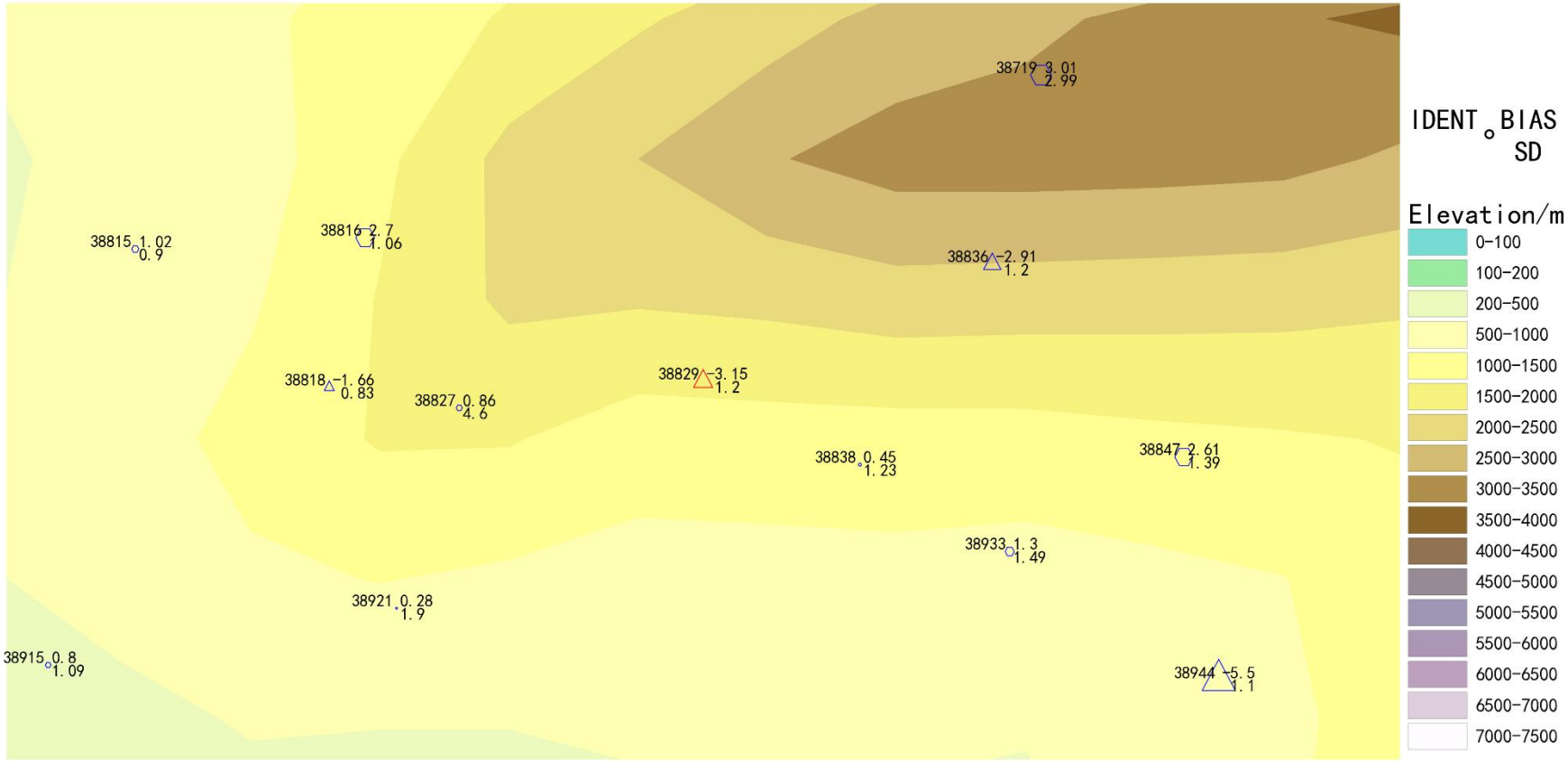

Figure 11 BIAS and SD of SLP for station 38829 (red) and surrounding stations (blue).

The number to the upper left of each symbol is the WMO IDENT, and those to the upper right are the values of BIAS and SD.

The size of each symbol is proportional to the value of BIAS, with hexagonal forms representing positive bias and triangular forms representing negative bias.

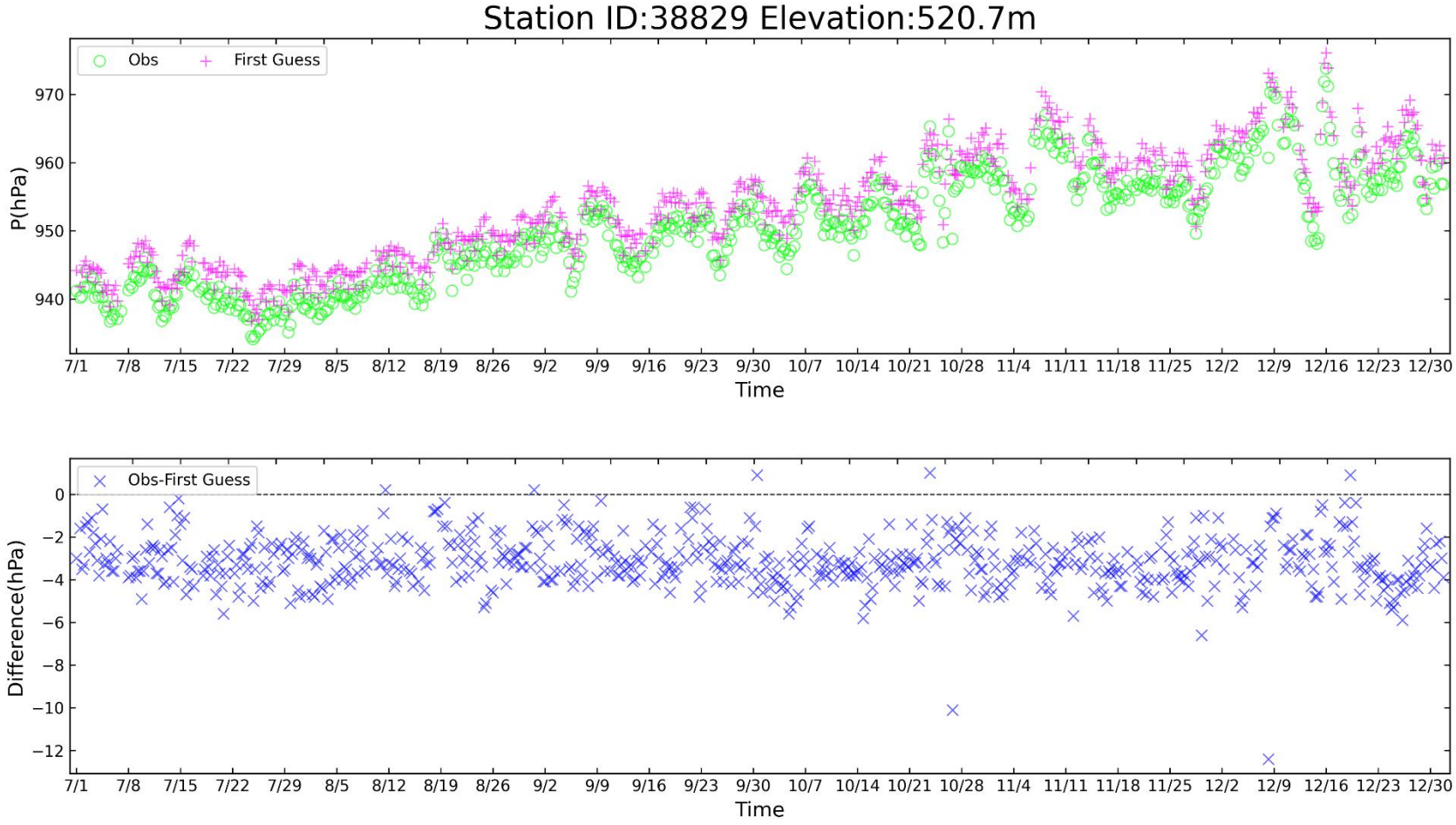

Figure 12 Time-series representation of SLP Obs minus FirstGuess for station 38829

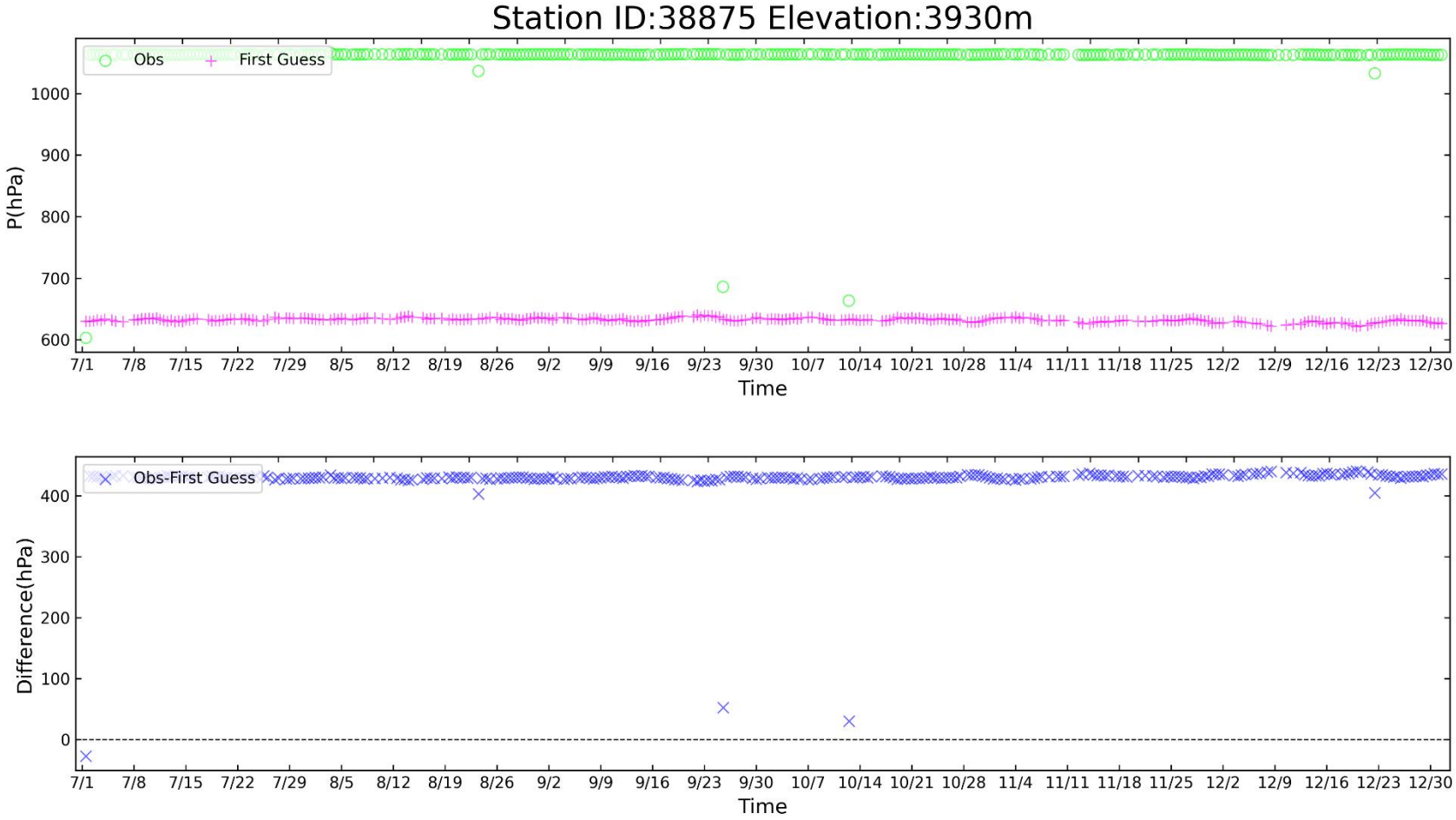

Figure 13 Time-series representation of SLP Obs minus FirstGuess for station 38875

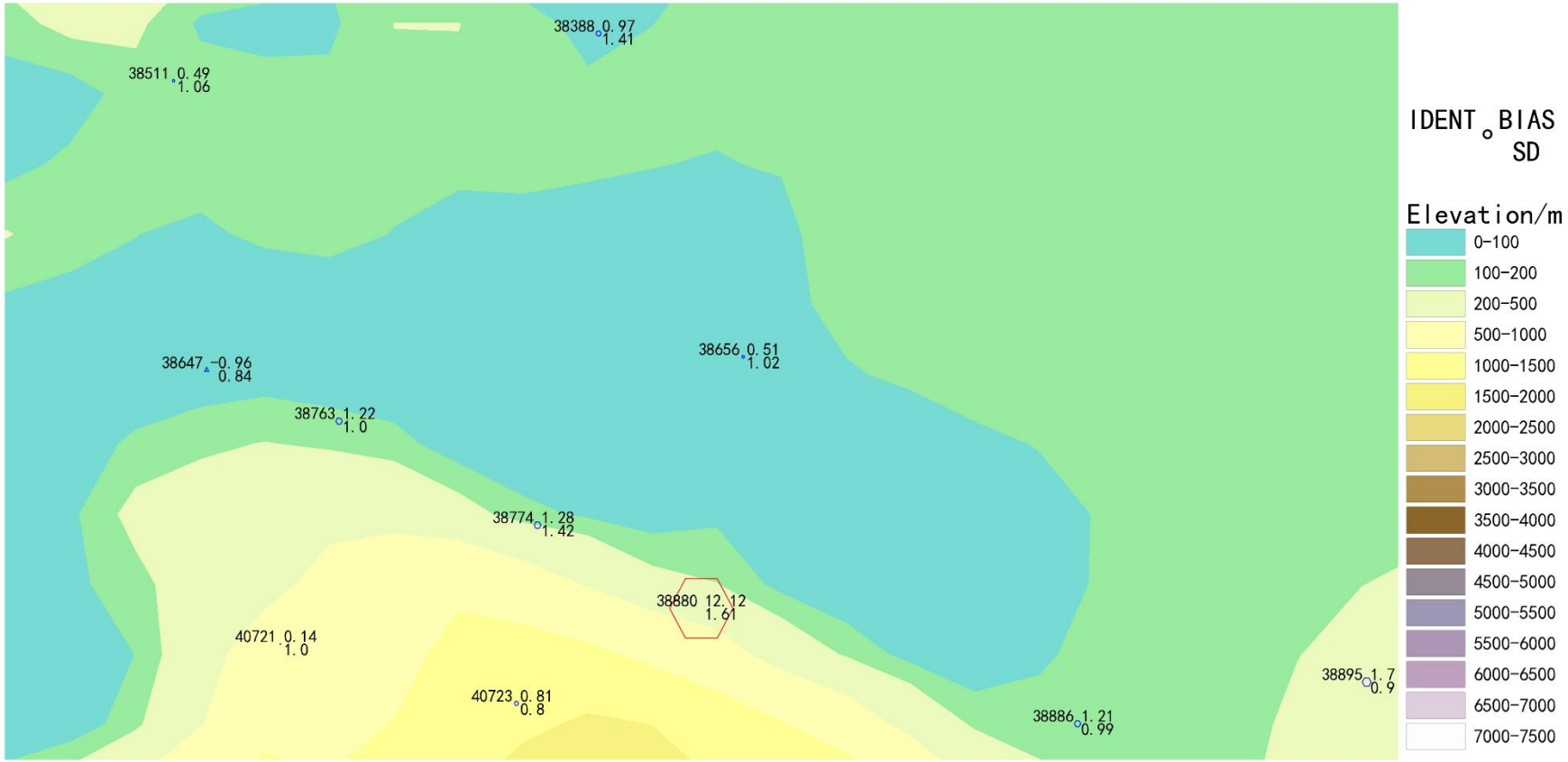

Figure 14 BIAS and SD of SLP for station 38880* (red) and surrounding stations (blue).

The number to the upper left of each symbol is the WMO IDENT, and those to the upper right are the values of BIAS and SD.

The size of each symbol is proportional to the value of BIAS, with hexagonal forms representing positive bias and triangular forms representing negative bias.

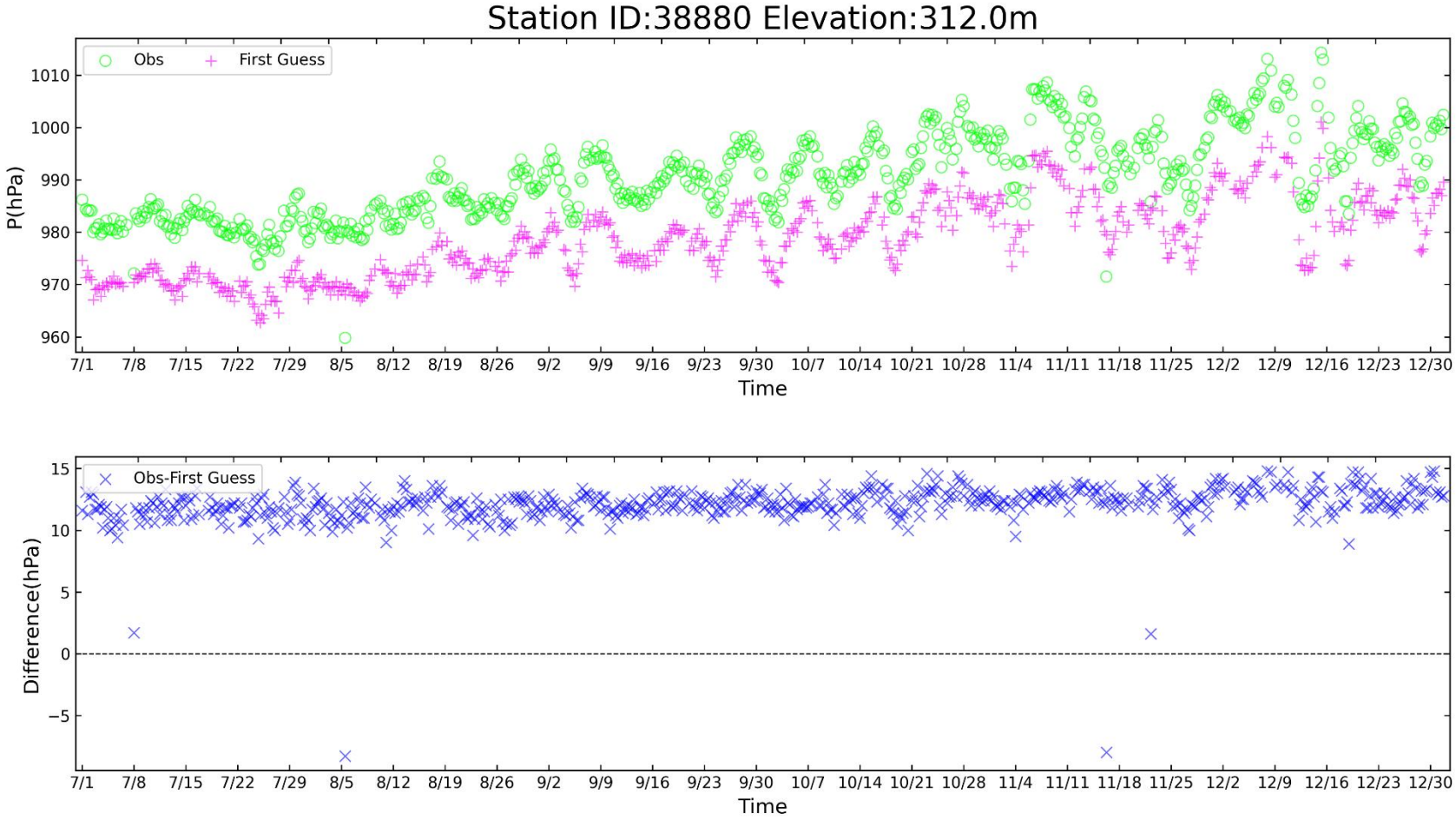

Figure 15 Time-series representation of SLP Obs minus FirstGuess for station 38880*

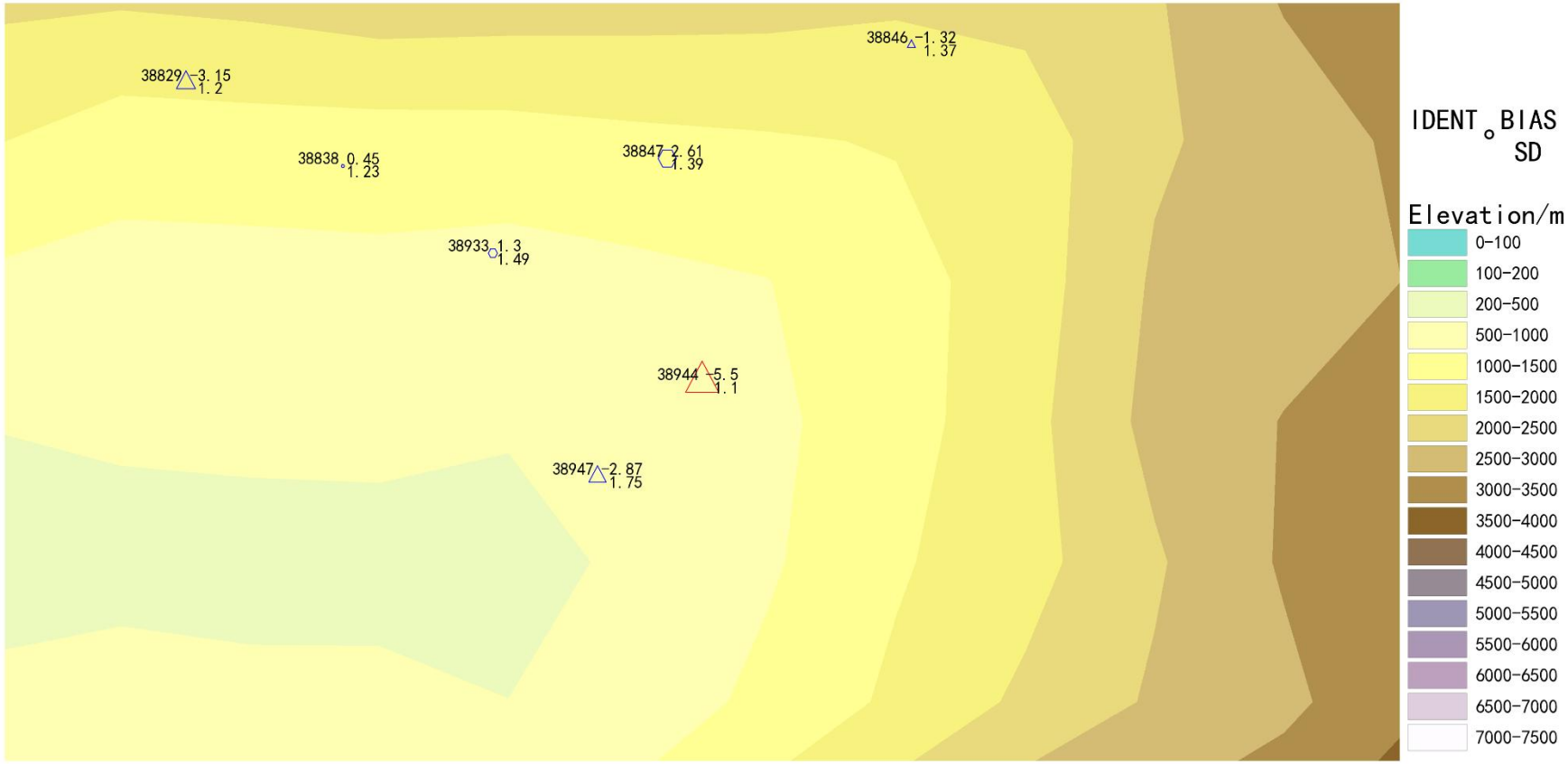

Figure 16 BIAS and SD of SLP for station 38944* (red) and surrounding stations (blue).

The number to the upper left of each symbol is the WMO IDENT, and those to the upper right are the values of BIAS and SD.

The size of each symbol is proportional to the value of BIAS, with hexagonal forms representing positive bias and triangular forms representing negative bias.

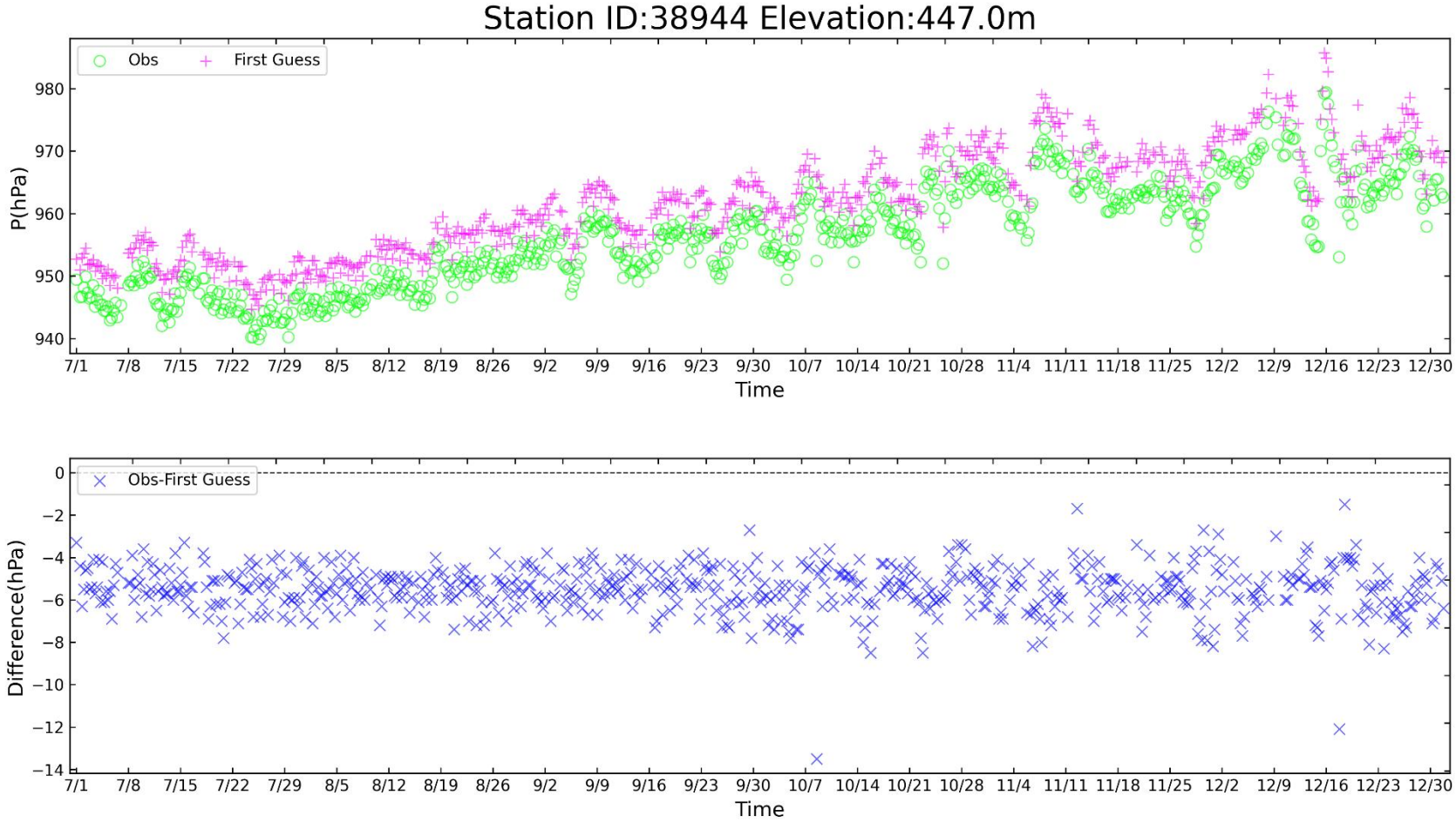

Figure 17 Time-series representation of SLP Obs minus FirstGuess for station 38944*

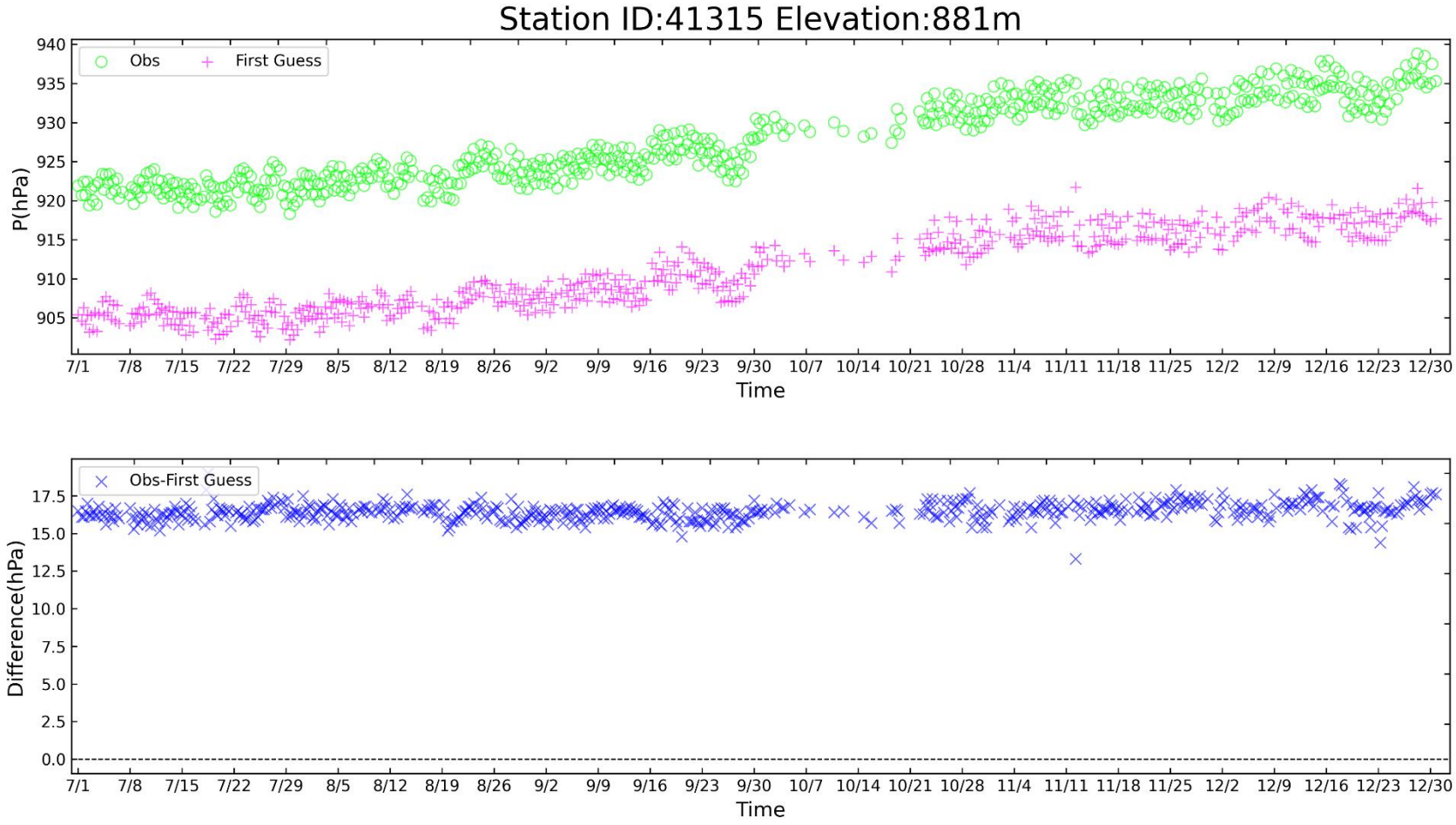

Figure 18 Time-series representation of SLP Obs minus FirstGuess for station 41315*

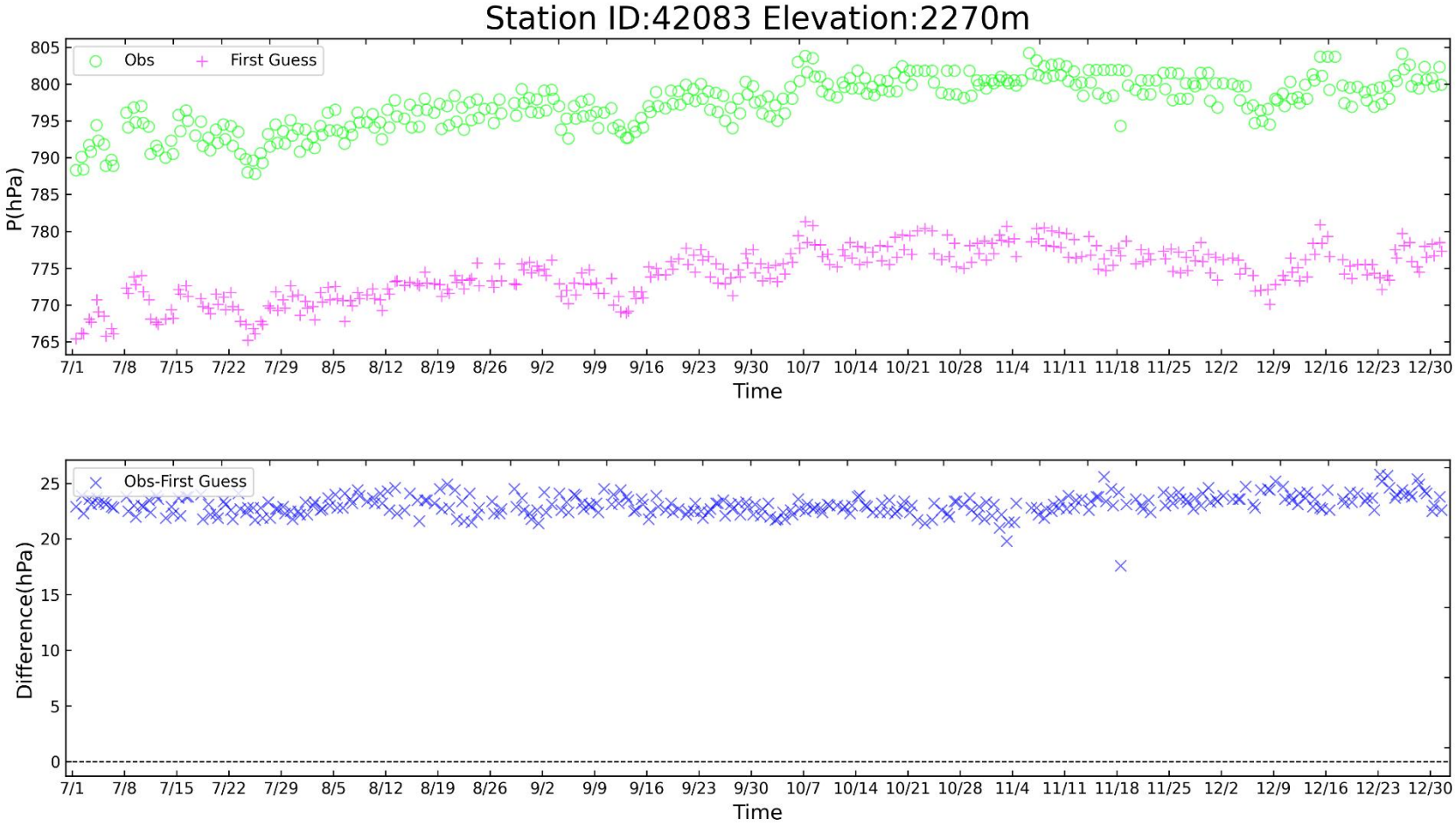

Figure 19 Time-series representation of SLP Obs minus FirstGuess for station 42083

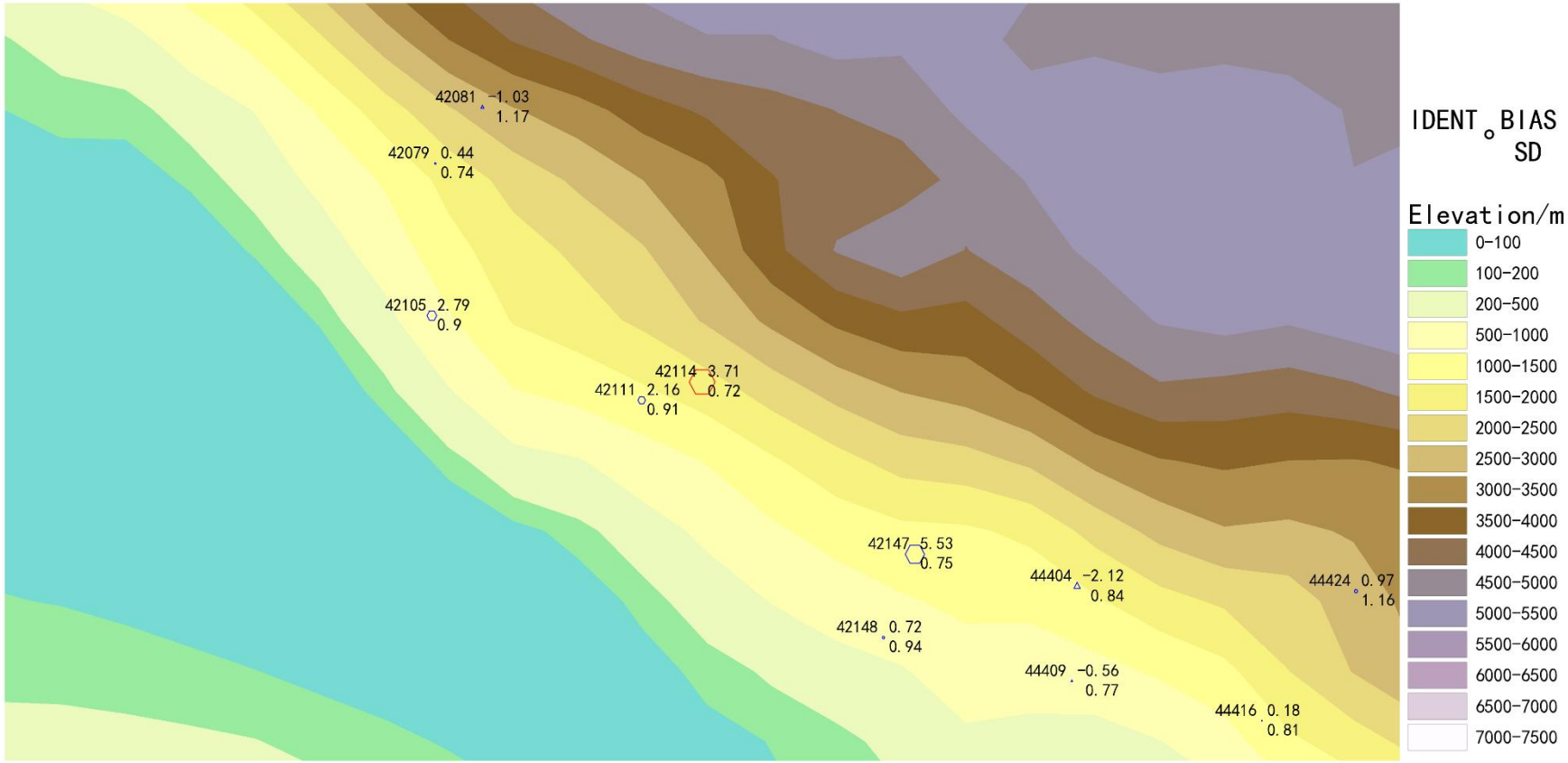

Figure 20 BIAS and SD of SLP for station 42114 (red) and surrounding stations (blue).

The number to the upper left of each symbol is the WMO IDENT, and those to the upper right are the values of BIAS and SD.

The size of each symbol is proportional to the value of BIAS, with hexagonal forms representing positive bias and triangular forms representing negative bias.

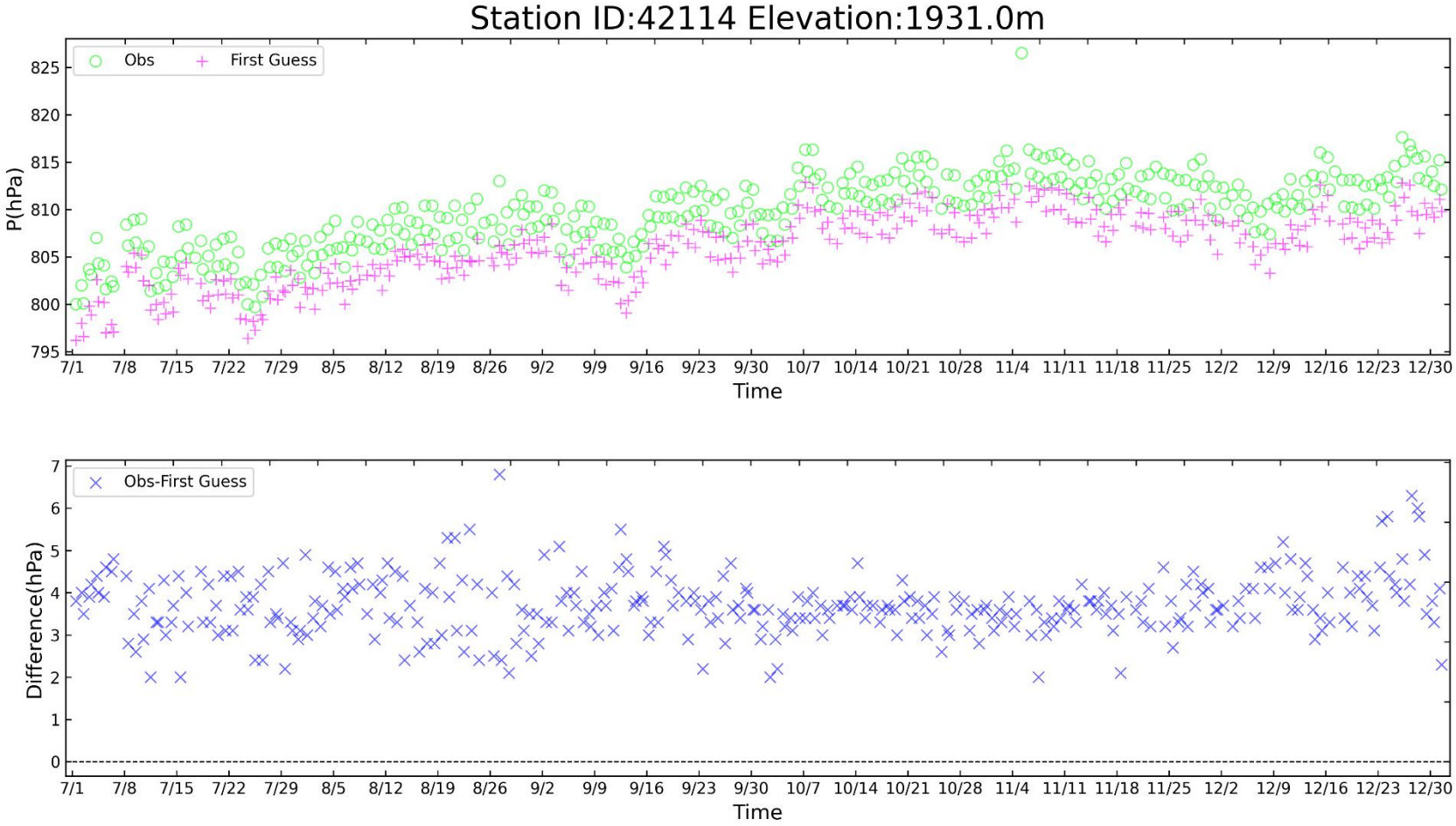

Figure 21 Time-series representation of SLP Obs minus FirstGuess for station 42114

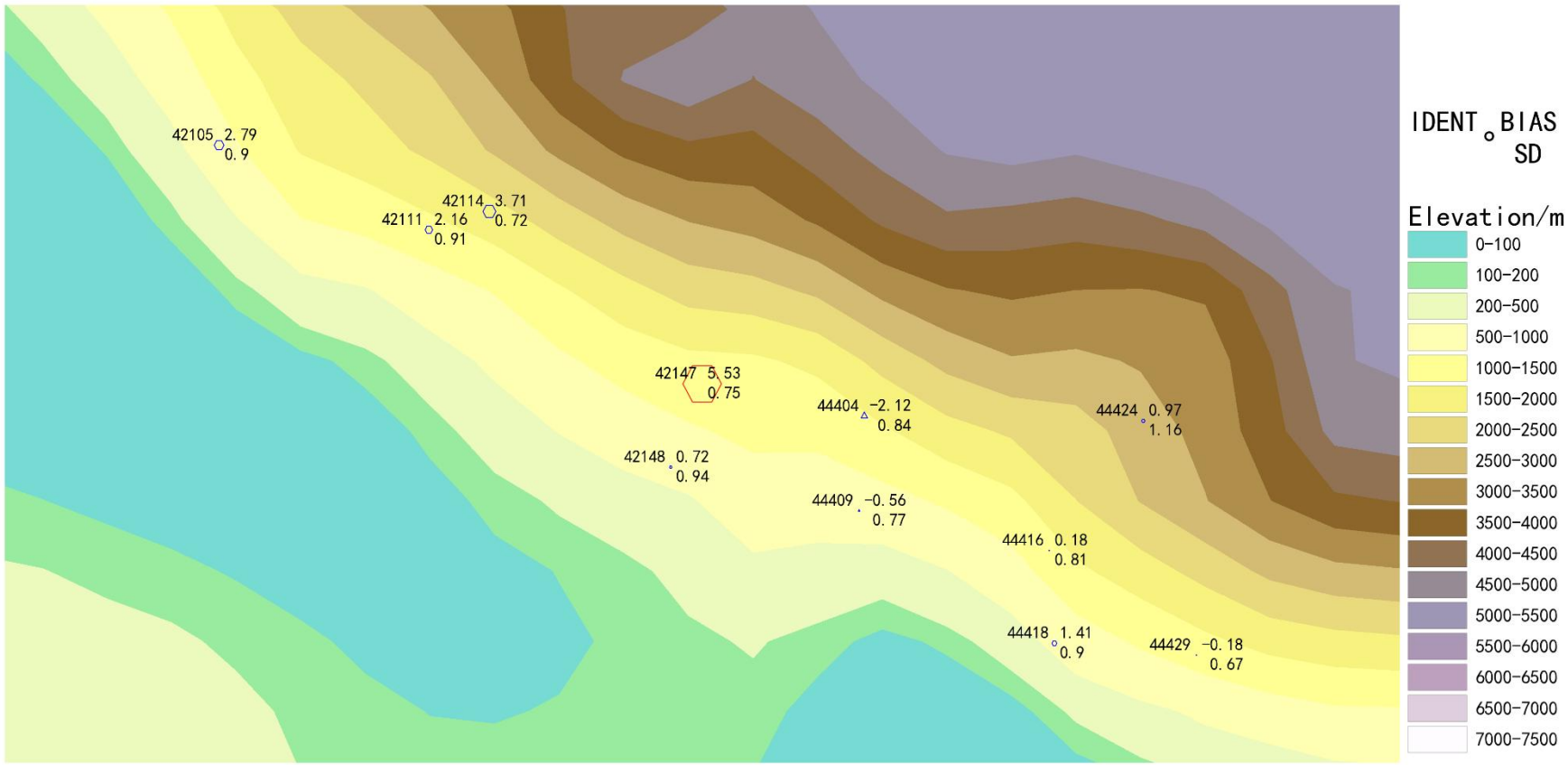

Figure 22 BIAS and SD of SLP for station 42147 (red) and surrounding stations (blue).

The number to the upper left of each symbol is the WMO IDENT, and those to the upper right are the values of BIAS and SD.

The size of each symbol is proportional to the value of BIAS, with hexagonal forms representing positive bias and triangular forms representing negative bias.

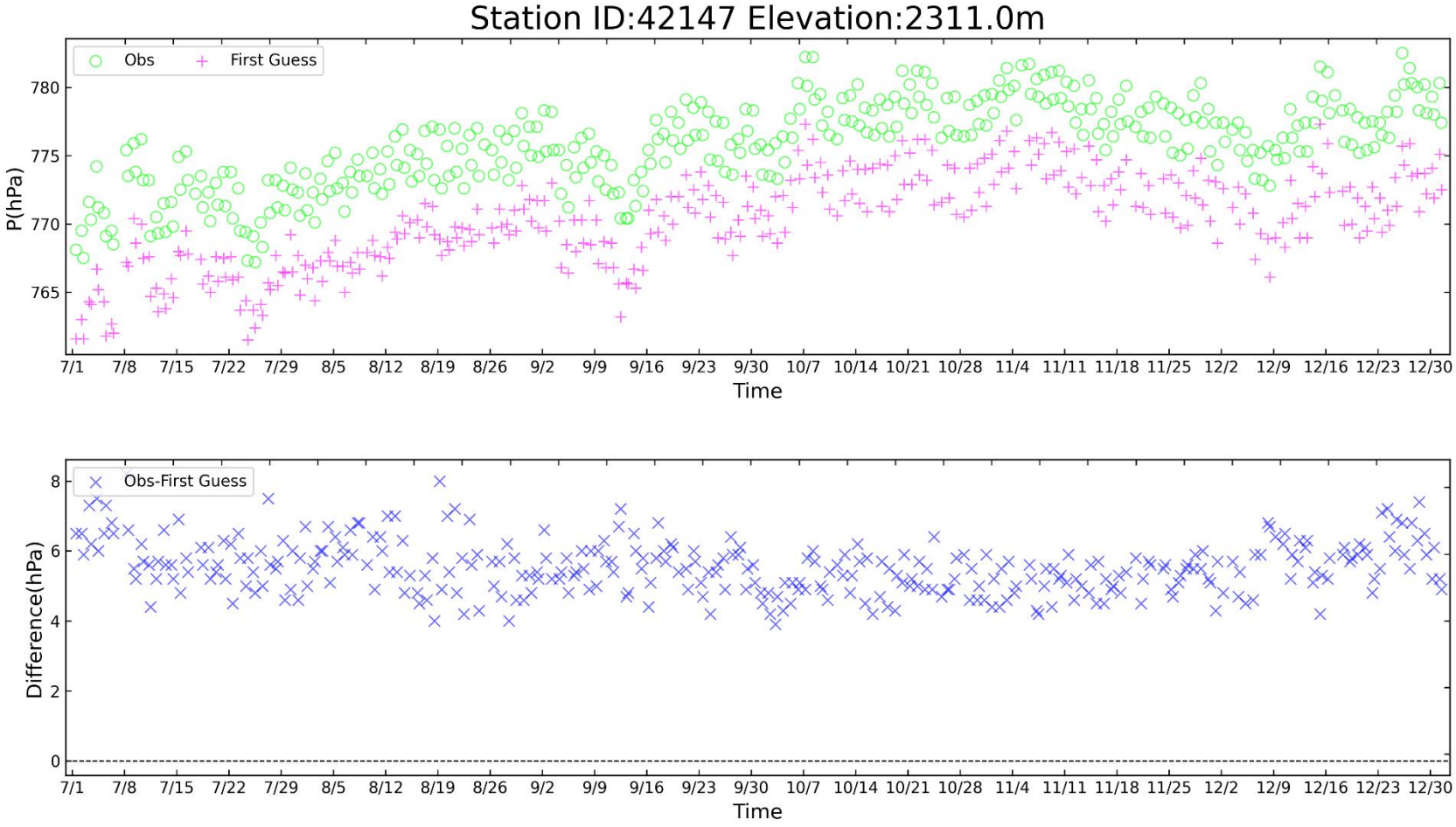

Figure 23 Time-series representation of SLP Obs minus FirstGuess for station 42147

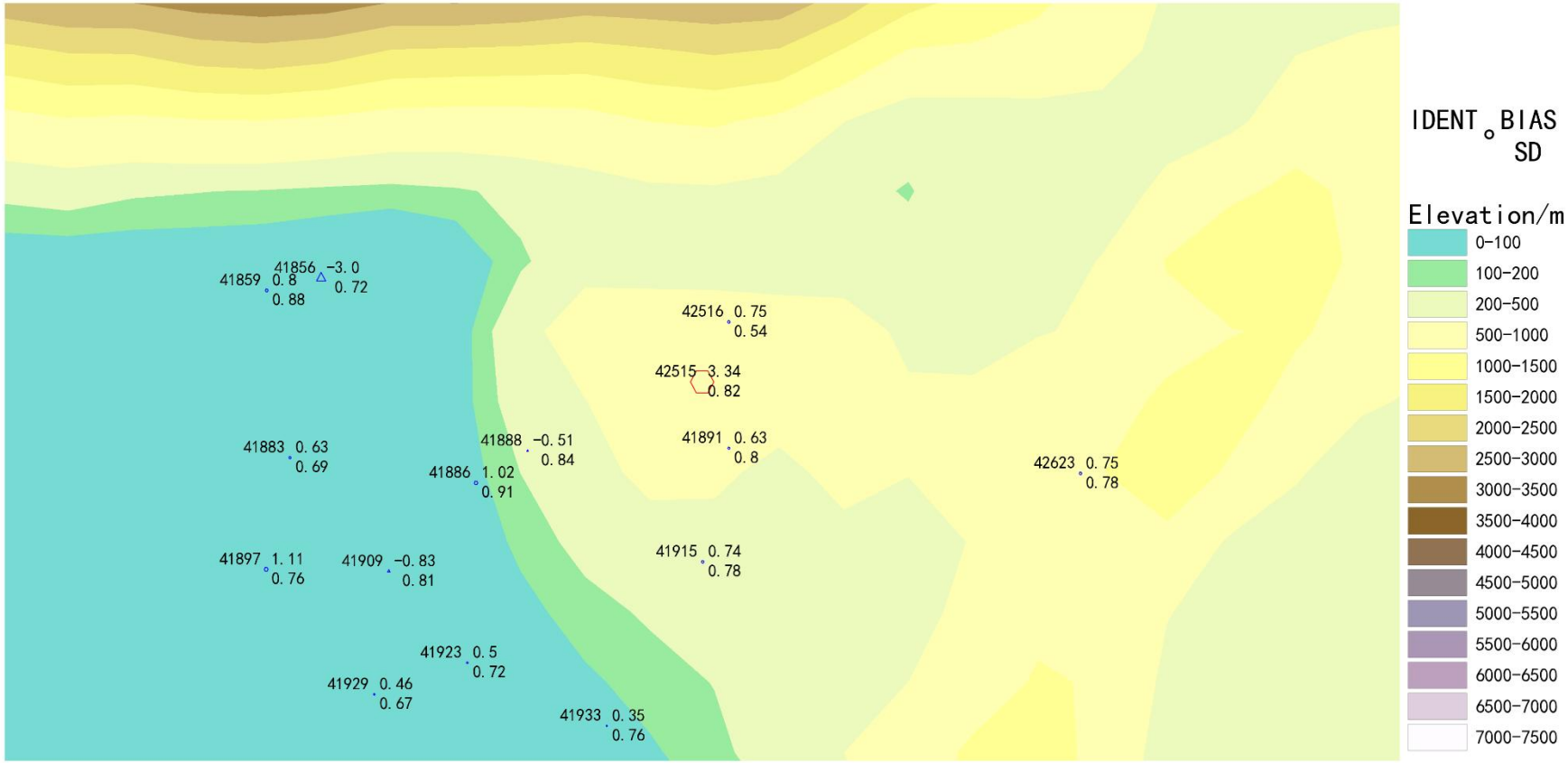

Figure 24 BIAS and SD of SLP for station 42515 (red) and surrounding stations (blue).

The number to the upper left of each symbol is the WMO IDENT, and those to the upper right are the values of BIAS and SD.

The size of each symbol is proportional to the value of BIAS, with hexagonal forms representing positive bias and triangular forms representing negative bias.

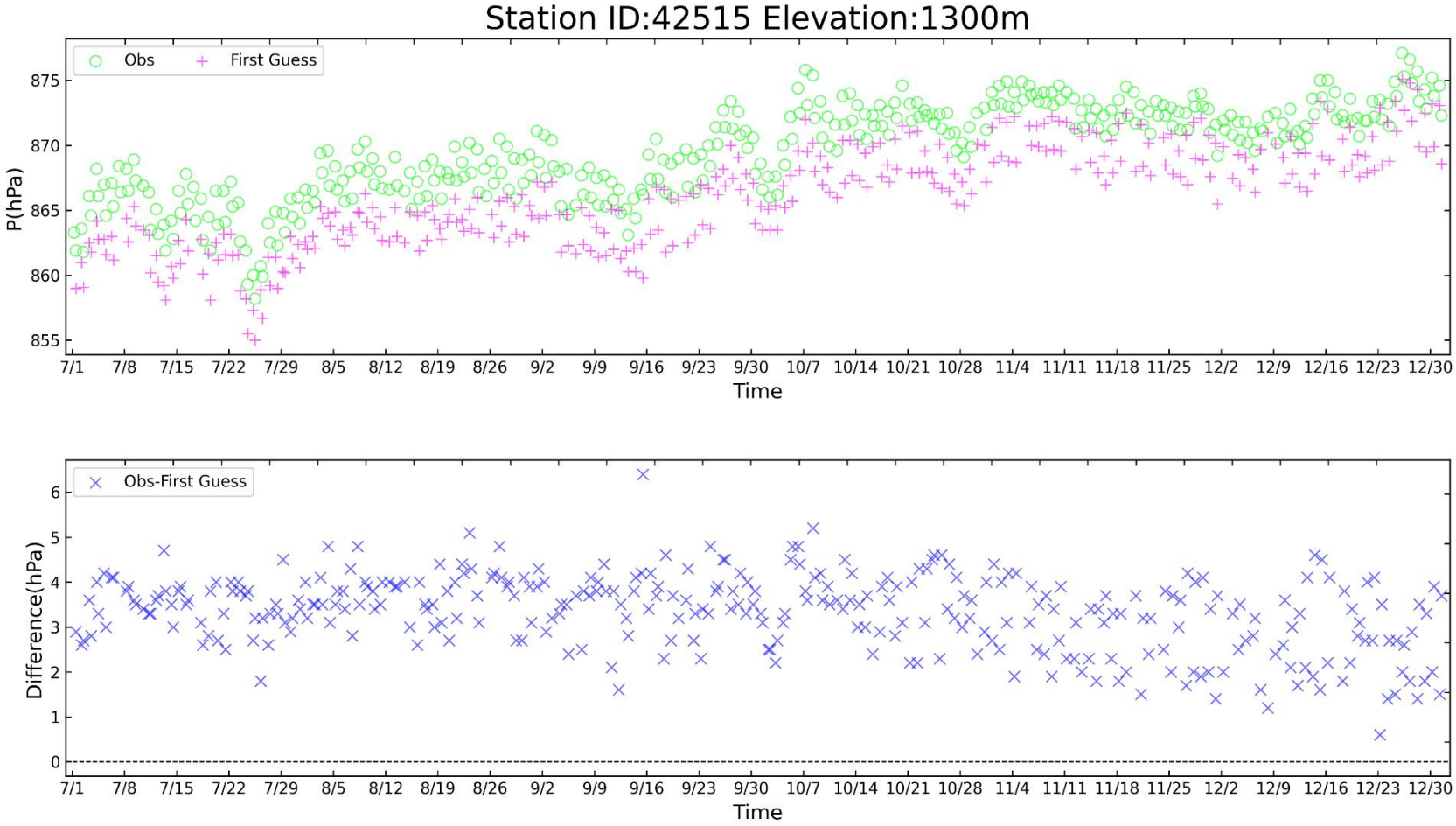

Figure 25 Time-series representation of SLP Obs minus FirstGuess for station 42515

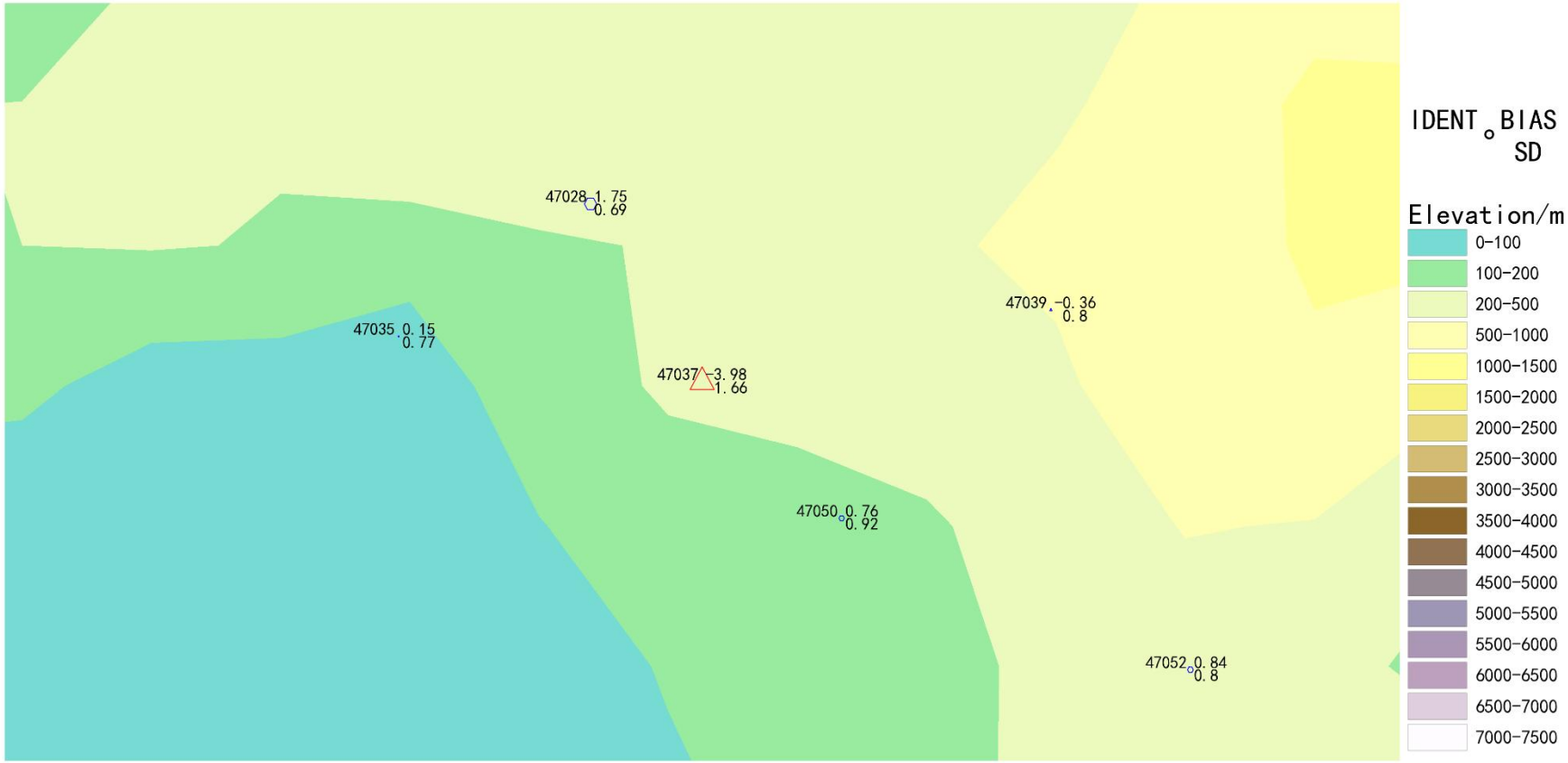

Figure 26 BIAS and SD of SLP for station 47037* (red) and surrounding stations (blue).
The number to the upper left of each symbol is the WMO IDENT, and those to the upper right are the values of BIAS and SD.
The size of each symbol is proportional to the value of BIAS, with hexagonal forms representing positive bias and triangular forms representing negative bias.

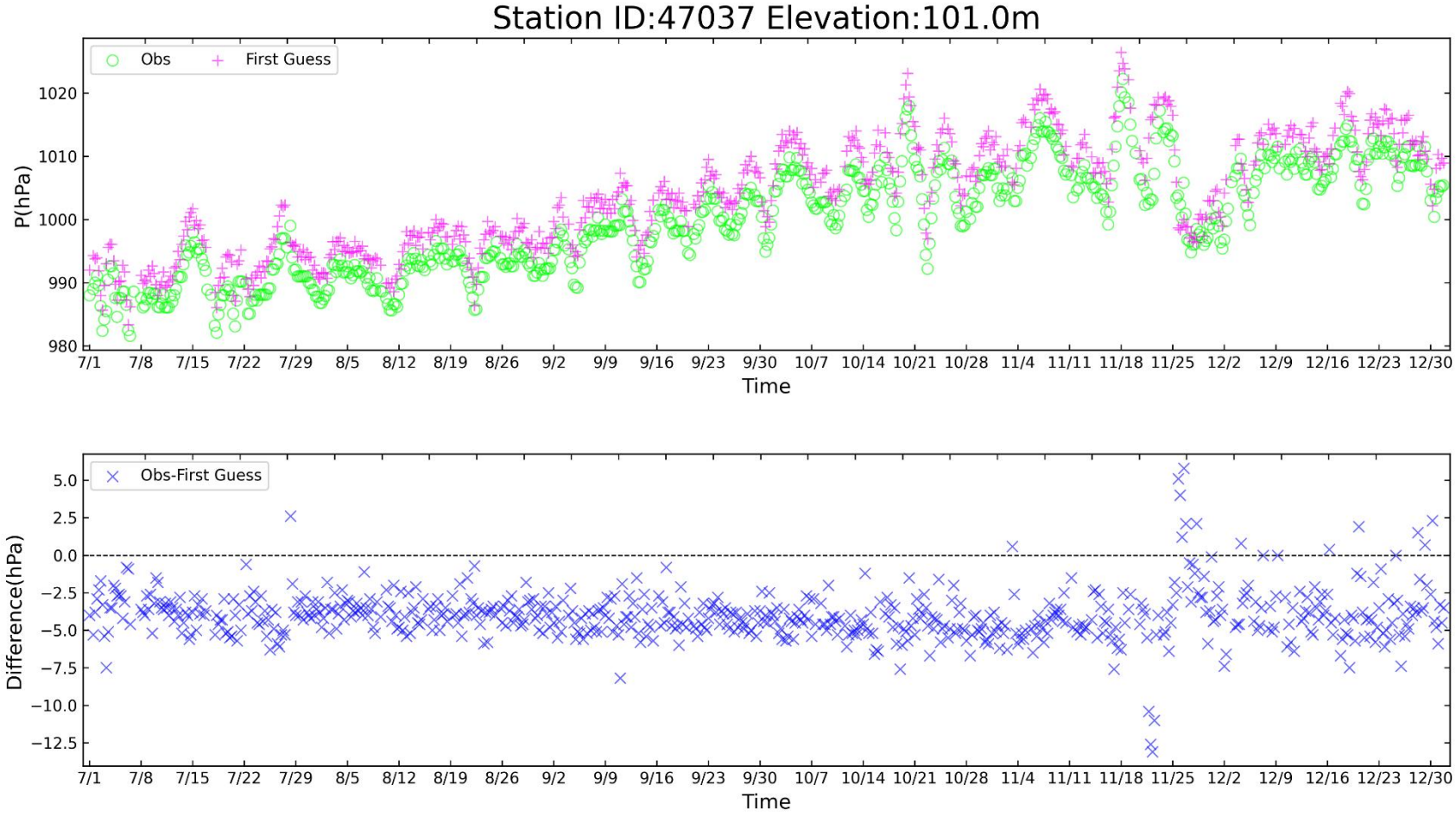

Figure 27 Time-series representation of SLP Obs minus FirstGuess for station 47037*

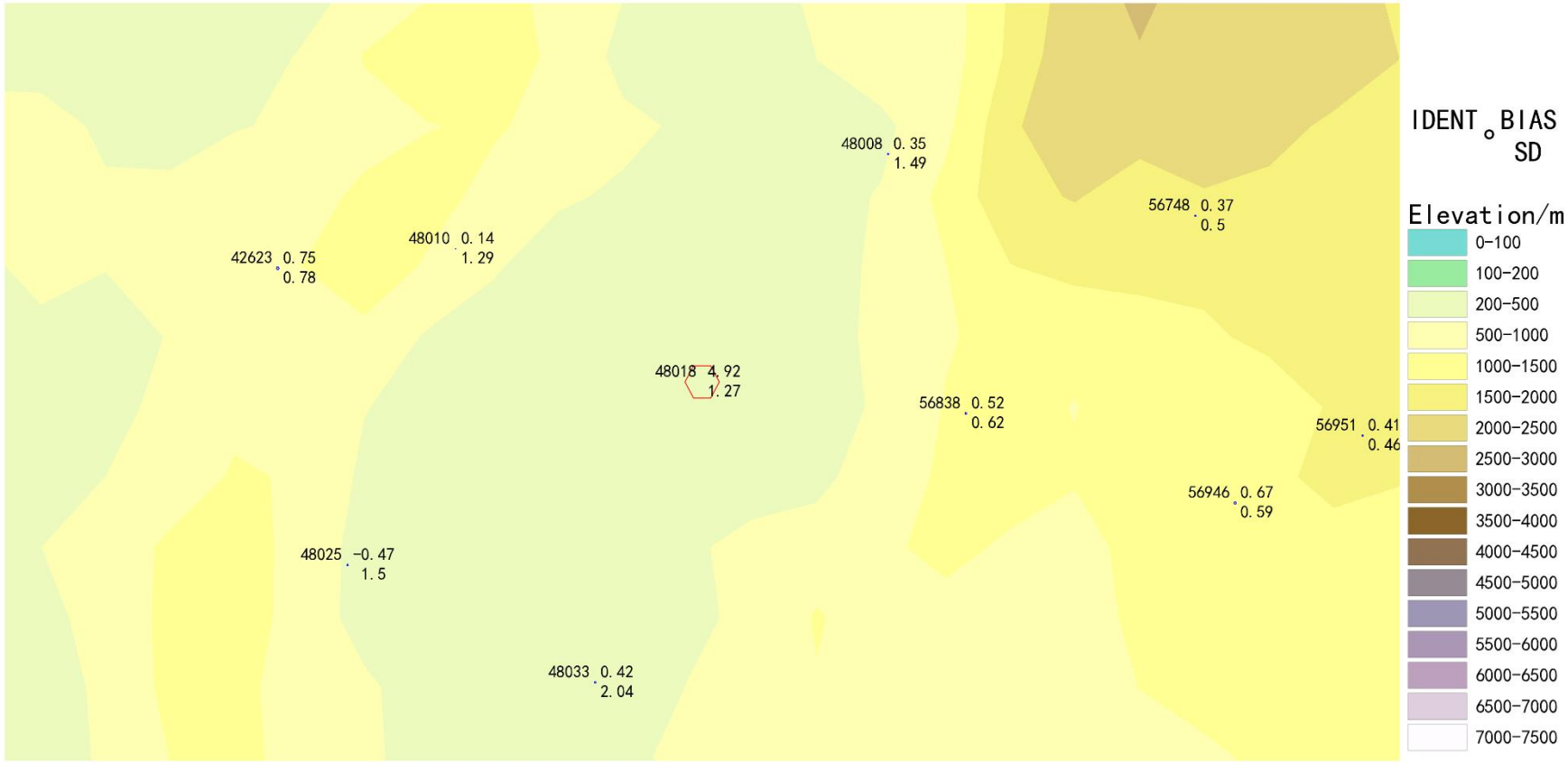

Figure 28 BIAS and SD of SLP for station 48018* (red) and surrounding stations (blue).
The number to the upper left of each symbol is the WMO IDENT, and those to the upper right are the values of BIAS and SD.
The size of each symbol is proportional to the value of BIAS, with hexagonal forms representing positive bias and triangular forms representing negative bias.

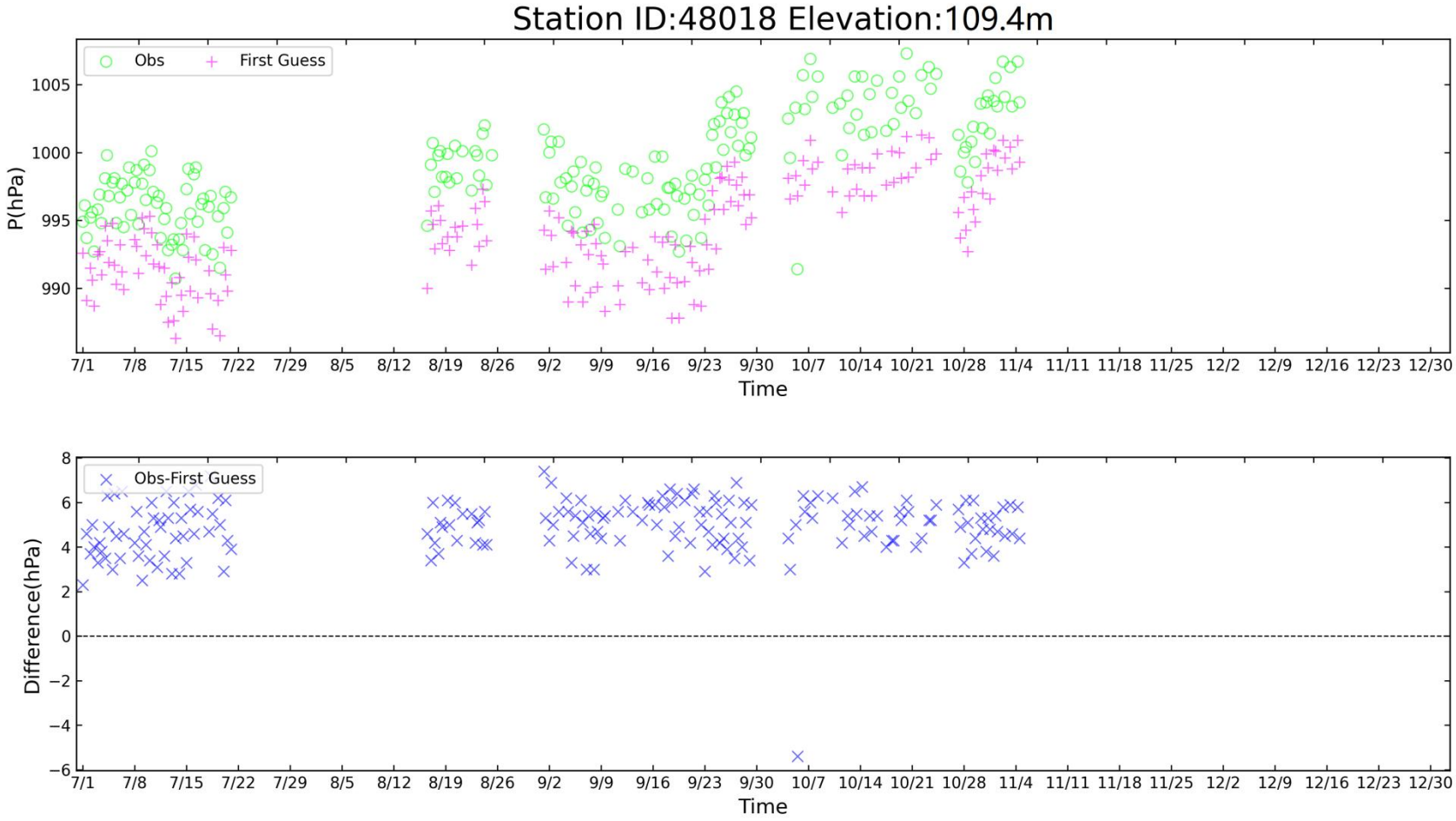

Figure 29 Time-series representation of SLP Obs minus FirstGuess for station 48018*

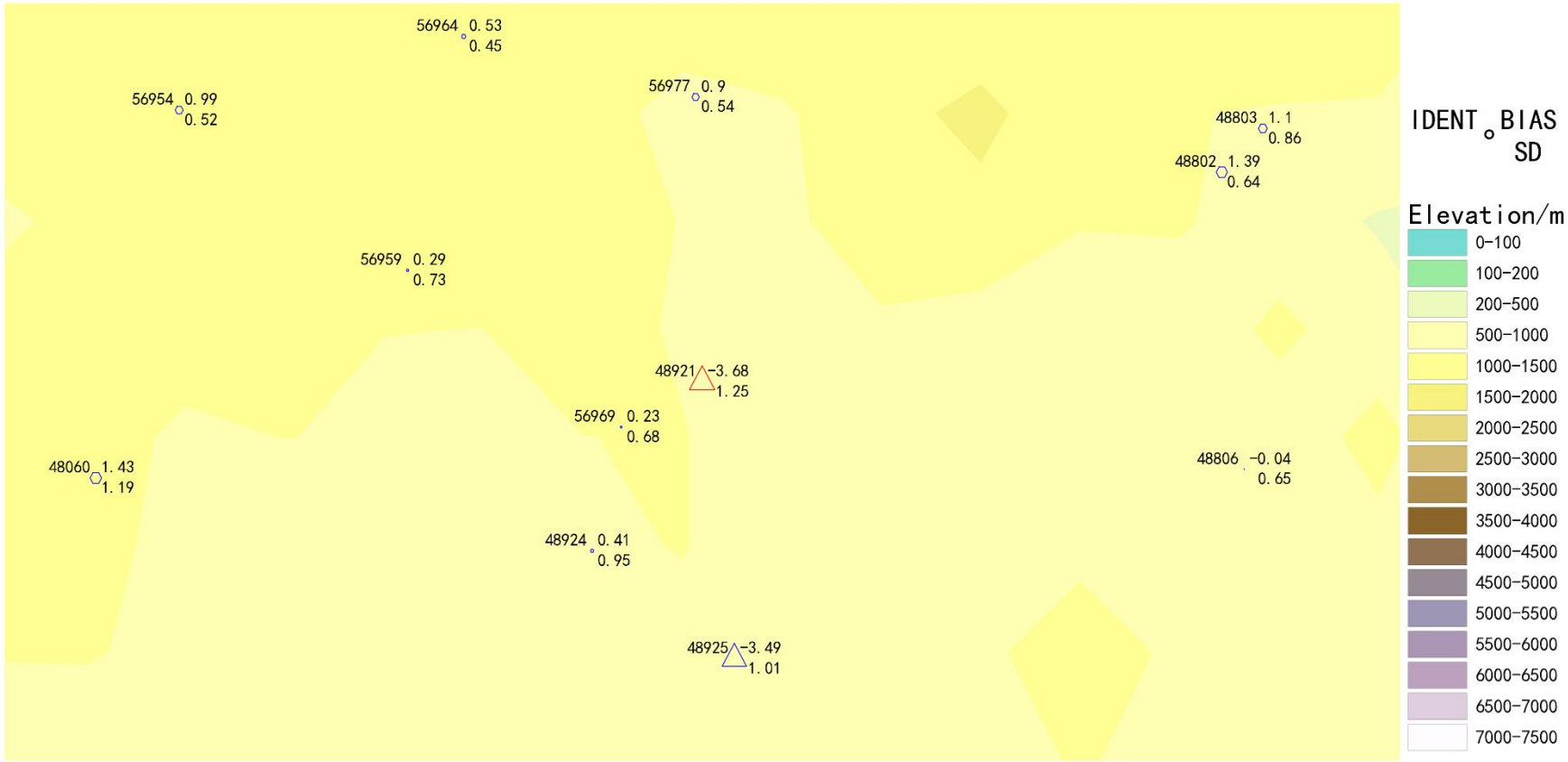

Figure 30 BIAS and SD of SLP for station 48921 (red) and surrounding stations (blue).

The number to the upper left of each symbol is the WMO IDENT, and those to the upper right are the values of BIAS and SD.

The size of each symbol is proportional to the value of BIAS, with hexagonal forms representing positive bias and triangular forms representing negative bias.

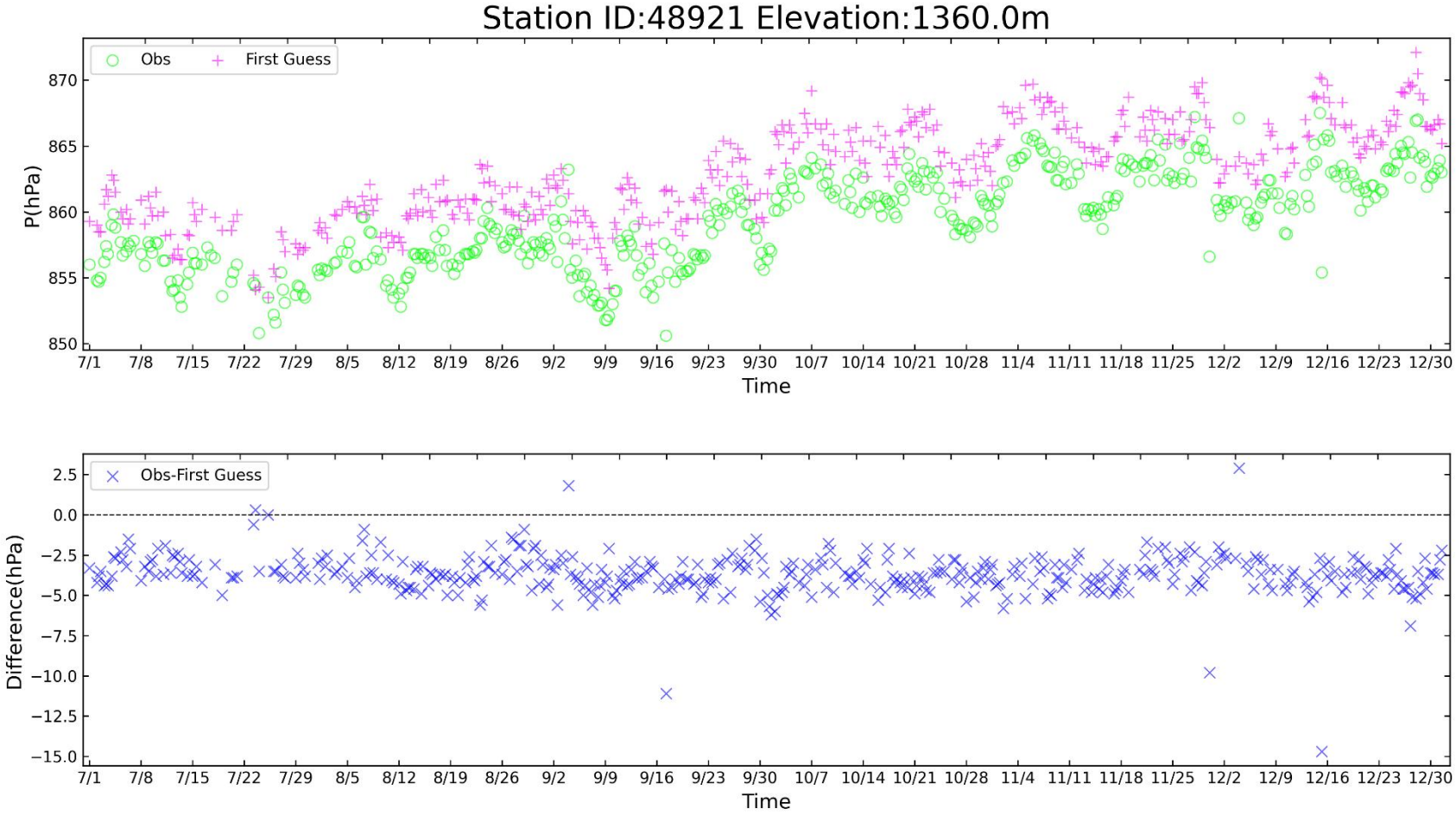

Figure 31 Time-series representation of SLP Obs minus FirstGuess for station 48921

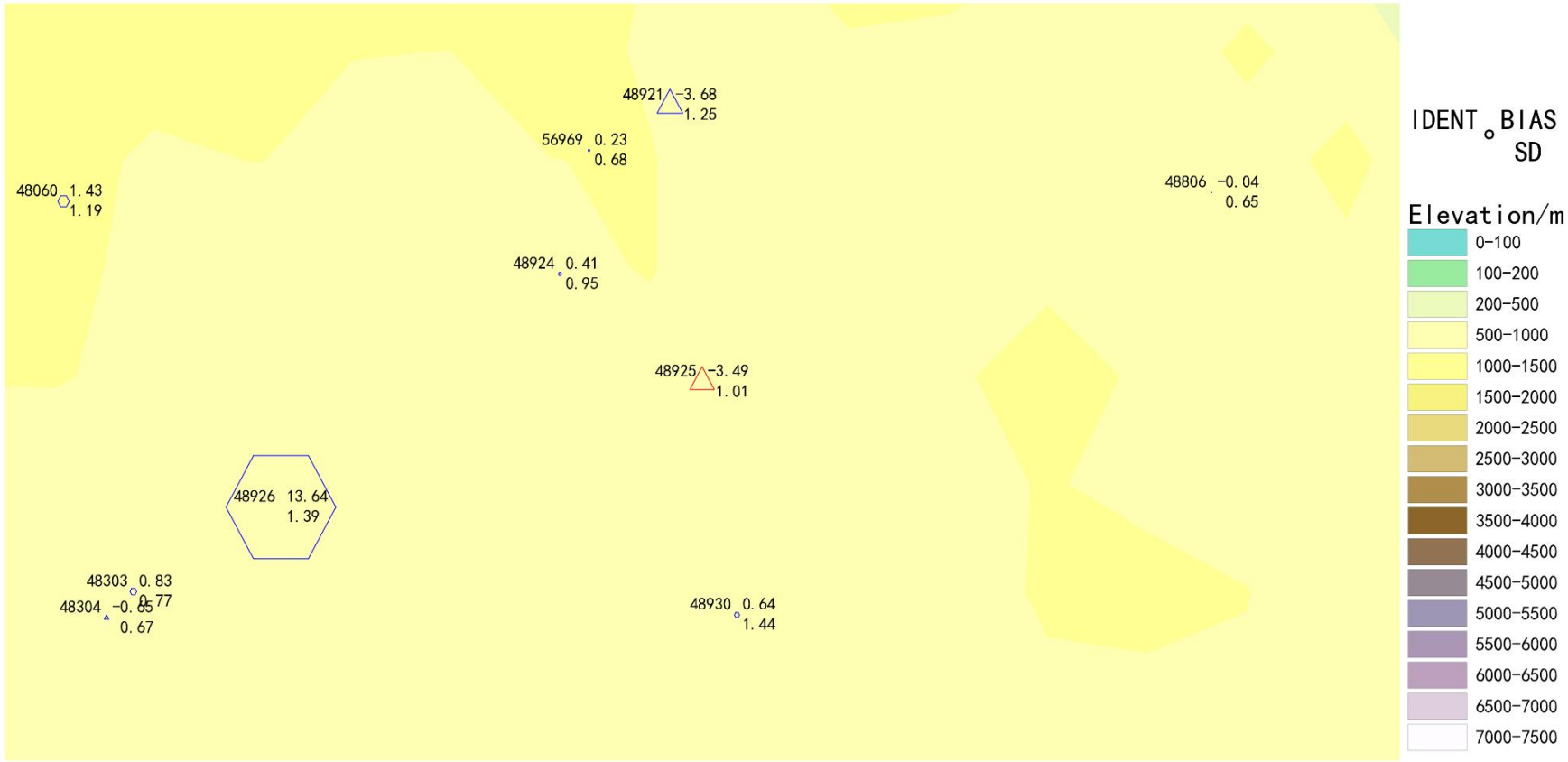

Figure 32 BIAS and SD of SLP for station 48925 (red) and surrounding stations (blue).

The number to the upper left of each symbol is the WMO IDENT, and those to the upper right are the values of BIAS and SD.

The size of each symbol is proportional to the value of BIAS, with hexagonal forms representing positive bias and triangular forms representing negative bias.

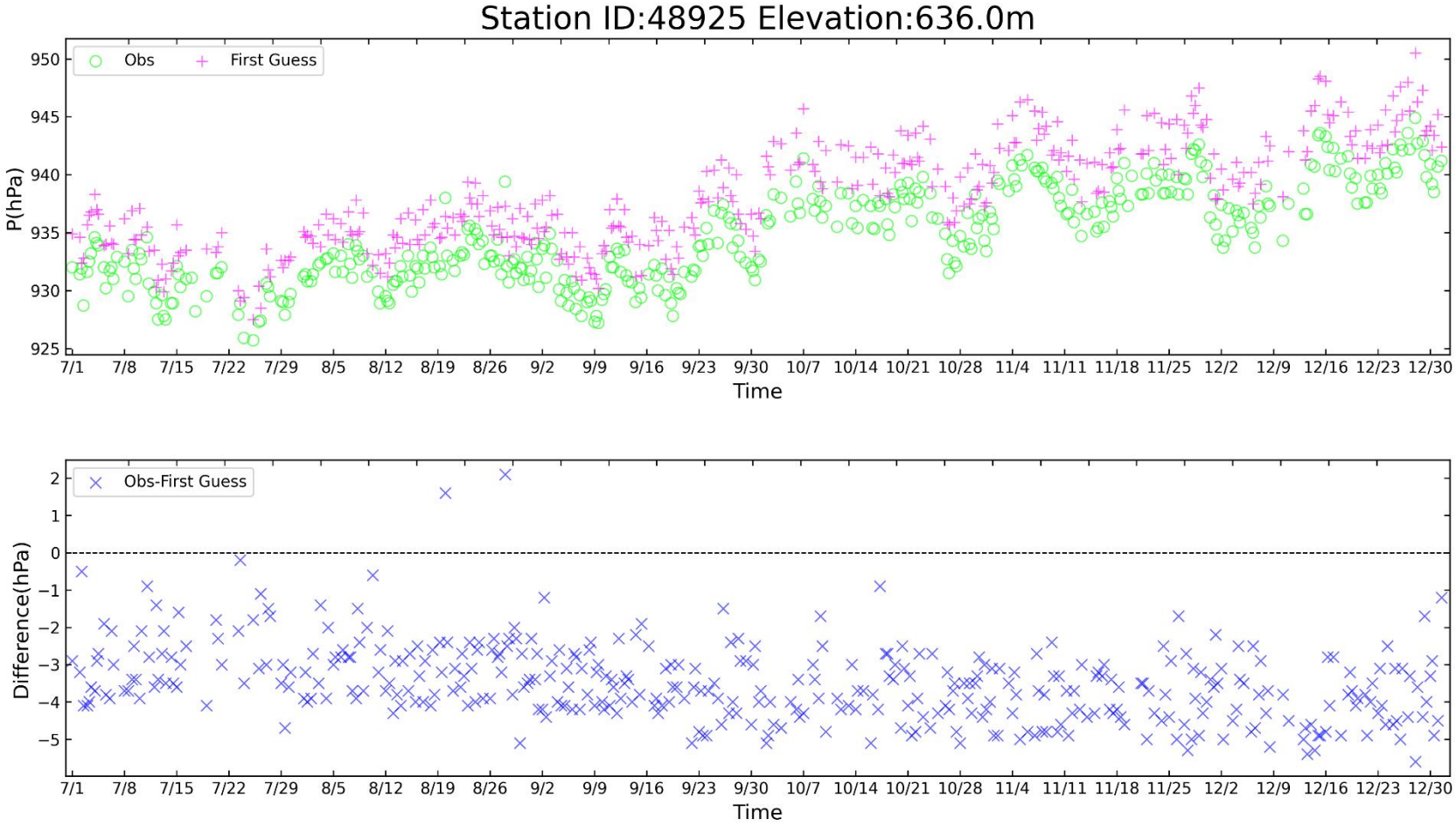

Figure 33 Time-series representation of SLP Obs minus FirstGuess for station 48925

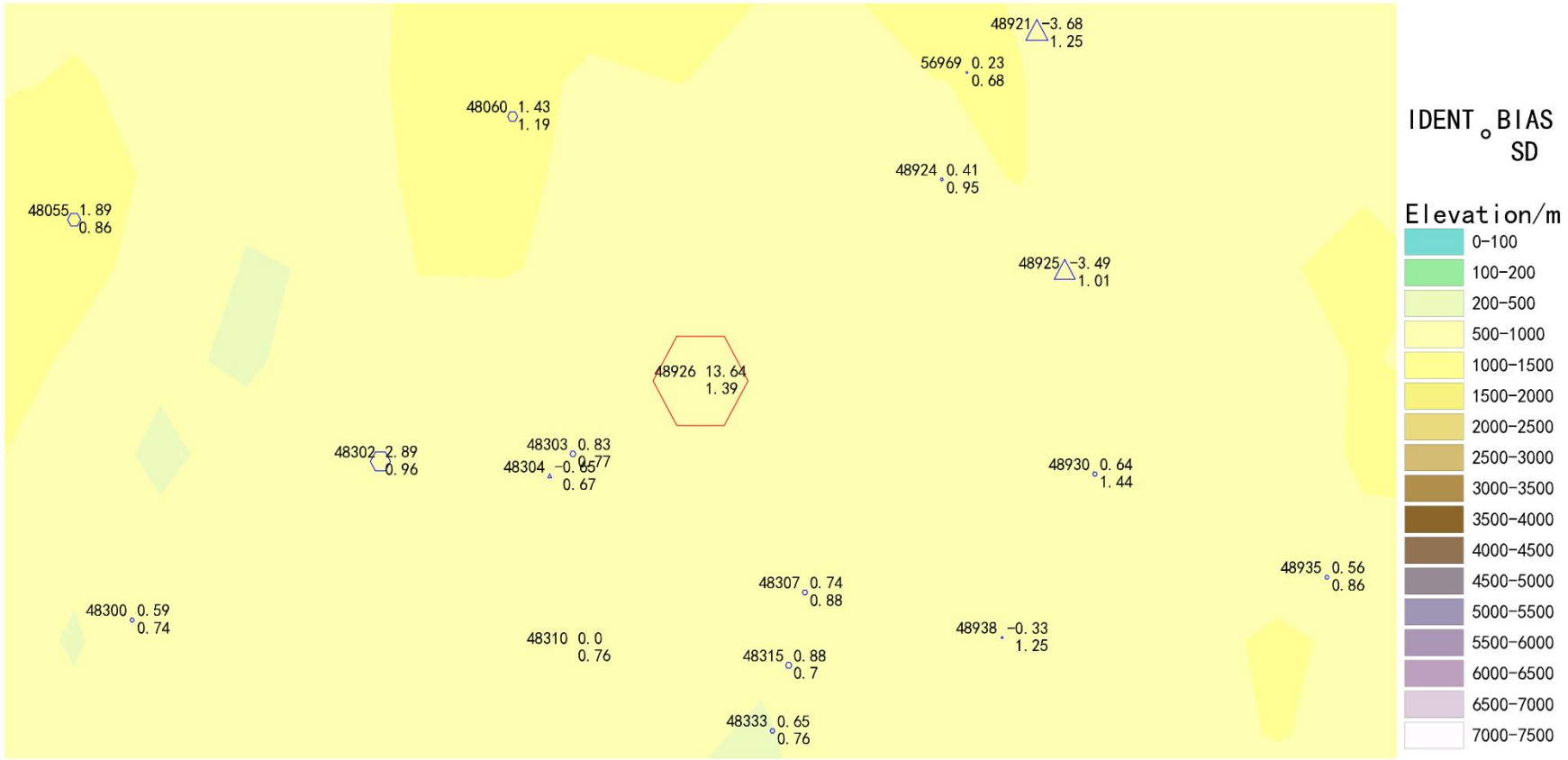

Figure 34 BIAS and SD of SLP for station 48926 (red) and surrounding stations (blue).

The number to the upper left of each symbol is the WMO IDENT, and those to the upper right are the values of BIAS and SD.

The size of each symbol is proportional to the value of BIAS, with hexagonal forms representing positive bias and triangular forms representing negative bias.

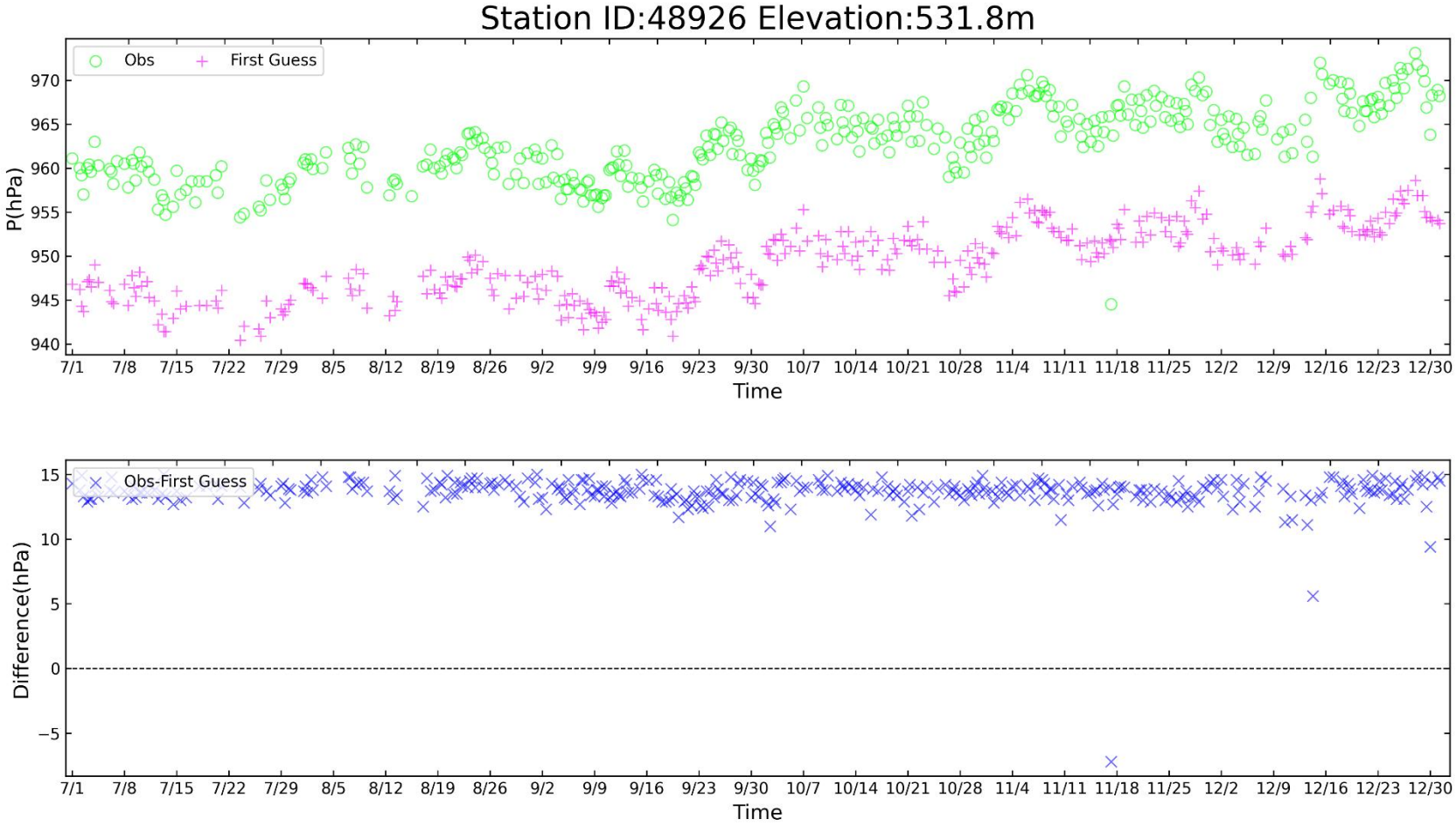

Figure 35 Time-series representation of SLP Obs minus FirstGuess for station 48926

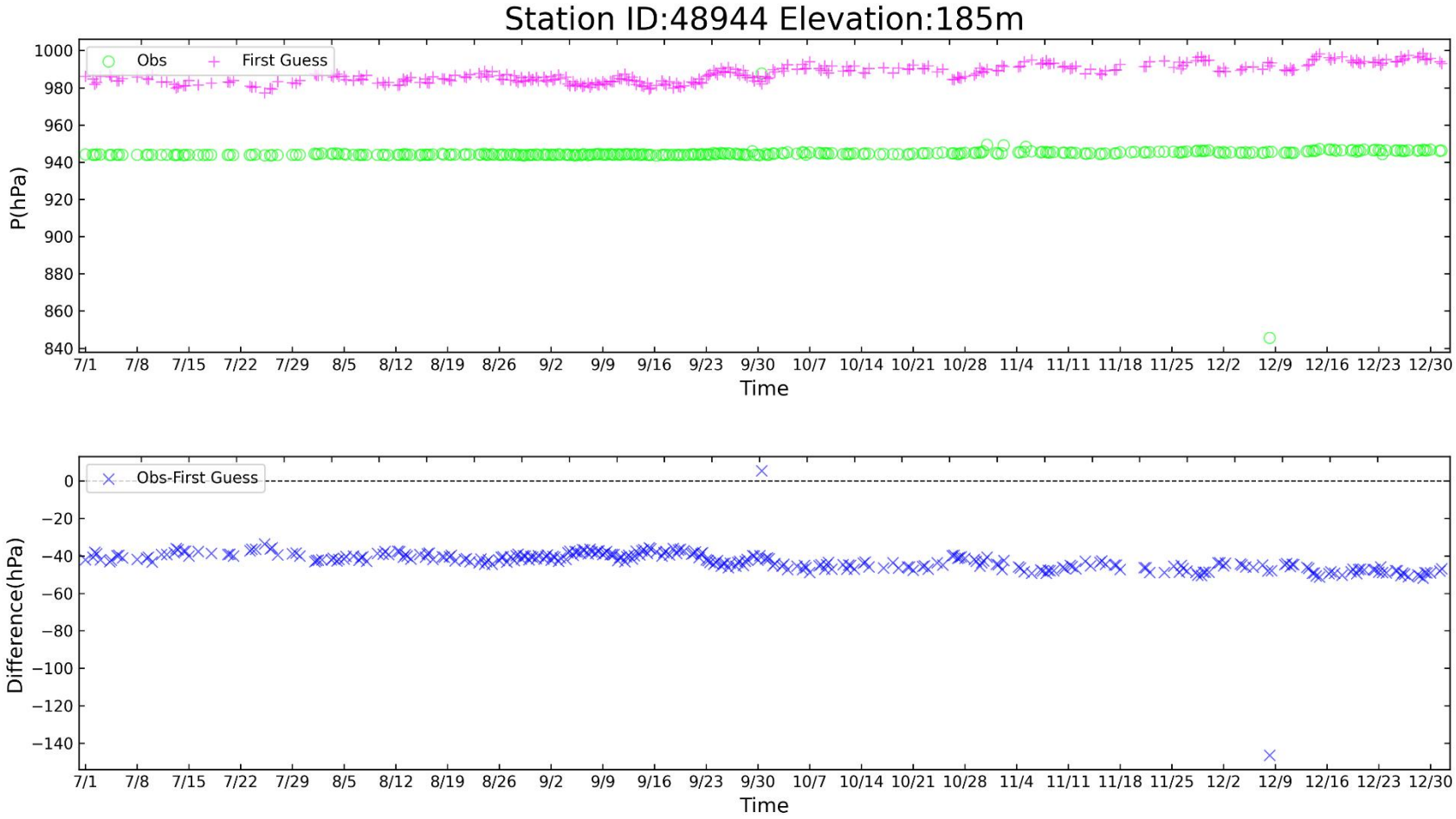

Figure 36 Time-series representation of SLP Obs minus FirstGuess for station 48944

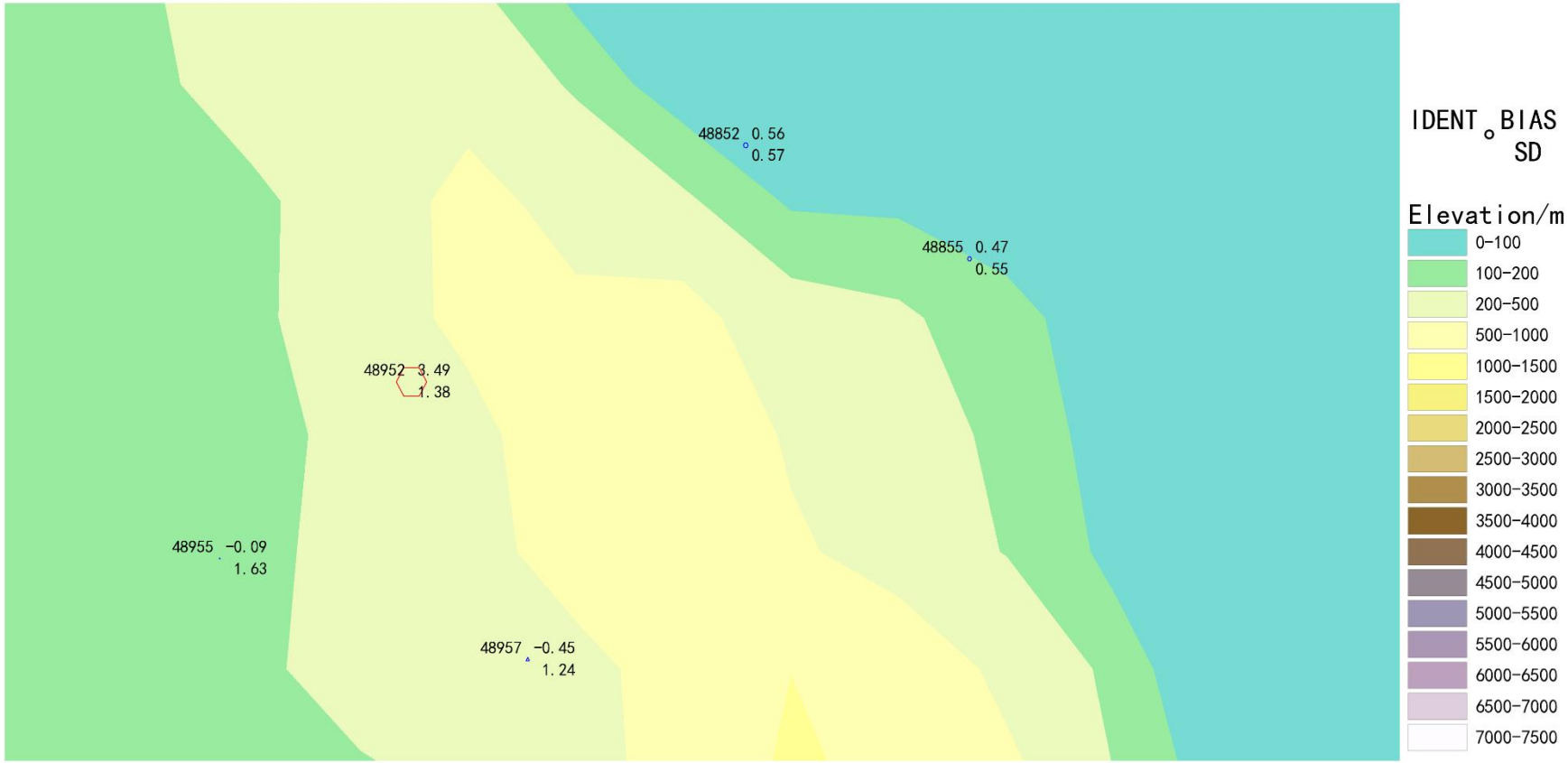

Figure 37 BIAS and SD of SLP for station 48952 (red) and surrounding stations (blue).

The number to the upper left of each symbol is the WMO IDENT, and those to the upper right are the values of BIAS and SD.

The size of each symbol is proportional to the value of BIAS, with hexagonal forms representing positive bias and triangular forms representing negative bias.

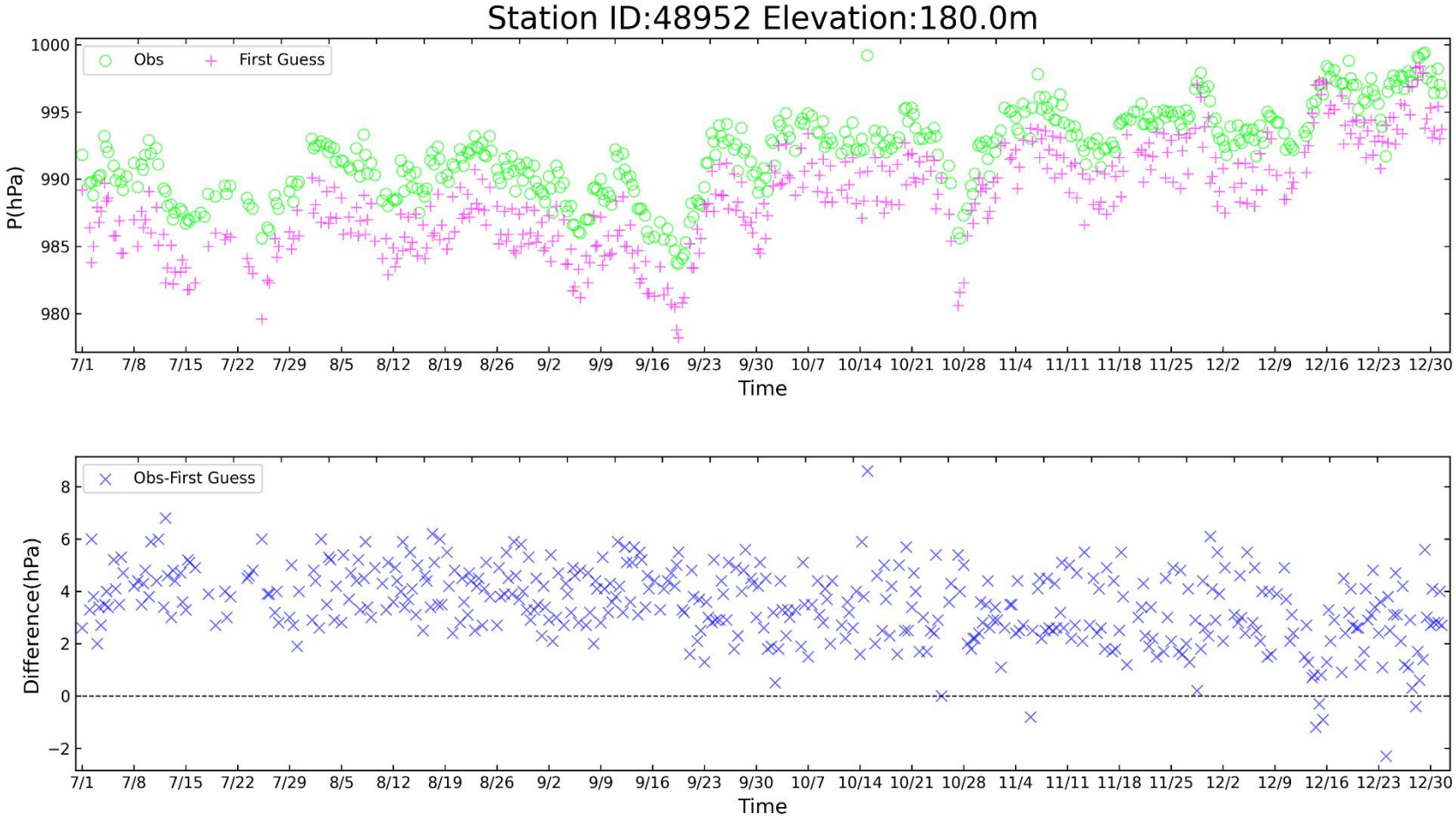

Figure 38 Time-series representation of SLP Obs minus FirstGuess for station 48952

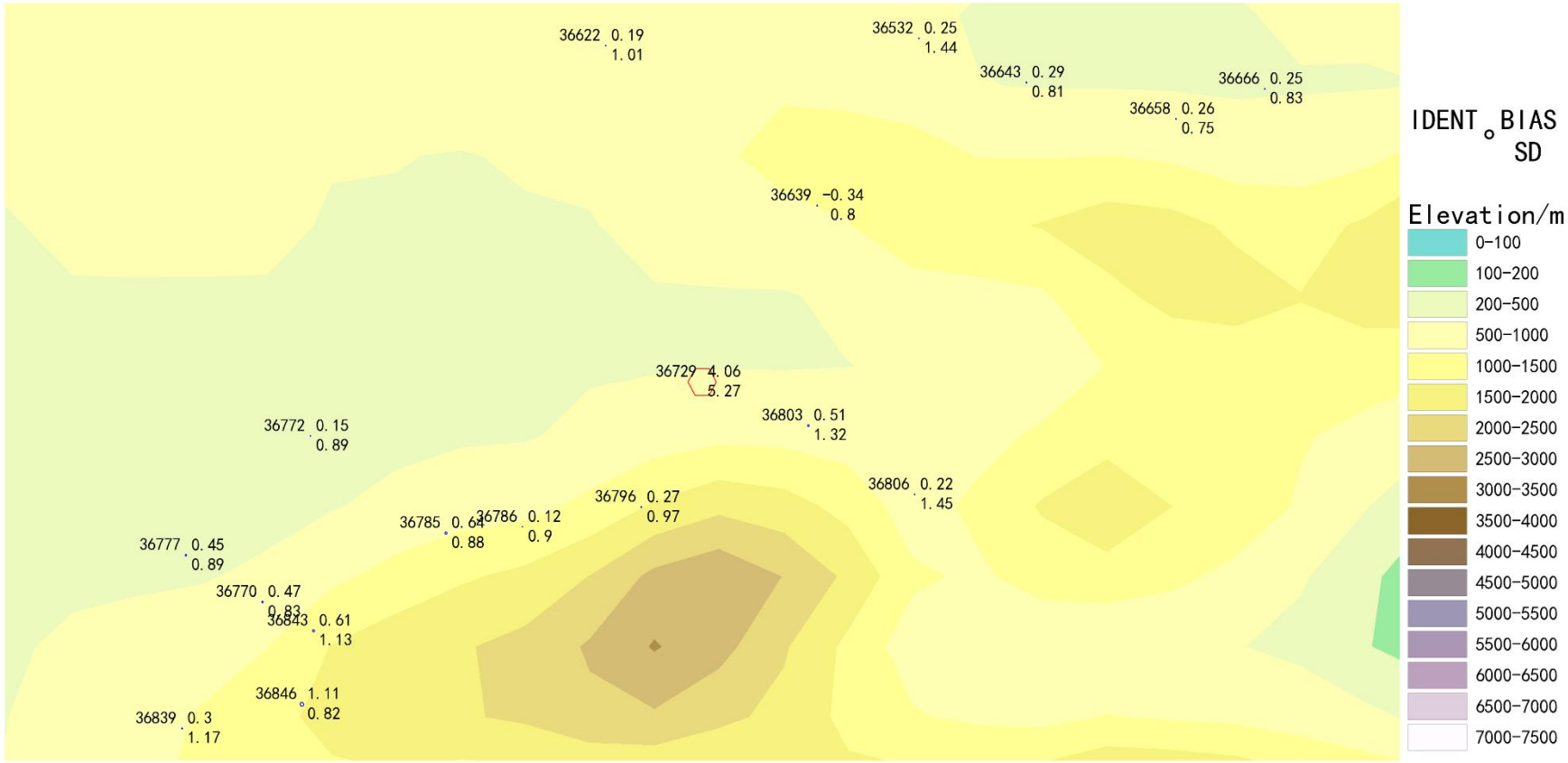

Figure 39 BIAS and SD of SLP for station 36729 (red) and surrounding stations (blue).

The number to the upper left of each symbol is the WMO IDENT, and those to the upper right are the values of BIAS and SD.

The size of each symbol is proportional to the value of BIAS, with hexagonal forms representing positive bias and triangular forms representing negative bias.

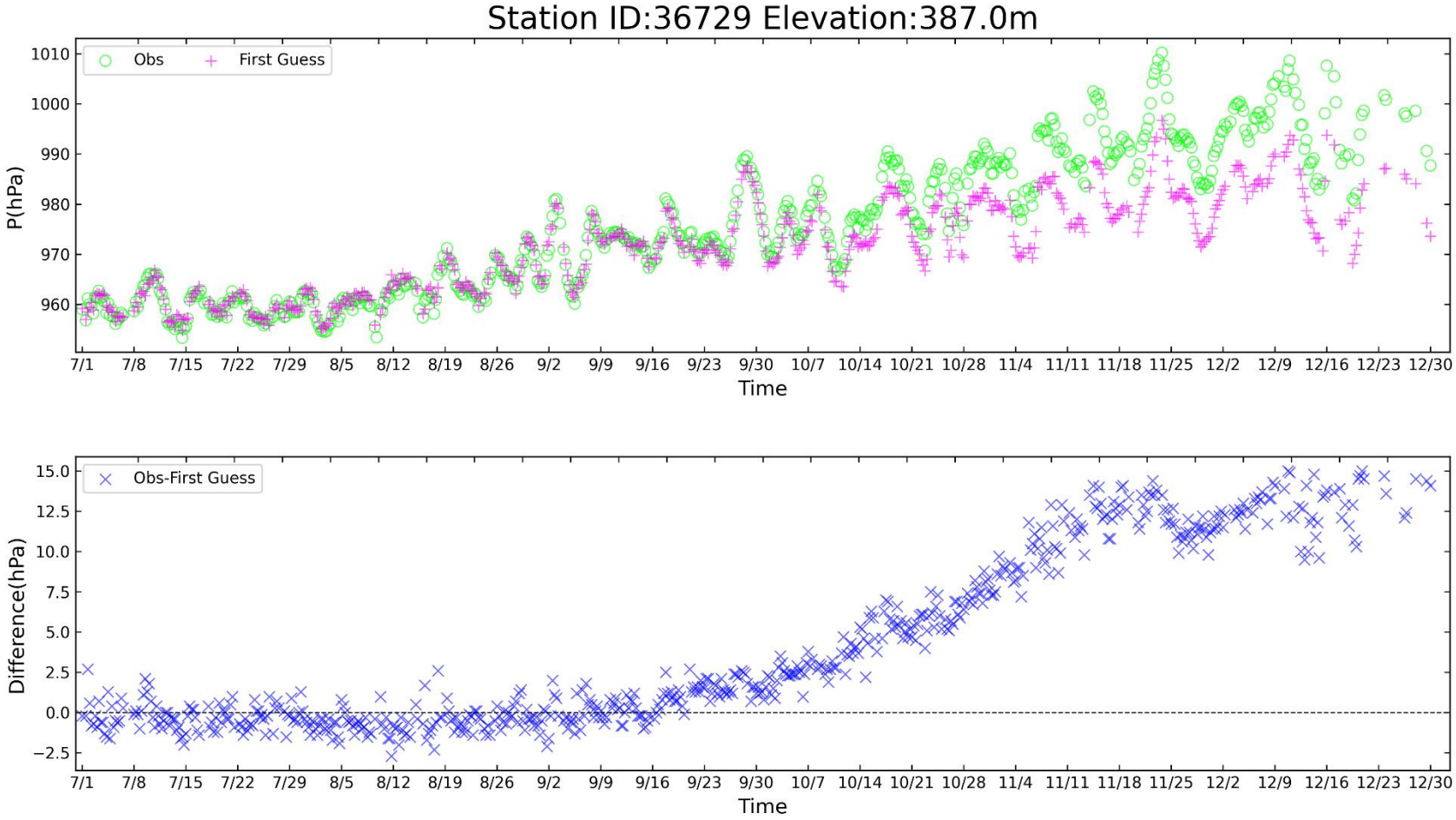

Figure 40 Time-series representation of SLP Obs minus FirstGuess for station 36729

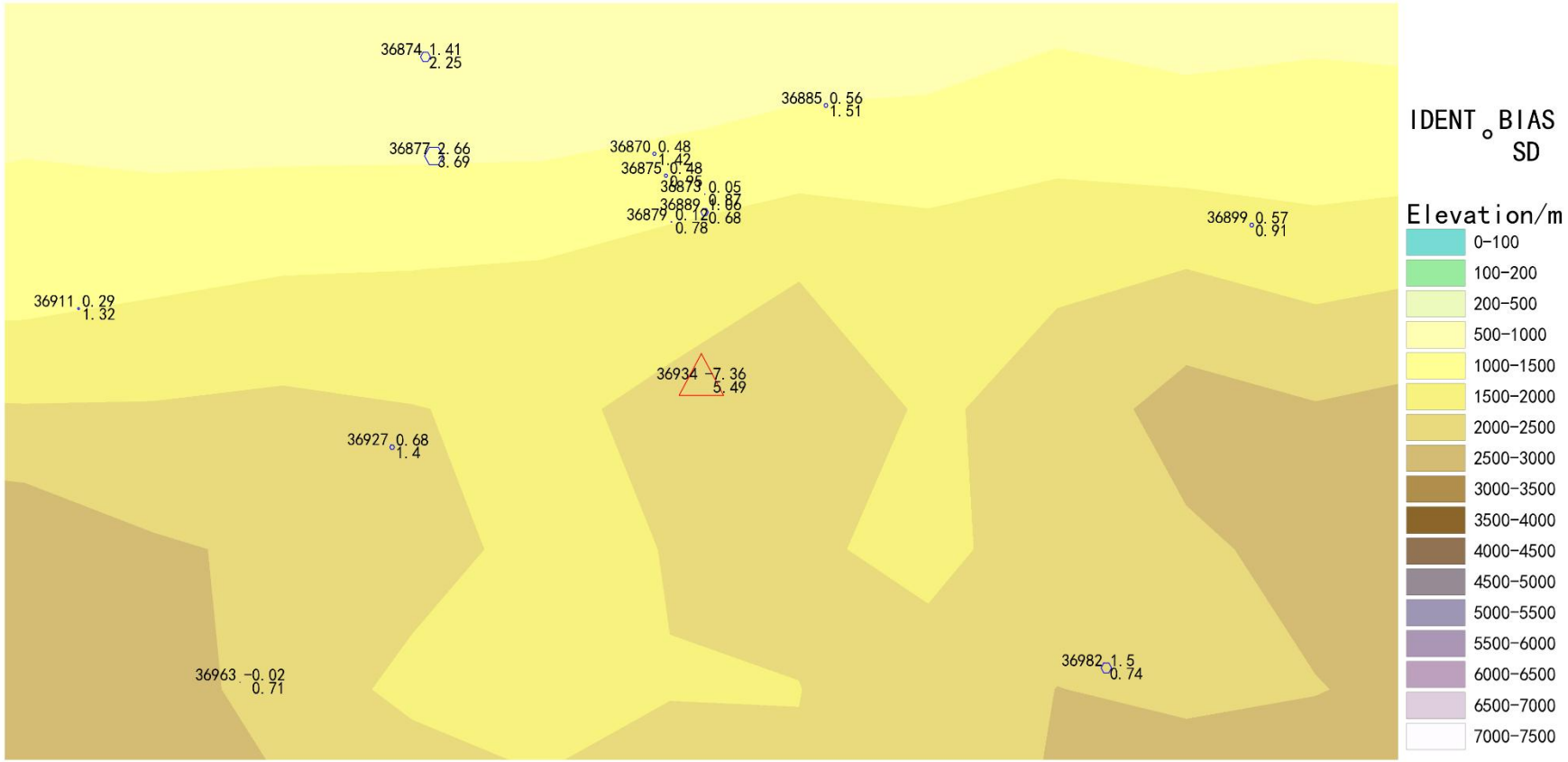

Figure 41 BIAS and SD of SLP for station 36934* (red) and surrounding stations (blue).

The number to the upper left of each symbol is the WMO IDENT, and those to the upper right are the values of BIAS and SD.

The size of each symbol is proportional to the value of BIAS, with hexagonal forms representing positive bias and triangular forms representing negative bias.

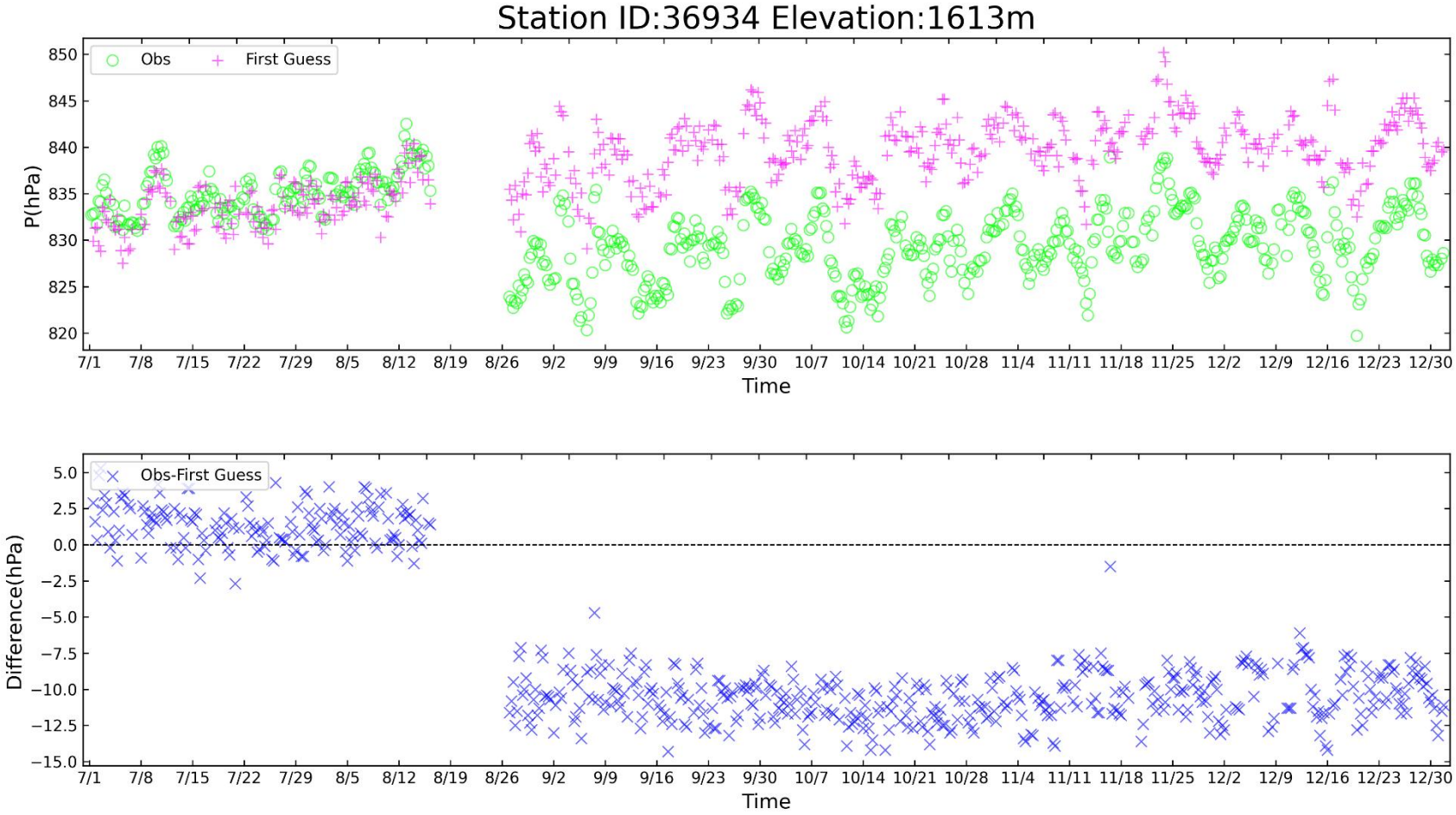

Figure 42 Time-series representation of SLP Obs minus FirstGuess for station 36934*

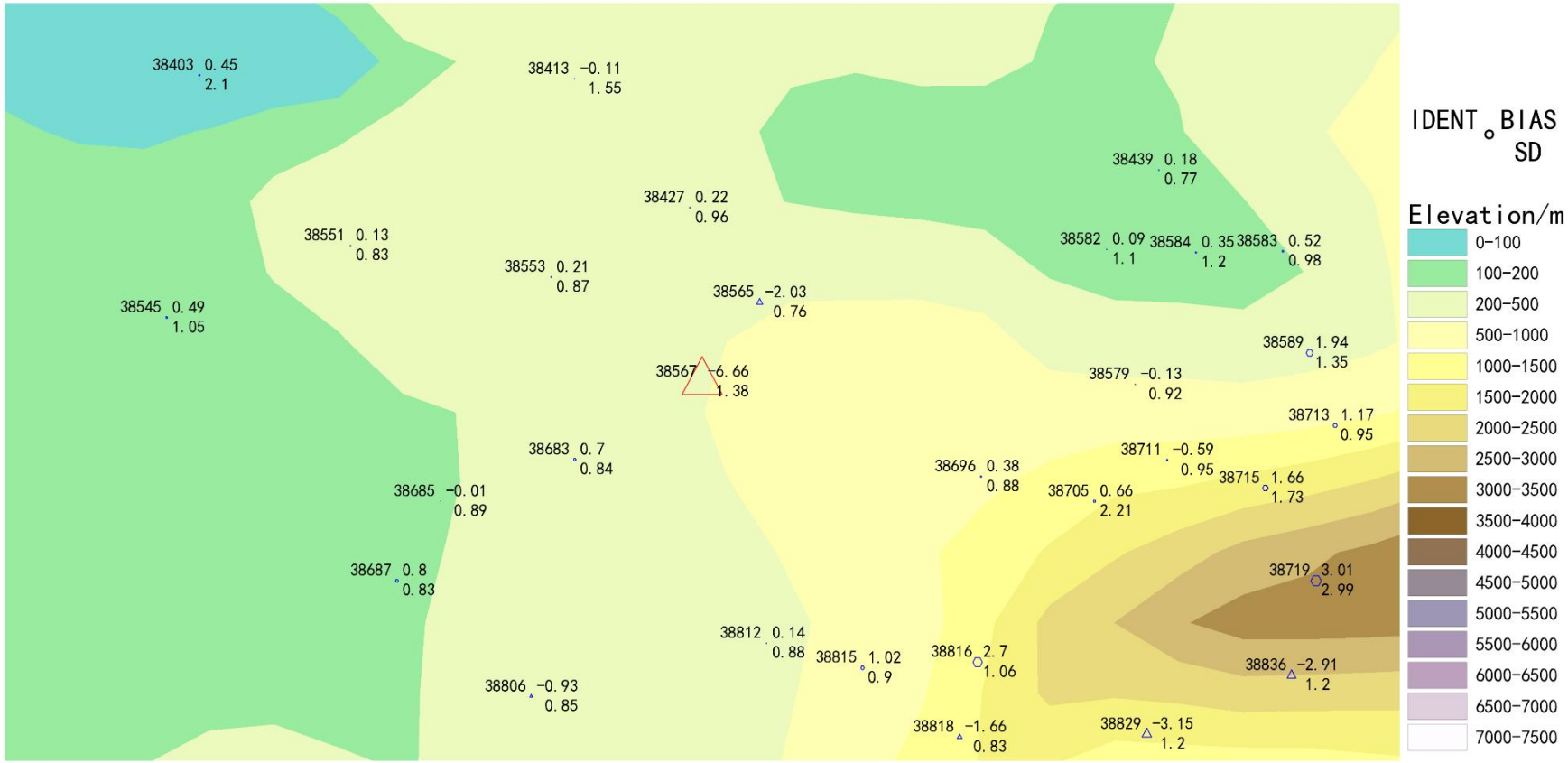

Figure 43 BIAS and SD of SLP for station 38567 (red) and surrounding stations (blue).

The number to the upper left of each symbol is the WMO IDENT, and those to the upper right are the values of BIAS and SD.

The size of each symbol is proportional to the value of BIAS, with hexagonal forms representing positive bias and triangular forms representing negative bias.

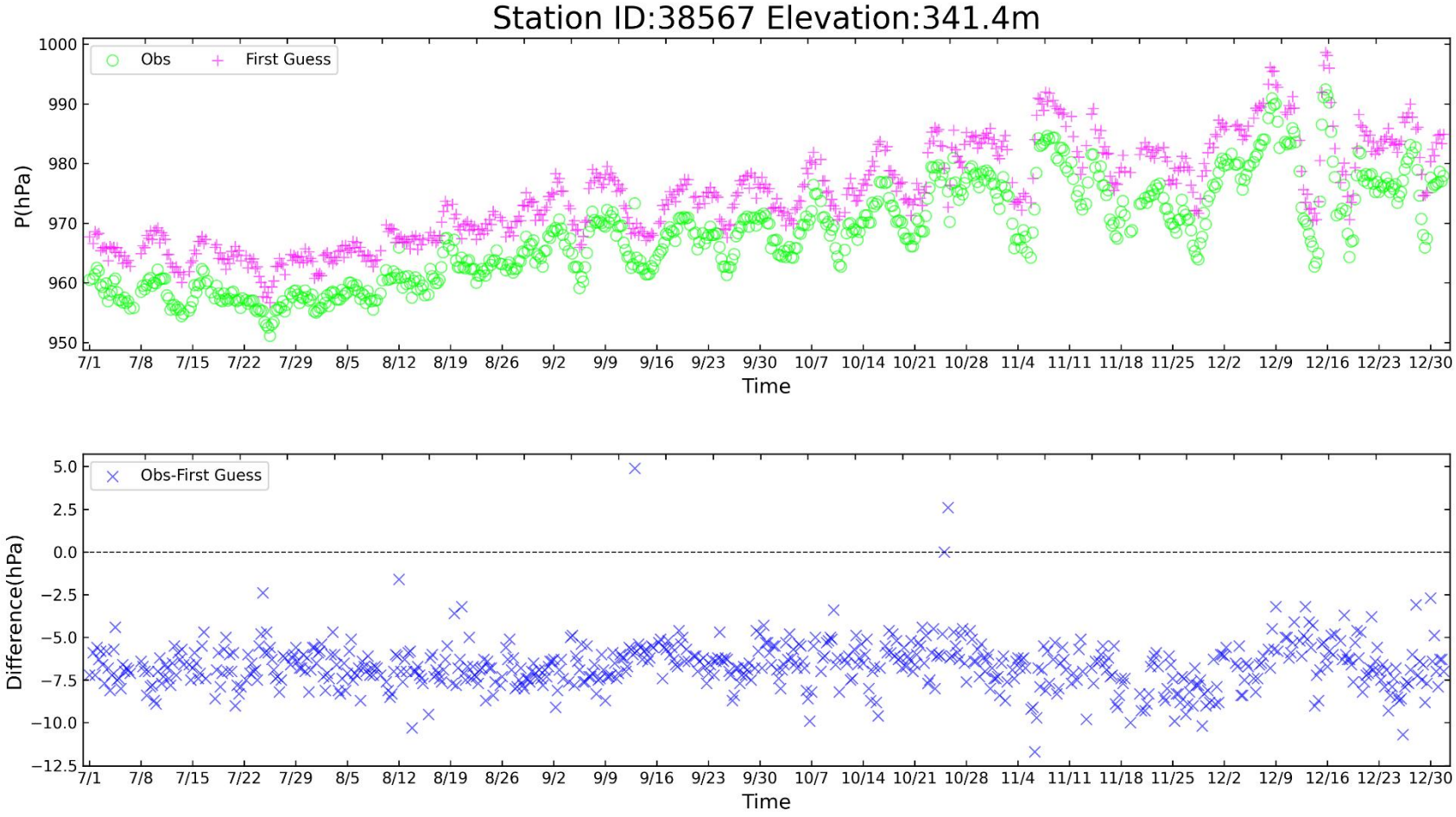

Figure 44 Time-series representation of SLP Obs minus FirstGuess for station 38567

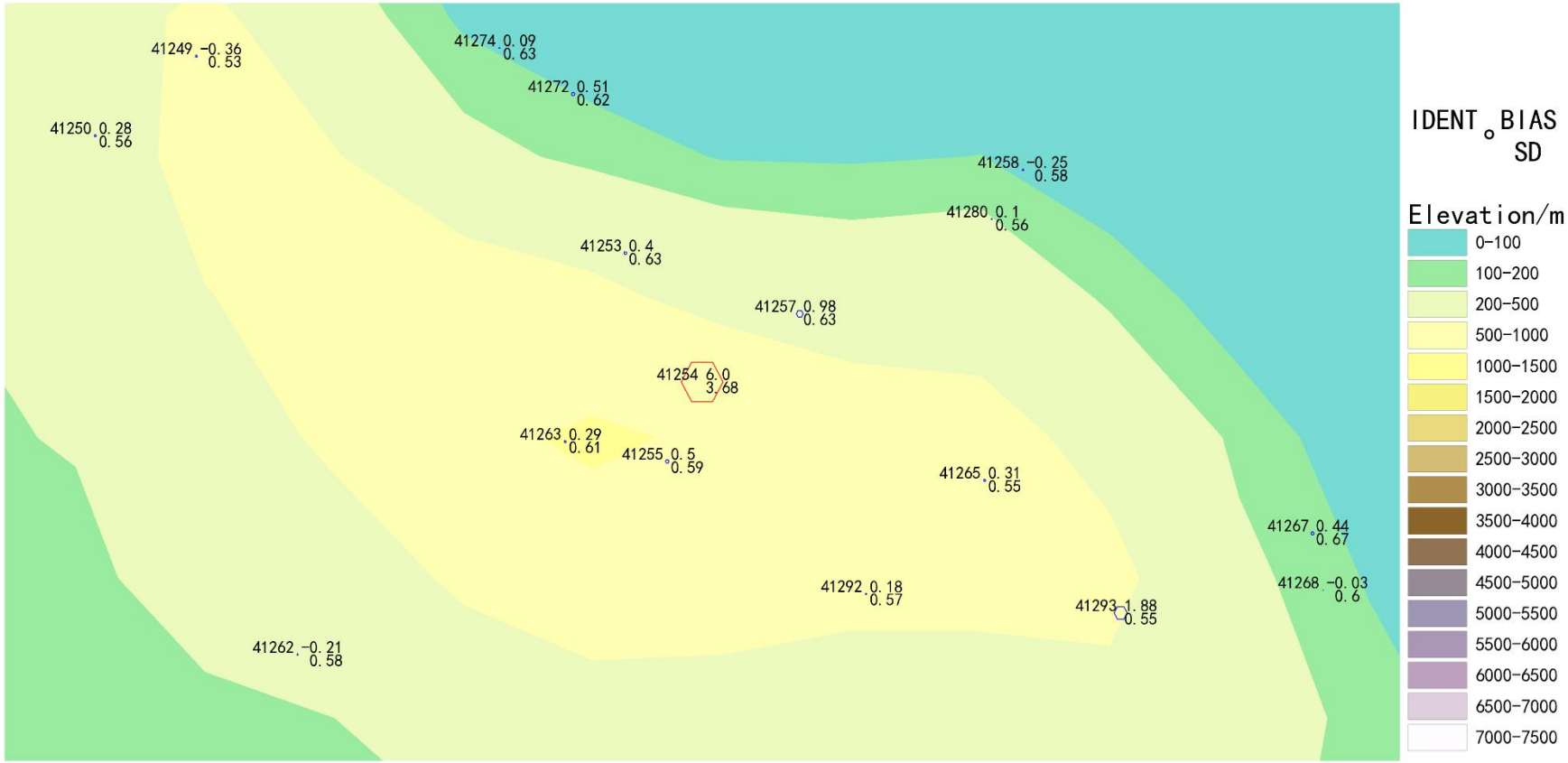

Figure 45 BIAS and SD of SLP for station 41565 (red) and surrounding stations (blue).

The number to the upper left of each symbol is the WMO IDENT, and those to the upper right are the values of BIAS and SD.

The size of each symbol is proportional to the value of BIAS, with hexagonal forms representing positive bias and triangular forms representing negative bias.

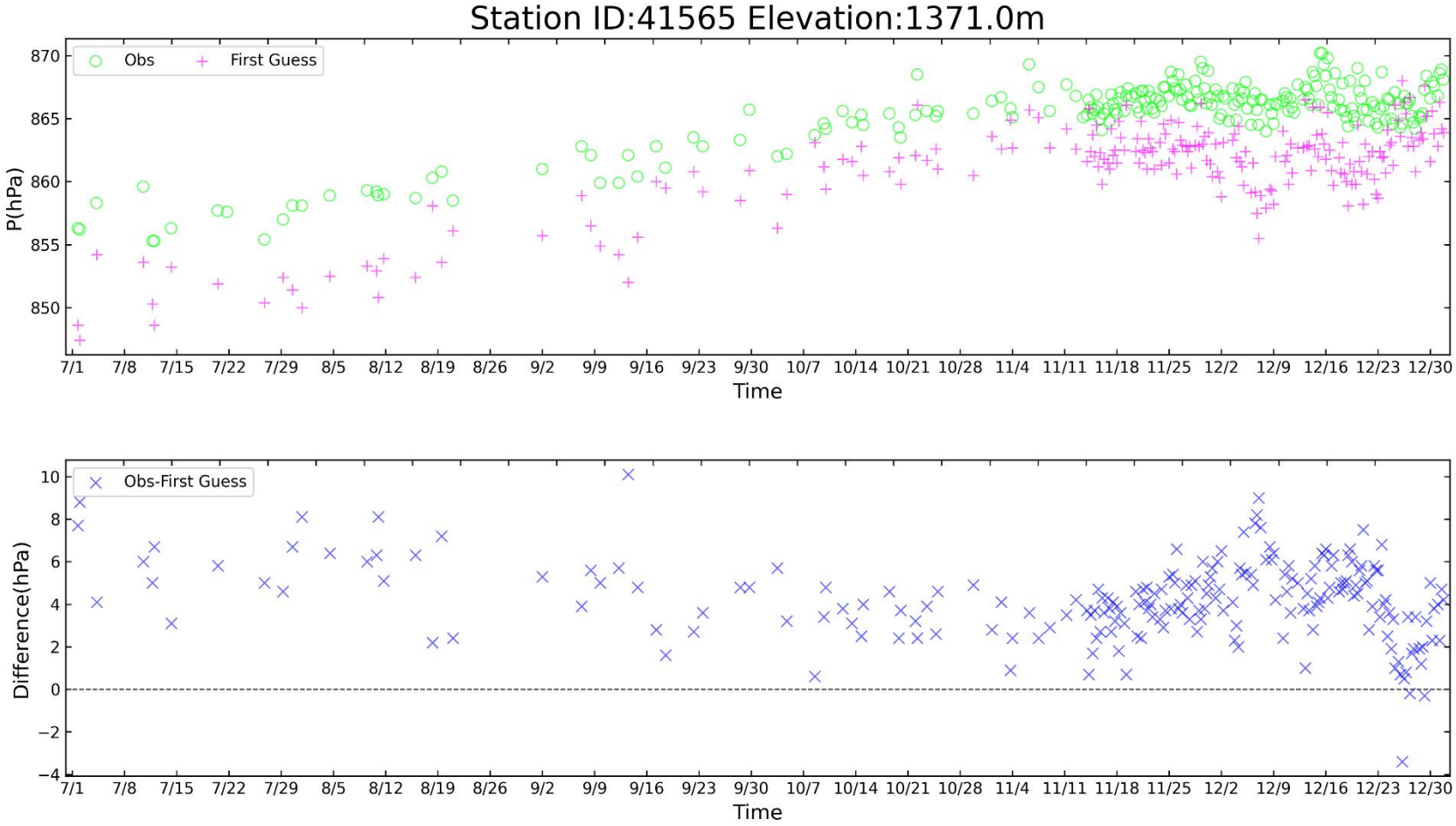

Figure 46 Time-series representation of SLP Obs minus FirstGuess for station 41565

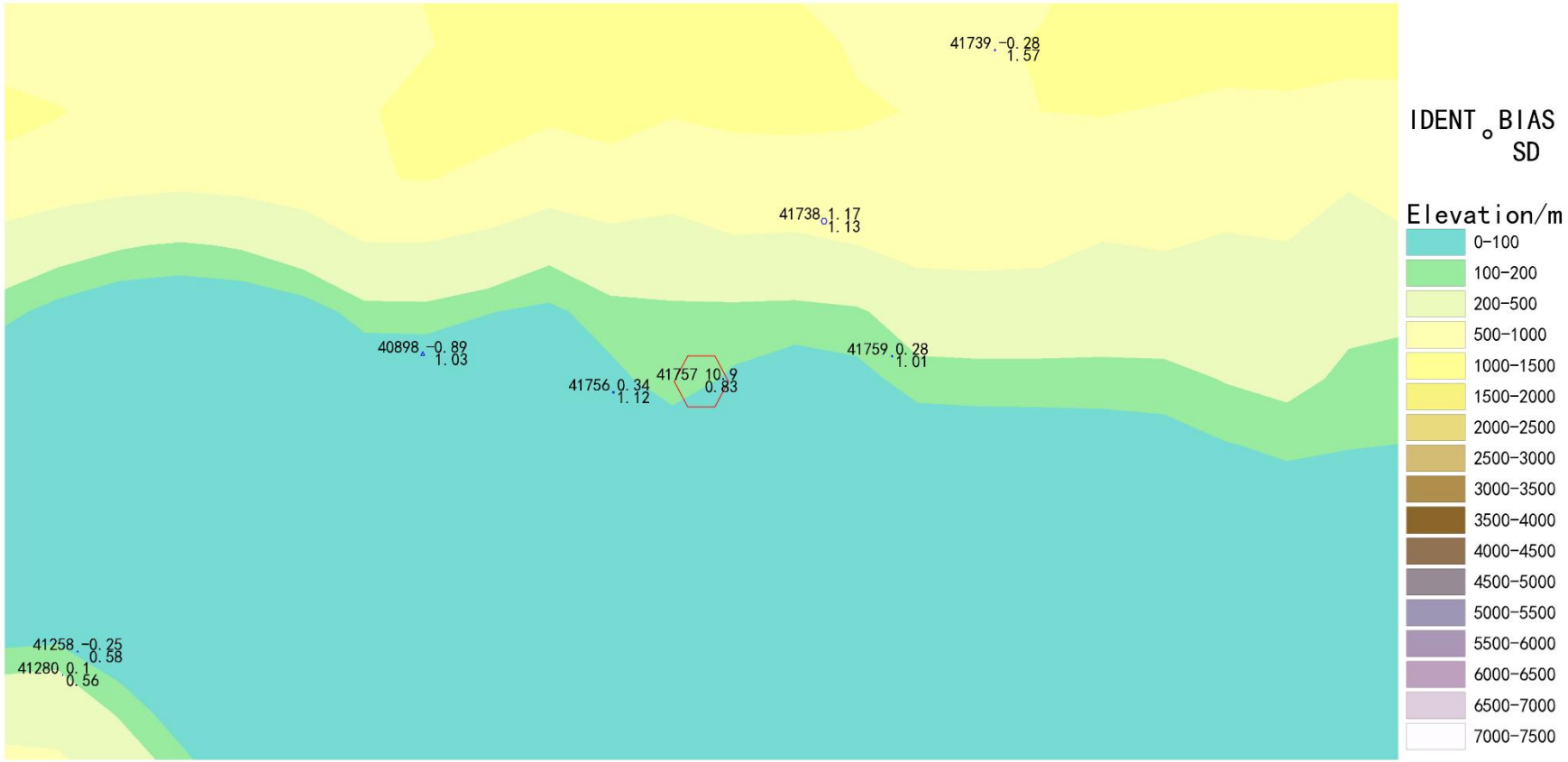

Figure 47 BIAS and SD of SLP for station 41757 (red) and surrounding stations (blue).

The number to the upper left of each symbol is the WMO IDENT, and those to the upper right are the values of BIAS and SD.

The size of each symbol is proportional to the value of BIAS, with hexagonal forms representing positive bias and triangular forms representing negative bias.

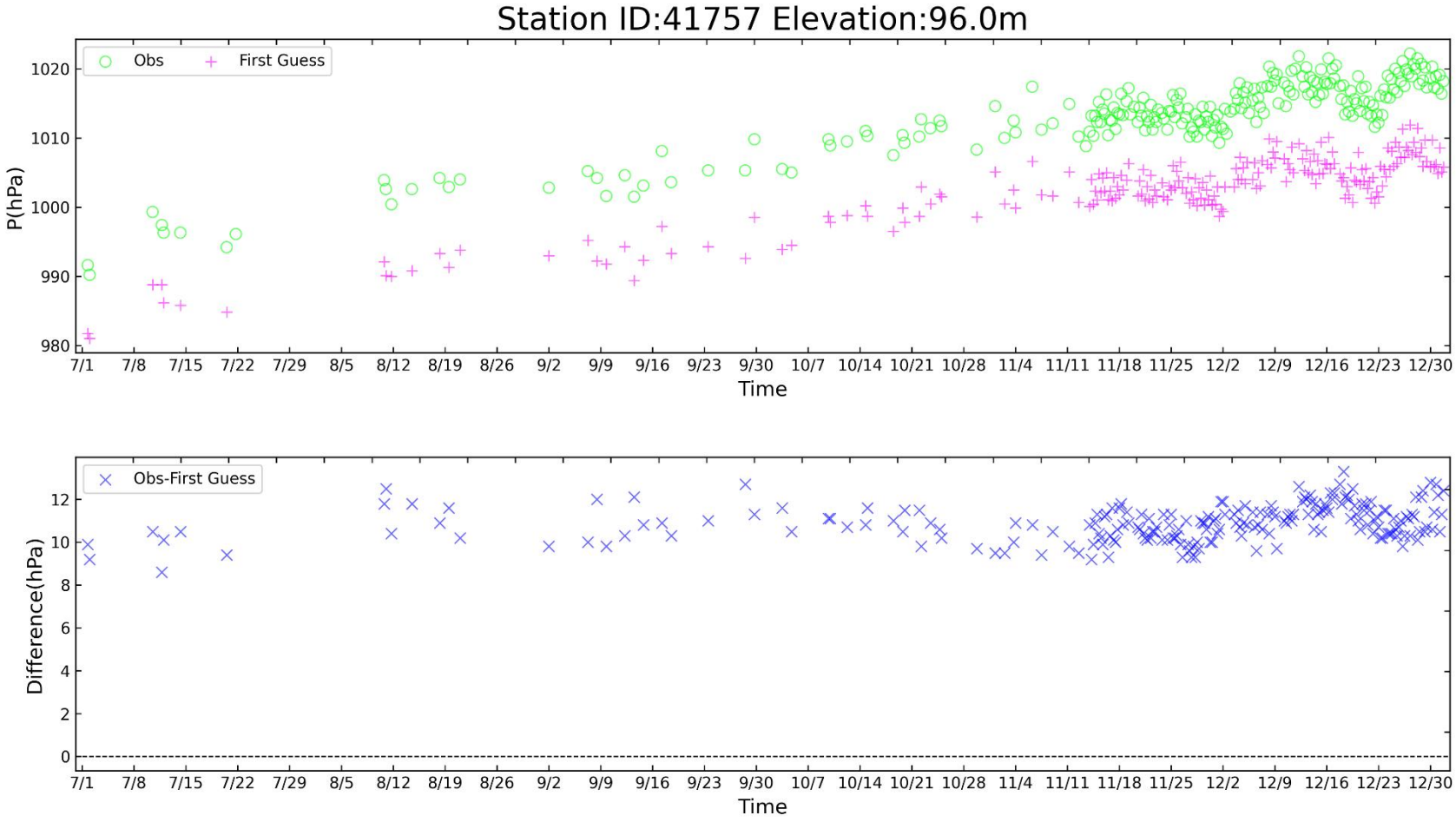

Figure 48 Time-series representation of SLP Obs minus FirstGuess for station 41757

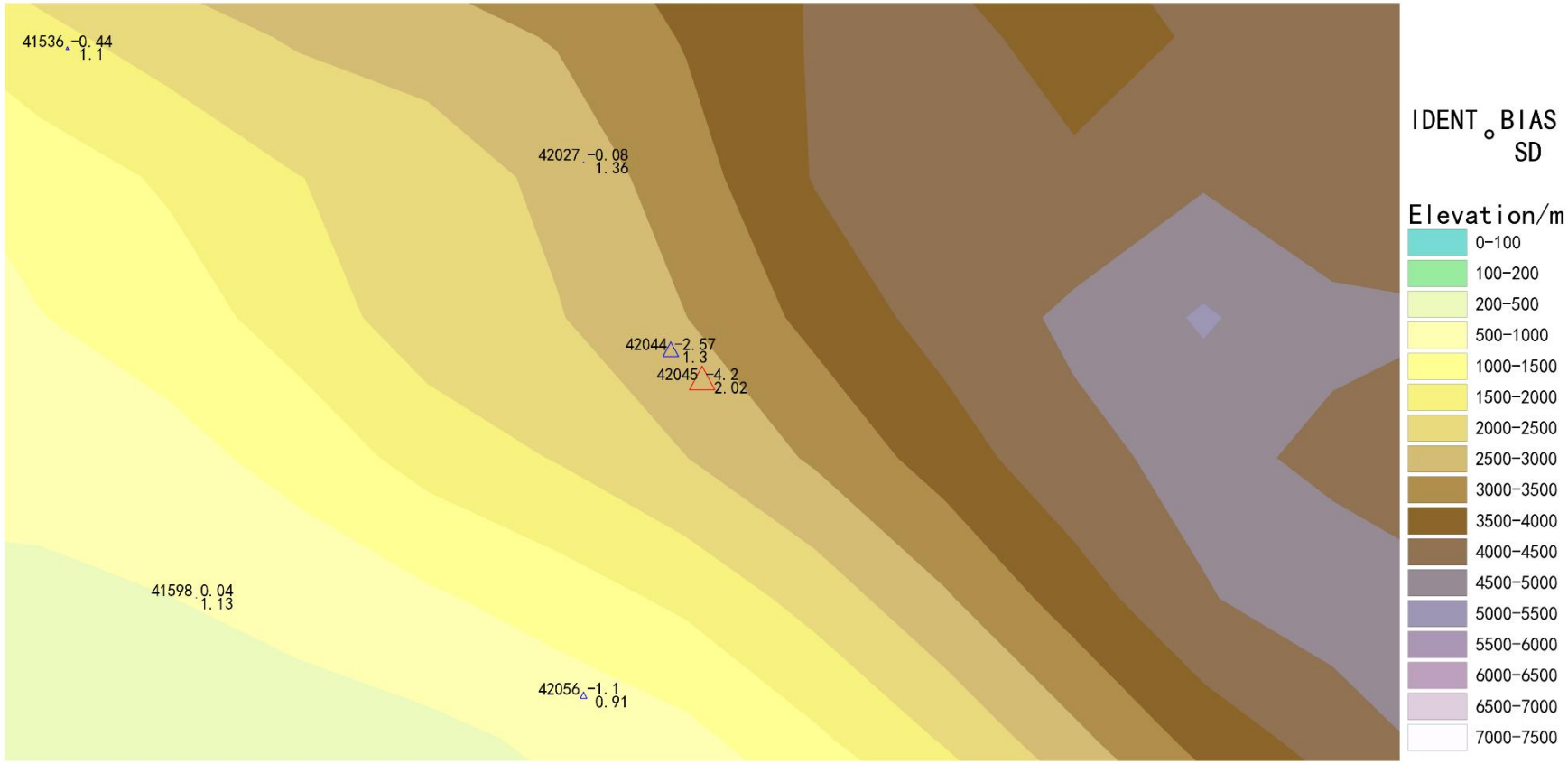

Figure 49 BIAS and SD of SLP for station 42045 (red) and surrounding stations (blue).
The number to the upper left of each symbol is the WMO IDENT, and those to the upper right are the values of BIAS and SD.
The size of each symbol is proportional to the value of BIAS, with hexagonal forms representing positive bias and triangular forms representing negative bias.

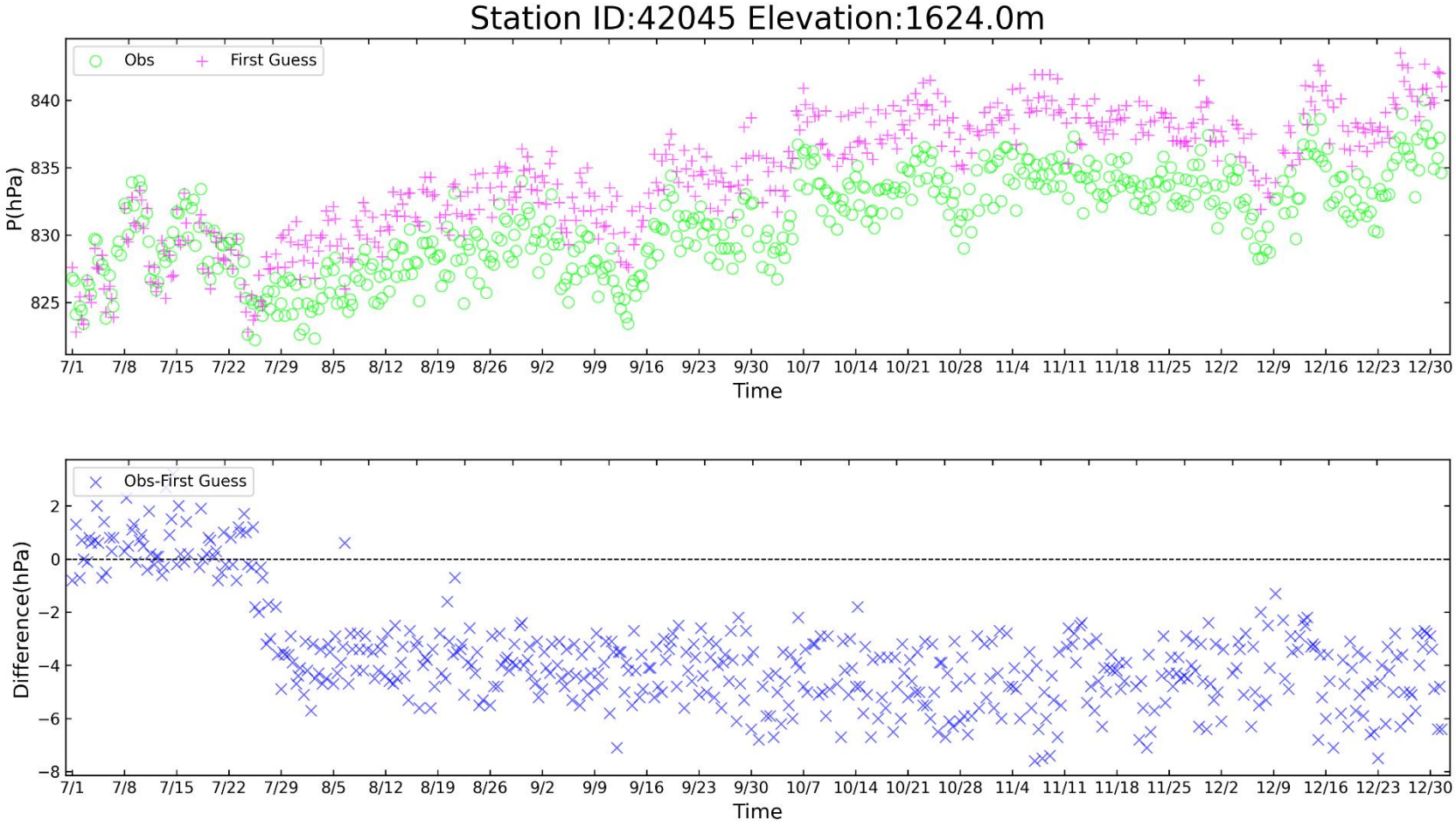

Figure 50 Time-series representation of SLP Obs minus FirstGuess for station 42045

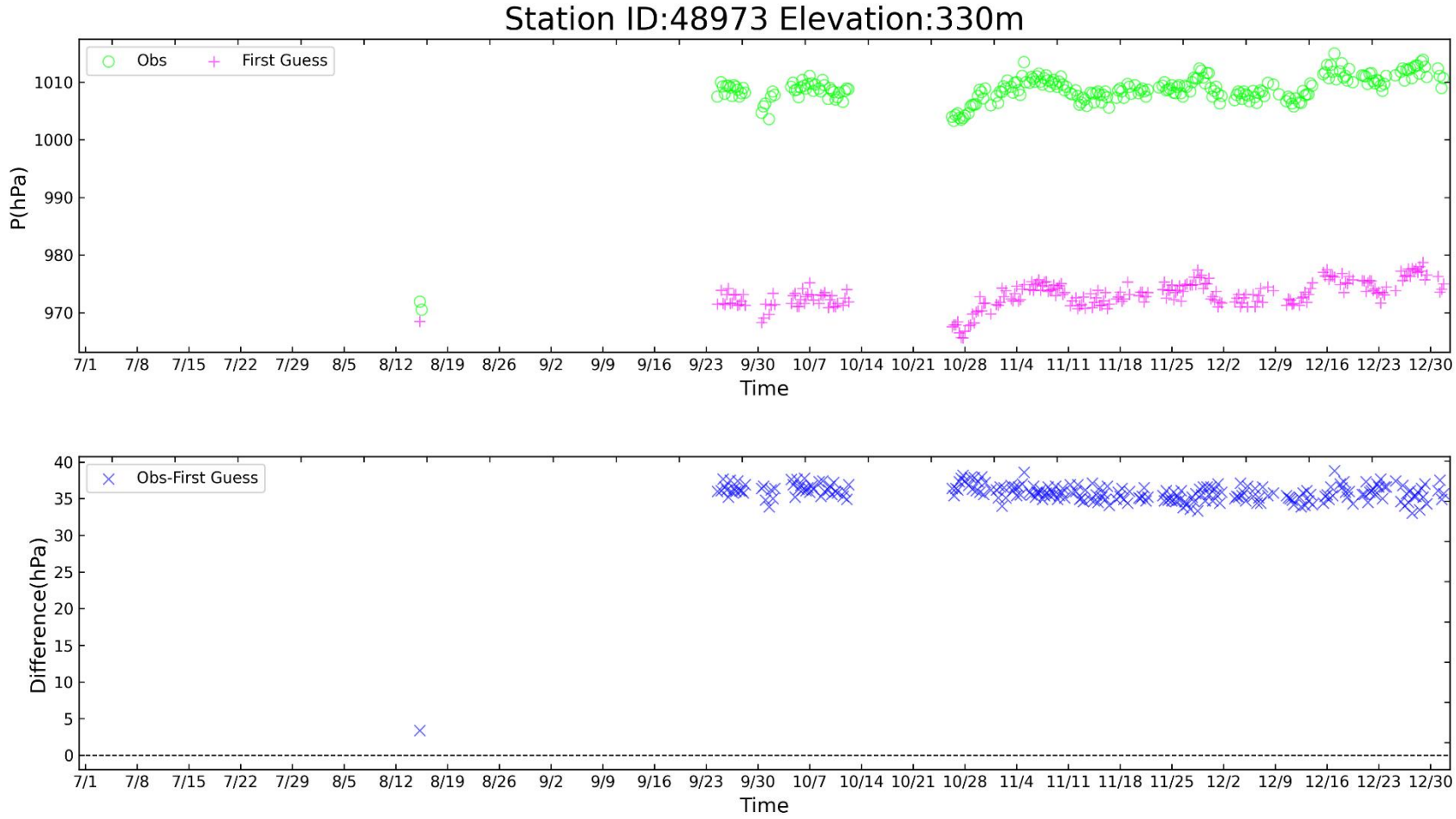

Figure 51 Time-series representation of SLP Obs minus FirstGuess for station 48973

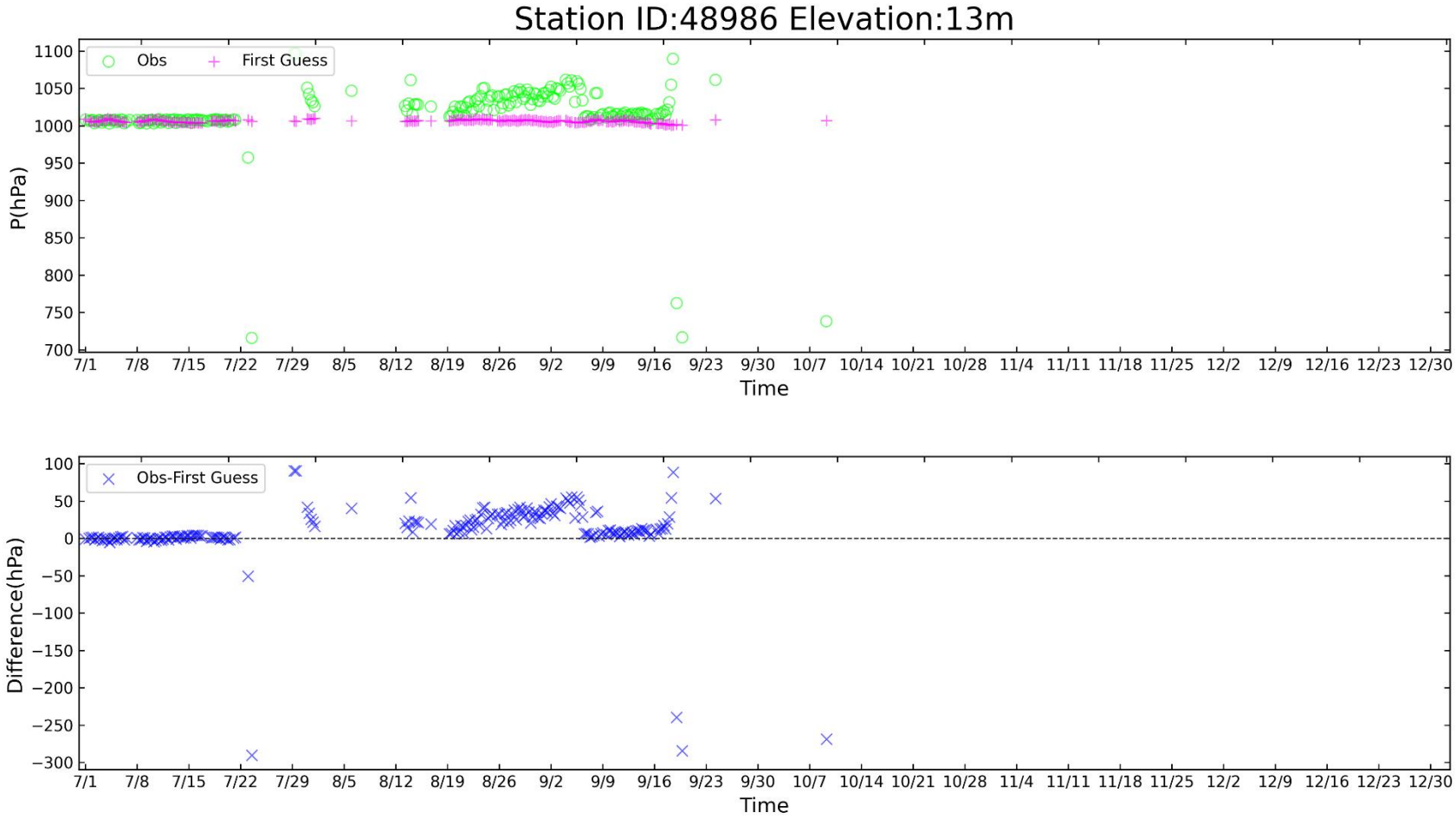

Figure 52 Time-series representation of SLP Obs minus FirstGuess for station 48986

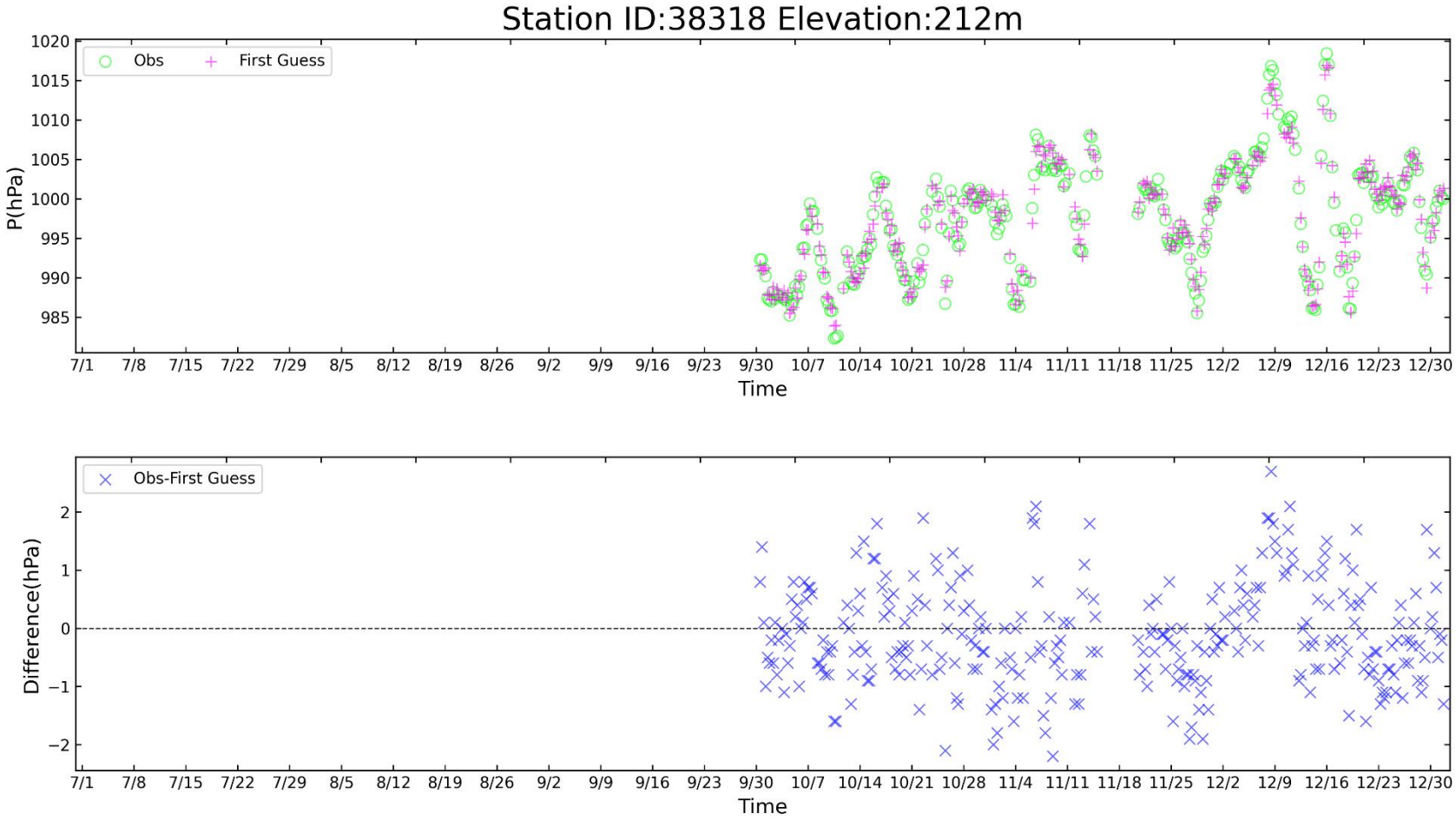

Figure 53 Time-series representation of SLP Obs minus FirstGuess for station 38318

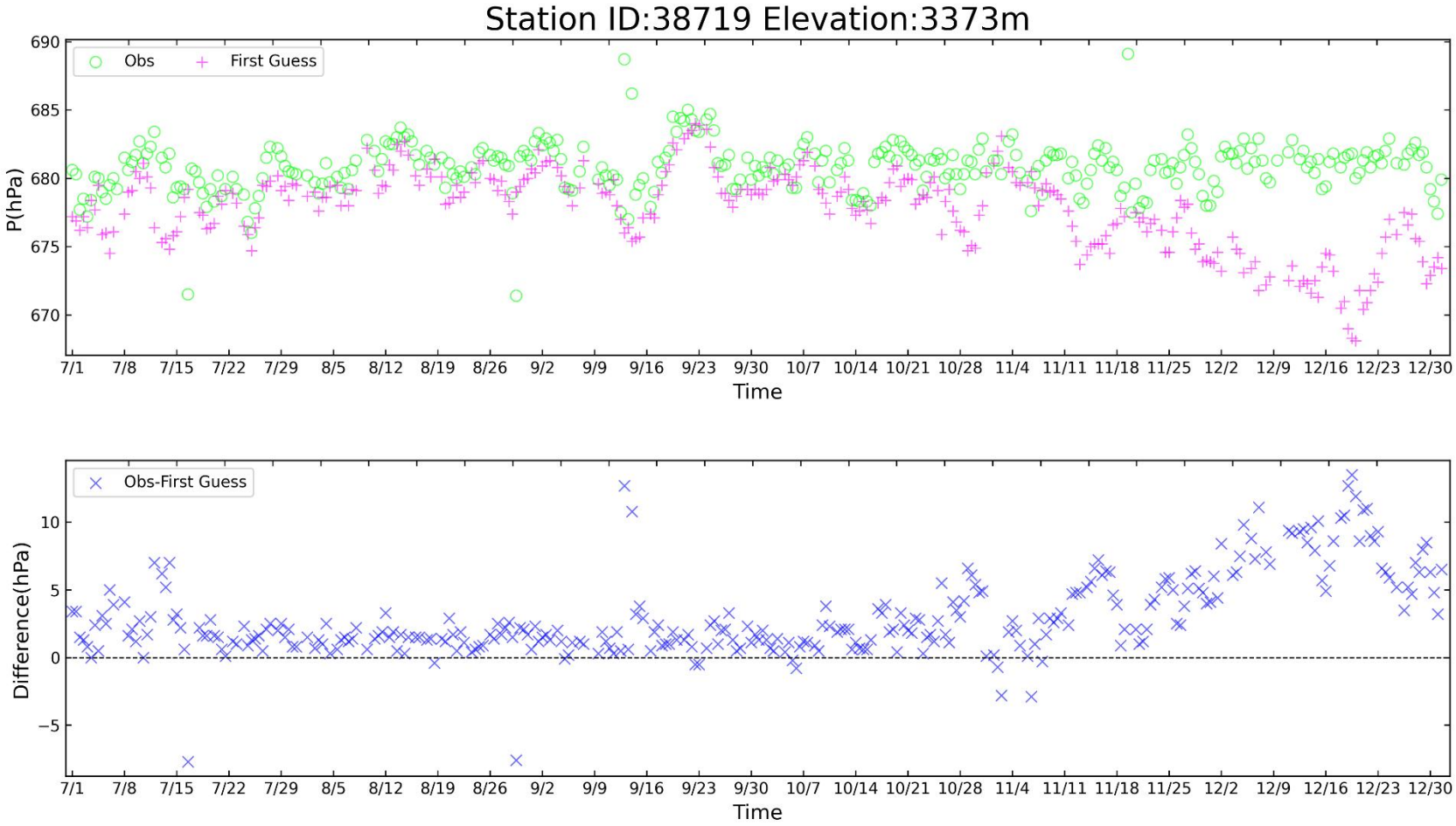

Figure 54 Time-series representation of SLP Obs minus FirstGuess for station 38719*

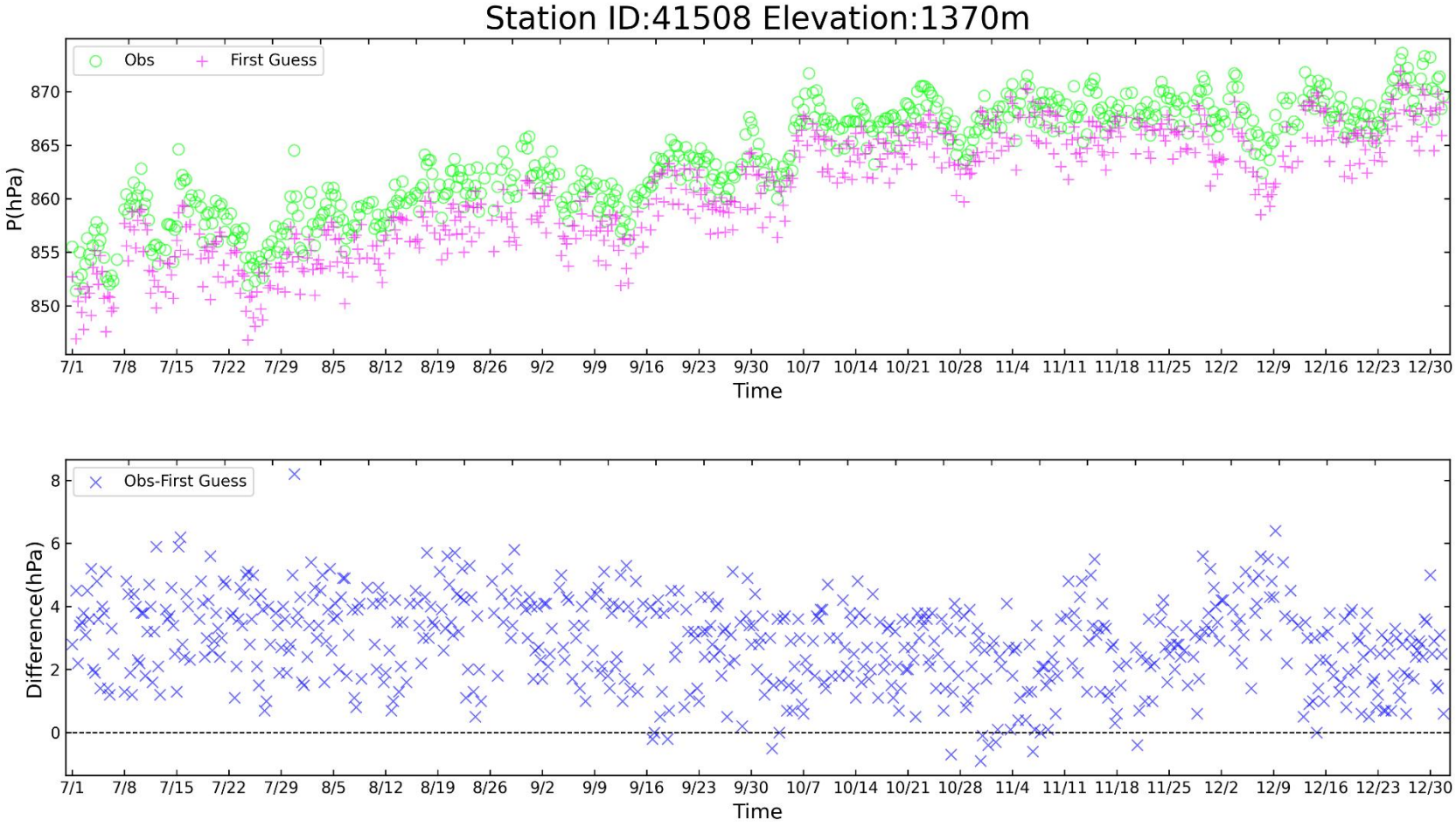

Figure 55 Time-series representation of SLP Obs minus FirstGuess for station 41508*

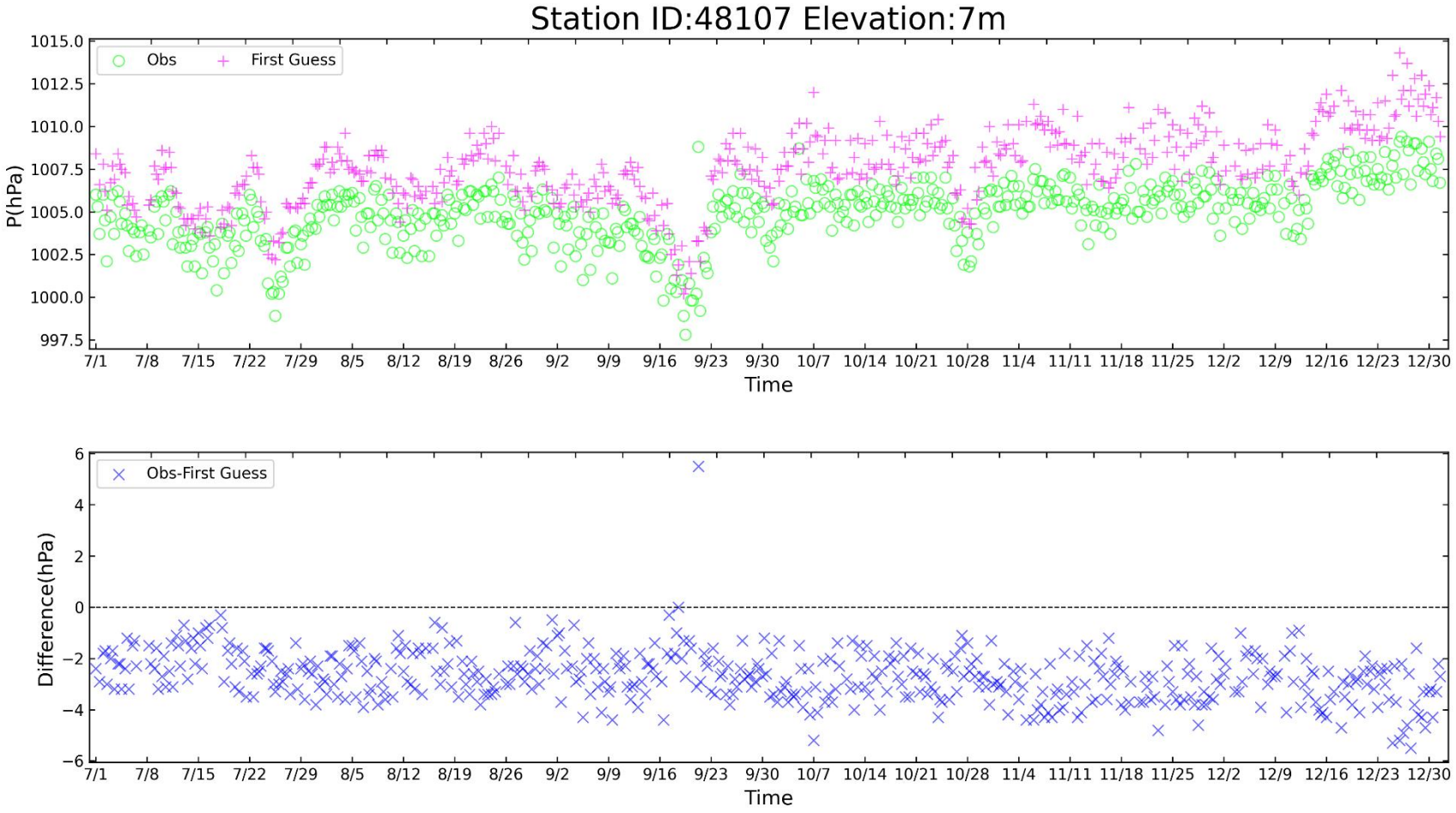

Figure 56 Time-series representation of SLP Obs minus FirstGuess for station 48107*

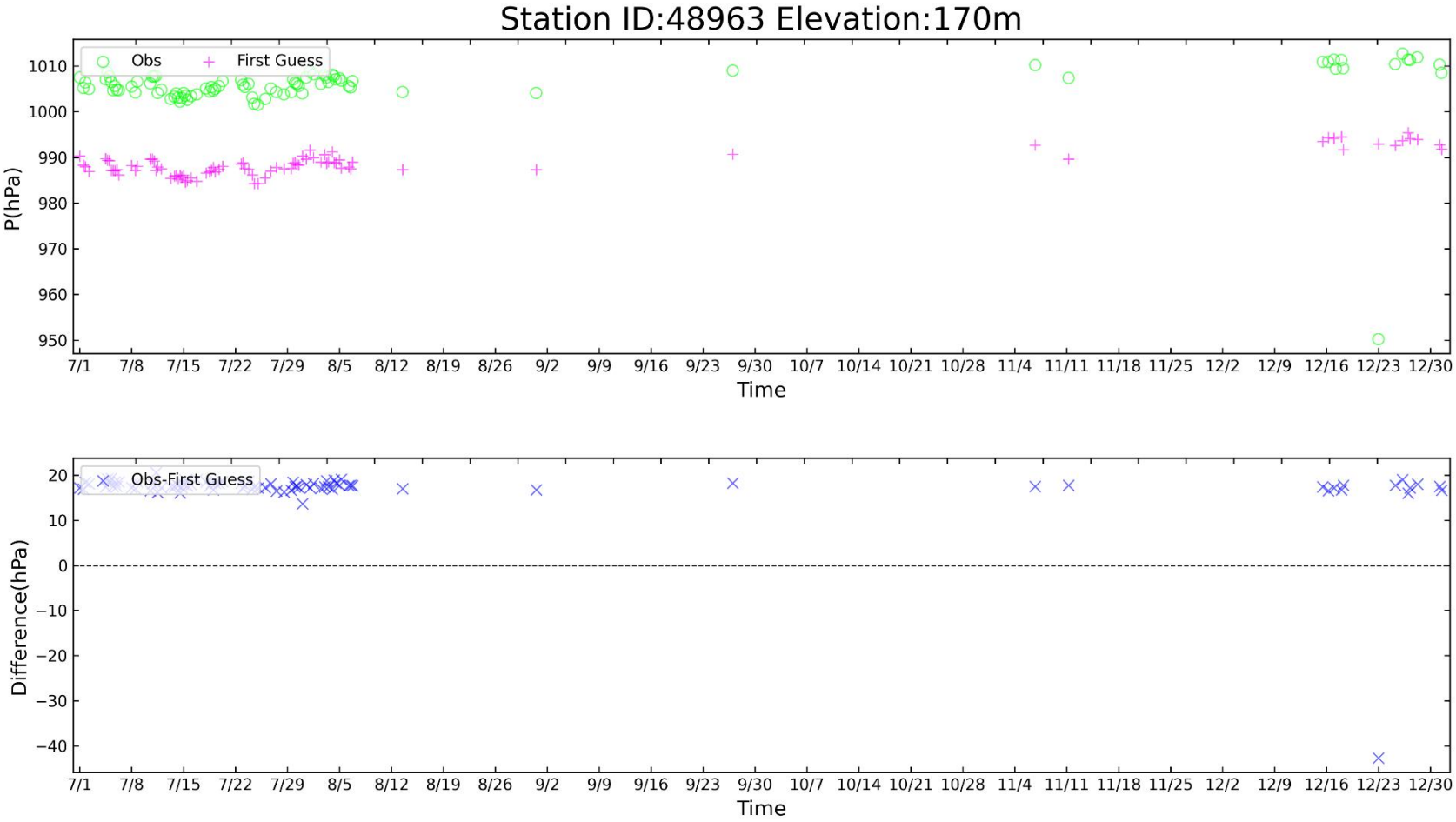

Figure 57 Time-series representation of SLP Obs minus FirstGuess for station 48963

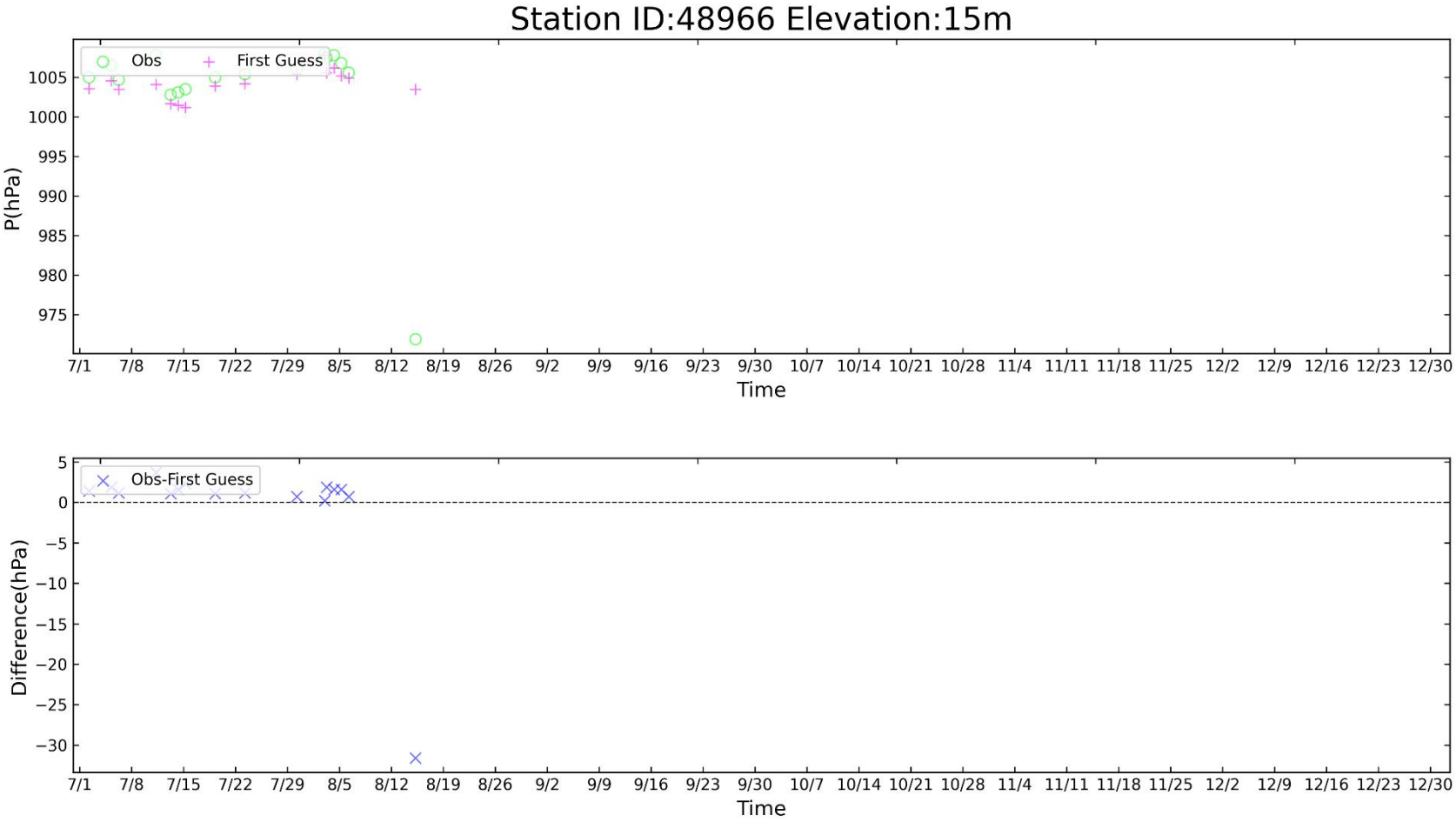

Figure 58 Time-series representation of SLP Obs minus FirstGuess for station 48966